Journal of Inclusion Phenomena and Molecular Recognition in Chemistry **24:** 61–132, 1996.

Review Article

Past, Present and Future of the Clathrate Inclusion Compounds Built of Cyanometallate Hosts*

TOSCHITAKE IWAMOTO
Department of Chemistry, College of Arts and Sciences, The University of Tokyo, Komaba, Meguro, Tokyo 153, Japan

Received: 19 February 1996; in final form: 11 March 1996

Abstract. One-, two- and three-dimensional CN-bridged metal complex structures made up of building blocks such as linear $[Ag(CN)_2]^-$, square planar $[Ni(CN)_4]^{2-}$ or tetrahedral $[Cd(CN)_4]^{2-}$, and of the complementary ligands such as ammonia, water, unidentate amine, bidentate α,ω-diaminoalkane, etc., are reviewed with an emphasis on their behaviour as hosts to afford clathrate inclusion compounds with guest molecules and as self-assemblies to form supramolecular structures with or without guests. The historical background is explained for Prussian blue and Hofmann's benzene clathrate based on their single crystal structure determinations. The strategies the author and coworkers have been applying to develop varieties of clathrate inclusion compounds from the Hofmann-type are demonstrated with the features observed for the developed structures determined by single crystal X-ray diffraction methods.

Key words: Crystal structure, dicyanoargentate, Hofmann-type clathrate, inorganic host, metal complex host, mineralomimetic chemistry, organic guest, tetracyanocadmate, tetracyanonickelate

Abbreviations for Ligands and Guests

mma:	$NMeH_2$
dma:	NMe_2H
tma:	NMe_3
mea:	$NH_2(CH_2)_2OH$
en:	$NH_2(CH_2)_2NH_2$
pn:	$NH_2CHMeCH_2NH_2$
tn:	$NH_2(CH_2)_3NH_2$
dabtn:	$NH_2(CH_2)_4NH_2$
daptn:	$NH_2(CH_2)_5NH_2$
dahxn:	$NH_2(CH_2)_6NH_2$
dahpn:	$NH_2(CH_2)_7NH_2$
daotn:	$NH_2(CH_2)_8NH_2$

* Presented at the Sixth International Seminar on Inclusion Compounds, Istanbul, Turkey, 27–31 August, 1995.

danon:	$NH_2(CH_2)_9NH_2$
dadcn:	$NH_2(CH_2)_{10}NH_2$
mtn:	$NMeH(CH_2)_3NH_2$
dmtn:	$NMe_2(CH_2)_3NH_2$
detn:	$NEt_2(CH_2)_3NH_2$
temtn:	$NMe_2(CH_2)_3NMe_2$
dien:	$NH_2(CH_2)_2NH(CH_2)_2NH_2$
pXdam:	p-$C_6H_4(NH_2CH_2)_2$
mXdam:	m-$C_6H_4(NH_2CH_2)_2$
py:	C_5H_5N pyridine
ampy:	$NH_2C_5H_4N$ aminopyridine
Clpy:	ClC_5H_4N chloropyridine
Mepy:	MeC_5H_4N methylpyridine
dmpy:	$Me_2C_5H_3N$ dimethylpyridine
bpy:	$NC_5H_4C_5H_4N$ bipyridine
quin:	C_7H_9N quinoline
iquin:	iso-C_7H_9N isoquinoline
qxln:	$C_8H_6N_2$ quinoxaline
Pe:	C_5H_{11}- pentyl
imH:	$C_3N_2H_4$ imidazole
pyrz:	$N(CHCH)_2N$ pyrazine
Mequin:	MeC_7H_8N methylquinoline
bppn:	$C_{13}H_{14}N_2$ 1,3-bis(4-pyridyl)propane
bpb:	$C_{14}H_8N_2$ 1,4-bis(4-pyridyl)butadiyne
N-Meim:	$C_3N_2H_3Me$ N-methylimidazole
2-MeimH:	$C_3N_2H_3Me$ 2-methylimidazole
dmf:	$HOCNMe_2$ dimethylformamide
hmta:	$C_6H_{12}N_4$ hexamethylenetetramine
o-phen:	$C_{12}H_8N_2$ 1,10-phenanthroline
den:	$HN(CH_2CH_2)_2NH$ piperazine
morph:	$HN(CH_2CH_2)_2O$ morpholine
ten:	$N(CH_2CH_2)_3N$ 1,4-diazabicyclo[2.2.2]octane
ameden:	$NH_2(CH_2)_2N(CH_2CH_2)_2NH$ N-(2-aminoethyl)piperazine

1. Introduction

From the end of the 19th to the beginning of the 20th century Alfred Werner had rationalised the composition of the molecular complexes formed between metal salt and inorganic or organic molecules as coordination complex compounds taking stereospecific structures. For example, the en-luteo salt $CoCl_3 \cdot 3en = [Cd(en)_3]Cl_3$, was interpreted in terms of the ionic compound comprised of the chloride anion and the octahedral cation of $[Co(en)_3]^{3+}$ in which the central cobalt atom was bonded by six N atoms of the three en ligands through the so-called side-valence value of 6, although there was still uncertainty about the bonding in Zeise's salt, $K[PtCl_3(C_2H_4)]$, discovered in 1827.

Stimulated by the discovery of Zeise's ethylene compound, Karl Andreas Hofmann examined the preparation of molecular complexes formed between metal salts and organic molecules. As chance would have it, he obtained a mauve crystalline product of composition $Ni(CN)_2 \cdot NH_3 \cdot C_6H_6$ from a concentrated ammoniacal solution of freshly precipitated nickel hydroxide by passing the coal gas used for lighting through the solution [1a]. Hofmann immediately assumed this and similar aniline and phenol compounds, $Ni(CN)_2 \cdot NH_3 \cdot PhNH_2$ and $Ni(CN)_2 \cdot NH_3 \cdot PhOH \cdot H_2O$, to be four-coordinate complexes of divalent Ni according to Werner's coordination theory [1b]. However, similar compounds with the composition $Ni(CN)_2 \cdot NH_3 \cdot G$ were obtained only with those organic molecules G whose molecular volumes were not greater than that of aniline. Hofmann's conclusion was as follows: the space-oriented valence force (covalent or coordination bonding) would not be able to form molecular compounds like these; the molecule (G) might be attracted as a whole and fill up a space upon the formation of the compound [1c]. His excellent view was verified by Herbert Marcus Powell in 1949–52, half a century after his discovery of the benzene compound [2].

The crystal structure of Hofmann's benzene compound is shown in Figure 1 as a more generalised form of the Hofmann-type benzene clathrate. Since there are two kinds of Ni atoms in the two-dimensional (2D) network, one in a square planar low-spin Ni^{2+} as the central metal of $[Ni(CN)_4]^{2-}$ and the other in an octahedral high-spin Ni^{2+} coordinated with four N atoms from four $[Ni(CN)_4]^{2-}$ entities and two N atoms from two NH_3 ligands at *trans* positions, the formula $[Ni(NH_3)_2Ni(CN)_4] \cdot 2C_6H_6$ should be given in place of the original $Ni(CN)_2 \cdot NH_3 \cdot C_6H_6$. The term clathrate first proposed by Powell for the quinol compound $3C_6H_4(OH)_2 \cdot SO_2$ [3] was applied to interpret the structure of Hofmann's benzene compound in which no direct chemical bonds were observed between the 2D metal complex network and the benzene molecule. His concept of the clathrate should be noted as an unprecedented view that a well-ordered chemical structure can be formed between two or more independent chemical species without direct or strong chemical bonds.

The Hofmann-type host structure demonstrates a typical example of a 2D network built of the square planar $[Ni(CN)_4]^{2-}$ entities and the second coordination centres accepting the N-donation from the square planar entities. Such a multidimensional structure involving cyanometallate anions and second coordination centres, but without a secondary or complementary ligand like NH_3 in the Hofmann-type, was proposed by Keggin and Miles in 1936 for the three-dimensional (3D) structures of Prussian blue and related complexes based on powder X-ray diffraction data [4]. As shown in Figure 2, the proposed structures had also a cage imprisoning K^+, which cation had been speculated to be present owing to the assumed compositions $K_2Fe^{II}[Fe^{II}(CN)_6]$ and $KFe^{III}[Fe^{II}(CN)_6]$. Apart from their validity, these structures in which a cube edged by —CN— bridges and cornered by coordination centres accommodates a 'guest' cation might provide the earli-

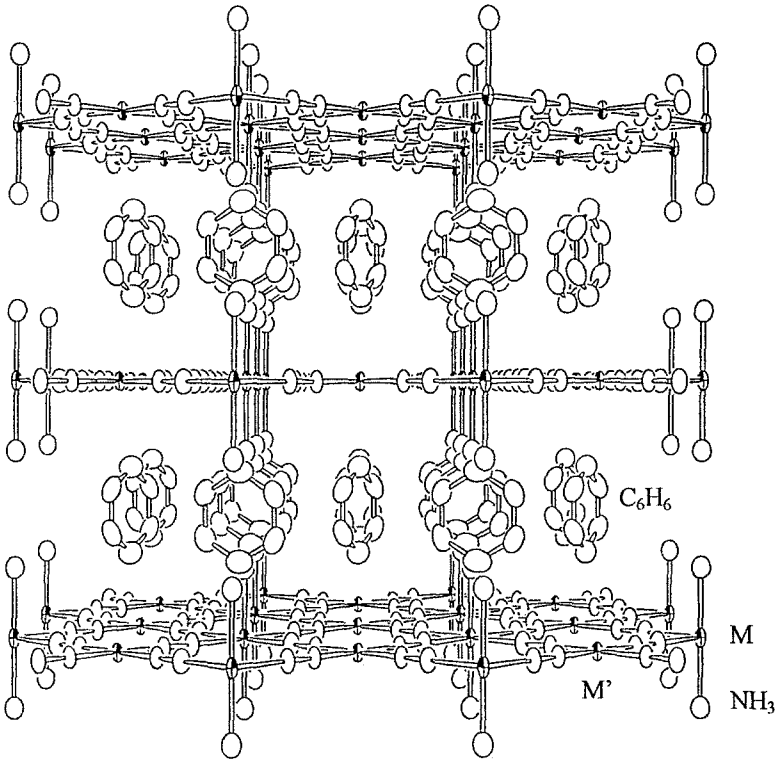

Figure 1. Hofmann-type benzene clathrate $[M(NH_3)_2M'(CN)_4]\cdot 2C_6H_6$. M: at octahedral position coordinated by two NH_3 ligands in trans positions; $M'(CN)_4$: square planar tetracyanometallate. In Hofmann's benzene clathrate M = M′ = Ni.

est example of a supramolecular structure, although there should be electrostatic interactions between the anionic host and the cationic guest.

Ludi and co-workers determined the single crystal structures for Prussian blue and a number of related complexes using single crystals prepared with extreme care; density measurements and chemical analyses were also carried out scrupulously [5,6]. No crystals showed the Keggin–Miles structure. In the case of Prussian blue, the primitive cubic unit cell has the *a* dimension of two Fe—CN—Fe spans, as shown in Figure 3. The $[Fe^{II}(CN)_6]^{4-}$ entity that had been speculated to be at the body centre position in the Keggin–Miles structure was missing; in place of the N-ends of the missing entity, waters of coordination ligated from the inside of the expanded cage in which additional water molecules were hydrogen-bonded to the aqua ligands. The composition based on the single crystal structure was given as $Fe^{III}_4[Fe^{II}(CN)_6]_3 \cdot xH_2O$ (x = *ca.* 15) [5]. Ludi's Prussian blue structure is also another example of a supramolecular structure in which a cube of the long spanned edges accommodates an assembly of water molecules with different roles, as ligands and as space-fillers to stabilise the crystal structure.

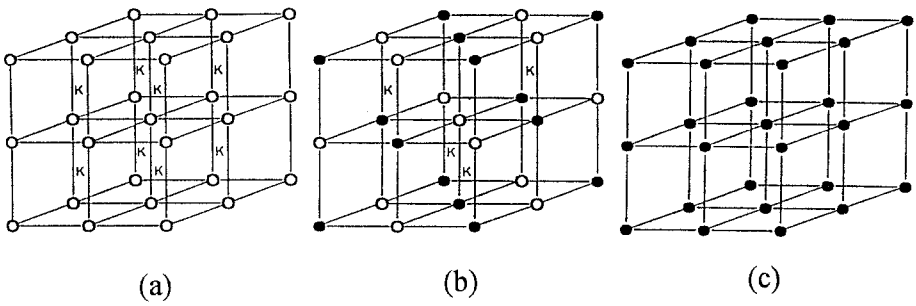

Figure 2. Keggin–Miles structures of Prussian blue complexes speculated for (a) $K_2Fe^{II}[Fe^{II}(CN)_6]$, (b) $KFe^{III}[Fe^{II}(CN)_6]$, and (c) $Fe^{III}[Fe^{III}(CN)_6]$. Open circle: Fe^{II}; solid circle: Fe^{III}; line: CN group. Each of the large cubes has about 10.2 Å of the edge length; each of the octant (small) cubes is occupied by a K^+ in (a), half of the octants arrayed with the T_d symmetry occupied by a K^+ in (b), but vacant in (c).

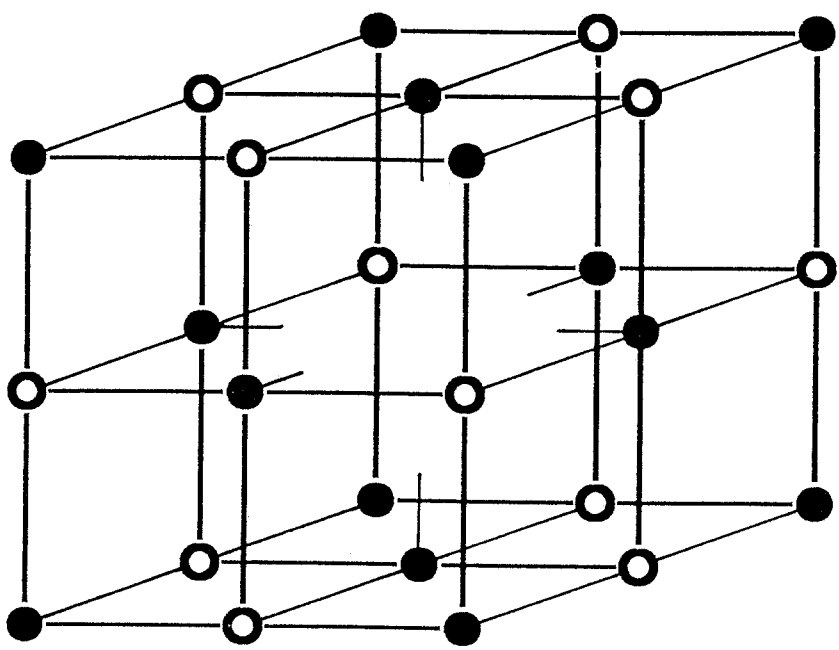

Figure 3. Ludi structure of $Fe_4^{III}[Fe^{II}(CN)_6]_3 \cdot xH_2O$ ($x \sim 15$). Solid circle: Fe^{III}; open circle: Fe^{II}; line between circles: CN group; the inside of the cube is filled up by hydrogen-bonded assembly of H_2O molecules six of which are coordinated to Fe^{III}.

The case of Prussian blue supports the fact that a solid state supramolecular structure should be verified, interpreted and understood on the basis of the single crystal structure. As will be exemplified later, it is often forgotten that similar compositions never assure structural similarities for inorganic polymeric compounds, although that is a common occurrence for organic compounds. In this review, the

cited compounds have been limited to those whose single crystal structures are available, unless stated otherwise.

2. Strategies to Develop New Series from the Hofmann-Type Structure

Since a few reviews [7] have already described the development from Hofmann's benzene clathrate to the Hofmann-type, together with some details of our strategies for developing novel series from the Hofmann-type, only the outlines are described in this review.

One of the structural features observed for the Hofmann-type is the layer structure of the flat 2D networks with the protrusion of the unidentate ammine ligands perpendicular to the flat network (Figure 1). The building blocks constructing the Hofmann-type host $[M(NH_3)_2M'(CN)_4]$ are divided into the three moieties, the square planar $[M'(CN)_4]^{2-}$, i.e., a moiety comprised of the primary coordination centre M′ and the primary ligand CN, the octahedral M as the second coordination centre, and the NH_3 as the complementary ligand coordinated to M. Our strategies are summarised as follows:

(1) to replace the NH_3 by other unidentate ligands such as H_2O, mma, dma, etc., in order to regulate the lipo- or hydrophilic characters of the interlayer cavities;
(2) to replace two NH_3 ligands facing each other in the interlayer space by an ambidentate bridging ligand such as α,ω-diaminoalkane $NH_2(CH_2)_nNH_2$, etc., in order to increase the lipophilic character of the cavities and to regulate the interlayer distance in the three-dimensional host;
(3) to replace the square planar $[M'(CN)_4]^{2-}$ by a tetrahedral tetracyanometallate such as $[Cd(CN)_4]^{2-}$, $[Hg(CN)_4]^{2-}$, in order to build up the three-dimensional host with CN bridges only;
(4) to replace the octahedral *trans*-$[M(NH_3)_2]^{2+}$ entity by two phenylalkylammonium cations $Ph(CH_2)_nNH_3^+$ in order to increase the lipophilic character of the interlayer space;

and

(5) to replace the —CN— span by a —NC—Ag—CN— span, i.e., to replace the $[Ni(CN)_4]^{2-}$ by $\{[Ag(CN)_2]^-\}_2$ in the formula, in order to elongate the span distance.

In these strategies, we almost always refer to the Hofmann-type host $[Cd(NH_3)_2\ Ni(CN)_4]$ as the theoretical prototype. Divalent Cd appears to be the most suitable second coordination centre linked by cyanometallate anions to form a multi-dimensional polymeric structure, the softness-hardness of Cd(II) as a Lewis acid being most appropriate for accepting the N atom of cyanometallate as a Lewis base.

As for naming of the derived series, Hofmann-L-type has been applied to denote the structures involving the 2D network topologically the same as that of

the Hofmann-type with ligand L for those obtained by strategies (1) and (2). For example, Hofmann-H_2O-type $[Cd(H_2O)_2Ni(CN)_4]$ host is obtained by strategy (1); Hofmann-diam-type in general is for $[Cd\{NH_2(CH_2)_nNH_2\}Ni(CN)_4]$ by strategy (2) (n = 2–9), where ligand L makes the host three-dimensional. Hofmann-Td-type is used to denote $[Cd(NH_3)_2M'(CN)_4]$ (M′ = Cd or Hg); those obtained by the combination of strategies (2) and (3) are denoted as L-Td-type.

3. Structures of the Hosts Involving the $Ni(CN)_4$ Entity and Related Complexes

3.1. General

Brief crystallographic data along with the numbering of compounds are summarised in Table I for those structures involving square planar $Ni(CN)_4$.

The tetracyanonickelate(II) anion, as well as tetracyanopalladate(II) and tetracyanoplatinate(II), can behave not only as a cross ligand as in the Hofmann-type structure to provide the four N-ends to the second coordination centres but also as a bidentate bridging ligand using only two of the four N-ends at *cis* or *trans* positions; a unidentate ligation, though possible, cannot join in a catenation. Including an imaginary mode T-1D using three N-ends, the catenation modes observed in the known single crystal structures are illustrated in Figure 4. Except for T-1D, all the modes have been observed in our crystal structures involving $Ni(CN)_4$; $[Ni(en)_2Pd(CN)_4]$ [53] may be an example of *trans*-1D catenation observed for d^8 square planar $M'(CN)_4$ other than $Ni(CN)_4$.

The second coordination centres linked by $Ni(CN)_4$ entities are in some cases additionally bridged by complementary ligands to reinforce the multi-dimensional structures of the hosts and related complexes. For example in the Hofmann-diam-type host, there are one-dimensional (1D) chains of $—[Cd—L—]_\infty$ successively linking the 2D networks; the catenation mode may be denoted as single-1D. Some typical catenation modes possible for the combinations of the second coordination centre M and bridging ligand L in the ratios of M:L of 1:1, 1:2 and 1:3 are shown in Figure 5; the modes other than triangle-2D have been observed in our structures.

Since in some real crystal structures the catenation structures exemplified in Figures 4 and 5 are deformed to a certain extent, or combined with one another, there may be some ambiguity in representing these as 1D and 2D modes rather than real 3D structures.

3.2. Hofmann-type analogous 2D host structures

When the secondary ligand L is bulky in the Hofmann-L-type, the interlayer space is filled up by the ligands themselves to leave no spaces for guests, e.g., Hofmann-tma-type complex **28**, Hofmann-py-type complexes **31** and **32**, etc. in Table I. The topology of the Hofmann-type host is reserved but the 2D network is puckered to some extent in the Hofmann-L-type complexes except for **28**.

Table I. Crustallographic data for the structures involving $Ni(CN)_4$ and related structures.

		Space group	*a*/Å	*b*/Å	*c*/Å	*α*/°	*β*/°	*γ*/°	*Z*	Ref.
	Hofmann-type clathrates									
1	$[Mn(NH_3)_2Ni(CN)_4]\cdot 2C_6H_6$	*P4/m*	7.432(6)	7.432	8.335(5)	90	90	90	1	8
2	$[Fe(NH_3)_2Ni(CN)_4]\cdot 2C_6H_6$	*P4/mmm*	7.353(2)	7.353	8.316(2)	90	90	90	1	9
3	$[Ni(NH_3)_2Ni(CN)_4]\cdot 2C_6H_6$	*P4/m*	7.242(7)	7.242	8.277(8)	90	90	90	1	2
4	$[Ni(NH_3)_2Ni(CN)_4]\cdot 2C_{12}H_{10}$	*I*422	7.240(3)	7.240	25.30(1)	90	90	90	2	10
5	$[Cu(NH_3)_2Ni(CN)_4]\cdot 2C_6H_6$	*P4/mcc*	7.345(3)	7.345	16.519(4)	90	90	90	2	11
6	$[Zn(NH_3)_2Ni(CN)_4]\cdot 2C_6H_6$*1	*P4/m*	7.3294(3)	7.3294	8.0722(4)	90	90	90	1	12
7	$[Cd(NH_3)_2Ni(CN)_4]\cdot 2C_6H_6$	*P4/m*	7.575(6)	7.575	8.317(5)	90	90	90	1	13
		P4/m	7.542(2)	7.542	8.308(4)	90	90	90	1	14
8	$[Cd(NH_3)_2Ni(CN)_4]\cdot 2C_4H_5N$	*P4/m*	7.5225(6)	7.5225	8.009(1)	90	90	90	1	15
9	$[Cd(NH_3)_2Ni(CN)_4]\cdot 2C_4H_8O_2$	*P4/m*	7.586(9)	7.586	8.082(6)	90	90	90	1	16
	Hofmann-type hydrates									
10	$[Ni(NH_3)_2Ni(CN)_4]\cdot {}^1/_2H_2O$	*Imma*	7.24	14.32	8.74	90	90	90	4	17
11	$[Cd(NH_3)_2Ni(CN)_4]\cdot {}^1/_2H_2O$	*Imma*	7.622(4)	14.992(13)	8.961(6)	90	90	90	4	18
	Hofmann-H_2O-type clathrates and hydrates									
12	$[Fe(H_2O)_2Ni(CN)_4]\cdot 2C_4H_8O_2$	*P2/m*	7.222(1)	7.470(1)	8.008(2)	90	94.11(1)	90	1	19
13	$[Cd(H_2O)_2Ni(CN)_4]\cdot 2C_4H_8O_2$	*P2/m*	7.3980(8)	7.6454(6)	8.0639(9)	90	93.703(9)	90	1	20
14	$[Fe(H_2O)_2Ni(CN)_4]\cdot 4H_2O$	*Pnma*	12.200(2)	14.028(2)	7.2327(9)	90	90	90	4	20
15	$[Cd(H_2O)_2Ni(CN)_4]\cdot 4H_2O$	*Pnma*	12.415(1)	14.296(1)	7.435(1)	90	90	90	4	21
		Pnma	12.393(2)	14.278(5)	7.427(1)	90	90	90	4	22
	Hofmann-mma-type clathrate									
16	$[Cd(mma)_2Ni(CN)_4]\cdot {}^3/_2(o\text{-}MeC_6H_4NH_2)$	$P2_1/a$	14.518(4)	19.303(5)	7.6695(9)	90	90.36(2)	90	4	23
	Hofmann-dma-type clathrates									
17	$[Cd(dma)_2Ni(CN)_4]\cdot {}^1/_2C_6H_6$*2	$P2_1/c$	14.100(6)	7.556(1)	15.418(7)	90	96.56(5)	90	4	24
18	$[Cd(dma)_2Ni(CN)_4]\cdot PhNH_2$	*Pmma*	25.940(3)	7.562(1)	10.416(2)	90	90	90	4	25
19	$[Cd(dma)_2Ni(CN)_4]\cdot o\text{-}MeC_6H_4NH_2$	*Pmma*	26.32(1)	7.6135(9)	10.36(1)	90	90	90	4	26

*1. Neutron diffraction data for powder sample at 25 K.

*2. The crystal axes have been converted from those in the original literature.

Table I. Continued

		Space group	*a*/Å	*b*/Å	*c*/Å	*α*/°	*β*/°	*γ*/°	*Z*	Ref.
19	$[Cd(dma)_2Ni(CN)_4]\cdot o\text{-}MeC_6H_4NH_2$ (cont'nd)	*Pmma*	26.380(3)	7.606(3)	10.335(7)	90	90	90	4	25
20	$[Cd(dma)_2Ni(CN)_4]\cdot m\text{-}MeC_6H_4NH_2$	*P2/m*	14.667(7)	7.612(1)	10.369(8)	90	115.52(6)	90	4	26
		P2/m	14.665(2)	7.607(1)	10.346(7)	90	115.12(2)	90	4	25
21	$[Cd(dma)_2Ni(CN)_4]\cdot p\text{-}MeC_6H_4NH_2$	$P\bar{1}$	14.61(1)	7.613(2)	10.63(1)	94.2(1)	118.2(2)	89.8(1)	2	26
		$P\bar{1}$	14.601(2)	7.6151(6)	10.609(2)	94.51(2)	118.05(1)	89.66(1)	2	25
22	$[Cd(dma)_2Ni(CN)_4]\cdot 2,3\text{-}Me_2C_6H_3NH_2$	*P2/m*	14.712(1)	7.596(1)	10.450(2)	90	113.50(1)	90	2	25
23	$[Cd(dma)_2Ni(CN)_4]\cdot 2,4\text{-}Me_2C_6H_3NH_2$	*P2/m*	14.658(2)	7.605(2)	10.608(9)	90	115.94(4)	90	2	25
24	$[Cd(dma)_2Ni(CN)_4]\cdot 2,5\text{-}Me_2C_6H_3NH_2$	*P2/m*	14.599(3)	7.607(1)	10.333(9)	90	115.07(3)	90	2	25
25	$[Cd(dma)_2Ni(CN)_4]\cdot 2,6\text{-}Me_2C_6H_3NH_2$	*Pmma*	26.634(2)	7.607(1)	10.366(3)	90	90	90	4	25
26	$[Cd(dma)_2Ni(CN)_4]\cdot 3,4\text{-}Me_2C_6H_3NH_2$	*Pmma*	27.123(4)	7.602(3)	10.398(6)	90	90	90	4	25
27	$[Cd(dma)_2Ni(CN)_4]\cdot 2,4,6\text{-}Me_3C_6H_2NH_2$	$P\bar{1}$	14.955(3)	7.5300(6)	14.852(5)	85.94(6)	111.74(2)	90.05(1)	2	25
	Hofmann-tma-type complex									
28	$[Cd(tma)_2Ni(CN)_4]$	*I4/mmm*	7.5174(6)	7.5174	13.968(3)	90	90	90	2	23
	Hofmann-mea-type(2) clathrate									
29	$[Cd(mea)_2Ni(CN)_4]\cdot C_4H_5N$	$Pna2_1$	14.691(1)	15.881(1)	7.575(1)	90	90	90	4	27
	Hofmann-den-type(2) clathrate									
30	$[Cd(den)_2Ni(CN)_4]\cdot 2PhOH$	$P\bar{1}$	6.947(2)	7.818(2)	13.132(4)	101.67(2)	96.56(5)	90.69(3)	1	28
	Hofmann-py-type and related complexes									
31	$[Fe(py)_2Ni(CN)_4]$	*C2/m*	15.526(3)	7.392(2)	7.067(9)	90	101.26(2)	90	2	9
32	$[Cd(py)_2Ni(CN)_4]$	*C2/m*	15.881(4)	7.540(6)	7.097(9)	90	106.83(8)	90	2	29
33	$[Cd(NH_3)(4\text{-}Clpy)Ni(CN)_4]$*3	*Ima2*	12.490(3)	14.238(8)	7.705(5)	90	90	90	4	30
34	$[Cd(NH_3)(2\text{-}NH_2\text{-}3\text{-}Mepy)Ni(CN)_4]$	$Pna2_1$	13.535(1)	13.607(1)	7.645(1)	90	90	90	4	31
		Pnma	13.535(1)	7.645(1)	13.607(1)	90	90	90	4	32
35	$[Cd(morph)_2Ni(CN)_4]$	*Pmna*	7.985(1)	6.695(2)	14.314(2)	90	90	90	2	20
	Hofmann-diam-type clathrates									
36	$[Cd(en)Ni(CN)_4]\cdot 2C_6H_6$	*P4/m*	7.675(3)	7.675	8.056(10)	90	90	90	1	33
		P4/mmm	7.657(1)	7.657	8.013(2)	90	90	90	1	14
37	$[Cd(en)Ni(CN)_4]\cdot 2C_4H_5N$	*Pmmm*	7.18(3)	7.641(10)	7.861(4)	90	90	90	1	34
		P4/mmm	7.590(1)	7.590	7.725(2)	90	90	90	4	15

*3. Possibility of *Imam* space group has been suggested.

Table I. Continued

		Space group	*a*/Å	*b*/Å	*c*/Å	*α*/°	*β*/°	*γ*/°	*Z*	Ref.
38	$[Cd(mea)Ni(CN)_4]\cdot 2C_6H_6$	*P4/mmm*	7.5229(2)	7.529	8.094(1)	90	90	90	1	27
39	$[Cd(l\text{-pn})Ni(CN)_4]\cdot {}^3/_2C_4H_5N$	*P422*	7.575(2)	7.575	7.742(2)	90	90	90	1	35
40	$[Cd(dl\text{-pn})Ni(CN)_4]\cdot {}^3/_2C_4H_5N$	*P4/m*	7.570(2)	7.570	7.741(2)	90	90	90	1	35
41	$[Cd(tn)Ni(CN)_4]\cdot 1.72(o\text{-}MeC_6H_4NH_2)$	*P2/m*	7.538(2)	9.314(5)	7.670(2)	90	91.03(2)	90	1	36m
42	$[Cd(tn)Ni(CN)_4]\cdot {}^1/_2(m\text{-}ClC_6H_4NH_2)$	*Pbam*	12.1714(7)	15.798(1)	7.737(1)	90	90	90	4	36m
43	$[Cd(dabtn)Ni(CN)_4]\cdot C_4H_5N$	*P2/m*	7.840(4)	7.634(2)	7.060(2)	90	90.15(6)	90	1	36e
44	$[Cd(dabtn)Ni(CN)_4]\cdot {}^3/_2PhNH_2$	$P\bar{1}$	9.774(3)	13.918(8)	7.715(4)	90.41(4)	90.43(5)	93.18(4)	2	36e
45	$[Cd(dabtn)Ni(CN)_4]\cdot {}^3/_2(o\text{-}MeC_6H_4NH_2)$	$P\bar{1}$	9.806(3)	14.388(3)	7.725(2)	89.71(2)	89.96(2)	98.12(2)	2	36j
46	$[Cd(dabtn)Ni(CN)_4]\cdot PhNMe_2$	$P2_1/m$	9.860(5)	15.267(6)	7.309(4)	90	113.92(4)	90	2	36j
47	$[Cd(dabtn)Ni(CN)_4]\cdot 2,5\text{-}Me_2C_6H_3NH_2$	$P2_1/m$	9.795(2)	15.010(2)	7.125(2)	90	105.56(1)	90	2	36b
48	$[Cd(daptn)Ni(CN)_4]\cdot o\text{-}MeC_6H_4NH_2$	*P4/mmm*	7.485(7)	7.485	10.06(3)	90	90	90	1	36j
49	$[Cd(daptn)Ni(CN)_4]\cdot m\text{-}MeC_6H_4NH_2$	*Pbam*	12.254(6)	20.62(1)	7.804(1)	90	90	90	4	36j
50	$[Cd(daptn)Ni(CN)_4]\cdot {}^3/_2(p\text{-}MeC_6H_4NH_2)$	$P2_1/a$	13.736(3)	22.014(4)	7.762(3)	90	91.04(3)	90	4	36m
51	$[Cd(dahxn)Ni(CN)_4]\cdot o\text{-}MeC_6H_4NH_2$	*P2/m*	9.541(2)	7.569(2)	7.199(1)	90	103.3(1)	90	1	36c
52	$[Cd(dahxn)Ni(CN)_4]\cdot m\text{-}MeC_6H_4NH_2$	$P\bar{1}$	9.725(2)	7.598(1)	7.177(1)	90.44(1)	98.80(1)	95.70(1)	1	36c
53	$[Cd(dahxn)Ni(CN)_4]\cdot p\text{-}MeC_6H_4NH_2$	*P2/m*	9.540(2)	7.611(1)	7.120(1)	90	100.95(1)	90	1	36h
54	$[Cd(dahxn)Ni(CN)_4]\cdot 2,4\text{-}Me_2C_6H_3NH_2$	*P2/m*	9.628(2)	7.613(1)	7.122(1)	90	100.01(1)	90	1	36h
55	$[Cd(dahpn)Ni(CN)_4]\cdot {}^3/_2(2\text{-Mequin})$	*Pbam*	13.599(2)	27.938(2)	7.619(2)	90	90	90	4	36m
56	$[Cd(daotn)Ni(CN)_4]\cdot C_6H_{13}OH$	*P2/m*	11.479(2)	7.782(1)	6.945(1)	90	105.29(1)	90	1	36i
57	$[Cd(daotn)Ni(CN)_4]\cdot PhMe$	*P2/m*	11.348(3)	7.652(2)	7.042(1)	90	106.07(2)	90	1	36l
58	$[Cd(daotn)Ni(CN)_4]\cdot o\text{-}MeC_6H_4NH_2$	*P2/m*	11.513(4)	7.626(1)	7.101(1)	90	109.63(3)	90	1	36j
59	$[Cd(daotn)Ni(CN)_4]\cdot p\text{-}MeC_6H_4NH_2$	$P\bar{1}$	11.52(1)	7.632(3)	7.039(4)	88.93(4)	109.71(5)	82.81(9)	1	36j
60	$[Cd(danon)Ni(CN)_4]\cdot {}^1/_2(o\text{-}C_6H_4Me_2)$	$P\bar{1}$	15.118(3)	14.048(4)	7.325(1)	91.50(2)	131.66(3)	107.50(2)	1	36k
61	$[Cd(pXdam)Ni(CN)_4]\cdot o\text{-}MeC_6H_4NH_2$	$P\bar{1}$	6.960(2)	7.718(2)	9.693(2)	90.61(2)	91.72(2)	90.17(2)	1	37
62	$[Cd(den)Ni(CN)_4]\cdot C_6H_6$	*Pmma*	14.065(7)	7.795(3)	7.631(5)	90	90	90	2	38
63	$[Cd(den)Ni(CN)_4]\cdot C_4H_5N$	*Pmma*	13.467(5)	7.741(4)	7.564(4)	90	90	90	2	38
64	$[Cd(den)Ni(CN)_4]\cdot CH_2Cl_2$	*Pmma*	12.615(3)	7.823(3)	7.502(3)	90	90	90	2	38
65	$[Cd(den)Ni(CN)_4]\cdot CH_2Br_2$	*Pmma*	12.972(2)	7.860(2)	7.491(2)	90	90	90	2	38
66	$[Cd(den)Ni(CN)_4]\cdot CH_2I_2$	*Pmma*	13.542(7)	7.867(1)	7.492(2)	90	90	90	2	38
67	$[Cd(den)Ni(CN)_4]\cdot CH_2ClCH_2Cl$	$P\bar{1}$	7.363(3)	7.617(2)	7.590(2)	84.03(2)	105.12(2)	89.61(3)	1	38

Table I. Continued

		Space group	*a*/Å	*b*/Å	*c*/Å	*α*/°	*β*/°	*γ*/°	*Z*	Ref.
68	$[Cd(den)Ni(CN)_4]\cdot PhOMe$	*Pmmm*	7.448(2)	7.686(2)	7.594(2)	90	90	90	1	38
69	$[Cd(den)Ni(CN)_4]\cdot MeCN$	*P2/m*	7.013(3)	7.710(2)	7.554(2)	90	113.09(3)	90	1	38
70	$[Cd(den)Ni(CN)_4]\cdot EtCN$	*P4/mmm*	7.568(1)	7.568	7.486(4)	90	90	90	1	38
71	$[Cd(den)Ni(CN)_4]\cdot(HOCH_2CH_2OH\cdot H_2O)$	*C2/m*	10.721(3)	10.743(3)	7.521(2)	90	94.30(2)	90	2	38
	$\{Cd(pn)Ni(CN)_4\}$ host clathrates with channel cavities									
72	$[Cd(pn)Ni(CN)_4]\cdot 0.32C_7H_{16}$	*A2/a*	14.014(5)	26.963(5)	7.576(3)	90	90	91.74(2)	4	39
73	$[Cd(pn)Ni(CN)_4]\cdot 0.36C_6H_{14}$	*A2/a*	13.987(2)	26.971(2)	7.595(2)	90	90	91.74(1)	4	39
74	$[Cd(pn)Ni(CN)_4]\cdot {}^1/_2C_5H_{12}$	*A2/a*	14.075(5)	27.026(3)	7.612(1)	90	90	89.82(1)	4	39
75	$[Cd(pn)Ni(CN)_4]\cdot {}^1/_2Et_2O$	*A2/a*	13.961(3)	26.998(3)	7.589(3)	90	90	89.16(1)	4	39
76	$[Cd(pn)Ni(CN)_4]\cdot {}^1/_2HOCH_2CH_2OH$	*A2/a*	13.897(6)	26.890(5)	7.607(1)	90	90	88.88(3)	4	39
77	$[Cd(pn)Ni(CN)_4]\cdot {}^1/_2Me(CH_2)_3Br$	*A2/a*	14.116(5)	26.839(4)	7.642(1)	90	90	90.19(3)	4	39
78	$[Cd(pn)Ni(CN)_4]\cdot 0.36Me(CH_2)_4Br$	*A2/a*	14.082(3)	26.943(7)	7.602(3)	90	90	90.43(3)	4	39
79	$[Cd(pn)Ni(CN)_4]\cdot {}^1/_2Cl_2CHCHCl_2$	*Pnma*	14.061(1)	27.192(3)	7.590(1)	90	90	90	4	39
80	$[Cd(pn)Ni(CN)_4]\cdot {}^1/_2MeCHClEt$	*Pnma*	14.183(1)	26.983(2)	7.615(1)	90	90	90	4	39
81	$[Cd(pn)Ni(CN)_4]\cdot {}^1/_2MeCHClCH_2Cl$	*Pnma*	14.104(3)	26.799(1)	7.657(1)	90	90	90	4	39
82	$[Cd(pn)Ni(CN)_4]\cdot {}^1/_2MeCHOHMe$	*Pnma*	14.157(3)	26.699(2)	7.586(2)	90	90	90	4	39
83	$[Cd(pn)Ni(CN)_4]\cdot {}^1/_2Cl(CH_2)_2Cl$	*Pnma*	13.916(3)	26.638(2)	7.631(4)	90	90	90	4	39
84	$[Cd(pn)Ni(CN)_4]\cdot {}^1/_2Br(CH_2)_2Br$	*Pnma*	13.981(1)	26.685(4)	7.698(2)	90	90	90	4	39
85	$[Cd(pn)Ni(CN)_4]\cdot {}^1/_2Cl(CH_2)_3Cl$	*Pnma*	14.104(7)	26.654(6)	7.645(6)	90	90	90	4	39
86	$[Cd(pn)Ni(CN)_4]\cdot {}^1/_2(Me_2CO\cdot H_2O)$	$Pn2_1a$	14.061(1)	27.192(3)	7.590(1)	90	90	90	4	39c
	$[Cd(danon \text{ or } dadcn)_2Ni(CN)_4]\cdot 2G$ clathrates									
87	$[Cd(danon)_2Ni(CN)_4]\cdot 2(2,6\text{-}Me_2C_6H_3NH_2)$	*P2/c*	14.460(2)	9.052(9)	17.190(2)	90	106.94(8)	90	2	40
88	$[Cd(danon)_2Ni(CN)_4]\cdot 2(2,3\text{-}Me_2C_6H_3NH_2)$	*P2/c*	14.446(1)	9.0513(5)	17.151(1)	90	106.403(6)	90	2	40
89	$[Cd(danon)_2Ni(CN)_4]\cdot 2(m\text{-}ClC_6H_4NH_2)$	*P2/c*	14.066(2)	9.010(3)	17.348(1)	90	104.936(7)	90	2	40
90	$[Cd(danon)_2Ni(CN)_4]\cdot 2(2\text{-}Cl\text{-}6\text{-}NO_2C_6H_3Me)$	*P2/c*	14.522(1)	8.9820(9)	17.294(1)	90	106.077(5)	90	2	40
91	$[Cd(danon)_2Ni(CN)_4]\cdot 2quin$	*P2/c*	14.380(4)	9.084(3)	17.051(1)	90	106.175(9)	90	2	40
92	$[Cd(danon)_2Ni(CN)_4]\cdot 2(3,5\text{-}Me_2C_6H_3NH_2)$	$P\bar{1}$	15.094(2)	8.626(1)	9.1290(8)	110.537(8)	92.472(9)	103.729(8)	1	40
93	$[Cd(danon)_2Ni(CN)_4]\cdot 2(2,4\text{-}Me_2C_6H_3NH_2)$	*C2/c*	28.59(1)	9.087(8)	17.239(7)	90	106.09(4)	90	4	40
94	$[Cd(danon)_2Ni(CN)_4]\cdot 2(o\text{-}MeC_6H_4NH_2)$	*C2/c*	28.12(1)	9.028(4)	17.18(1)	90	105.56(5)	90	4	40
95	$[Cd(danon)_2Ni(CN)_4]\cdot 2(m\text{-}C_6H_4NMe_2)$	*C2/c*	28.838(6)	9.060(6)	17.078(6)	90	106.37(2)	90	4	40

Table I. Continued

		Space group	a/Å	b/Å	c/Å	α/°	β/°	γ/°	Z	Ref.
96	$[Cd(danon)_2Ni(CN)_4]\cdot 2(p\text{-}MeC_6H_4NH_2)$	$C2/c$	29.32(2)	9.080(3)	16.961(7)	90	107.84(4)	90	4	40
97	$[Cd(danon)_2Ni(CN)_4]\cdot 2(2,5\text{-}Me_2C_6H_3NH_2)$	$C2/c$	29.20(2)	9.134(4)	17.107(5)	90	107.81(3)	90	4	40
98	$[Cd(danon)_2Ni(CN)_4]\cdot 2(4\text{-}Me\text{-}2\text{-}NO_2C_6H_3NH_2)$	$C2/c$	27.785(2)	8.946(1)	17.448(2)	90	104.066(46	90	4	40
99	$[Cd(danon)_2Ni(CN)_4]\cdot 2(4\text{-}CNC_6H_4NH_2)$	$P2_1/a$	8.436(2)	29.354(2)	19.008(3)	90	106.09(2)	90	2	40
100	$[Cd(danon)_2Ni(CN)_4]\cdot 2(2,4,6\text{-}Me_3C_6H_2NH_2)$	$C2/c$	58.643(3)	9.070(3)	17.171(3)	90	106.89(1)	90	8	40
101	$[Cd(dadcn)_2Ni(CN)_4]\cdot 2(m\text{-}MeC_6H_4NH_2)$	$P\bar{1}$	15.930(5)	8.237(3)	8.570(4)	101.07(4)	101.69(3)	89.67(4)	1	40
102	$[Cd(dadcn)_2Ni(CN)_4]\cdot 2(p\text{-}MeC_6H_4NH_2)$	$P\bar{1}$	16.009(4)	8.251(3)	8.787(8)	102.96(4)	101.79(4)	88.38(4)	1	40
103	$[Cd(dadcn)_2Ni(CN)_4]\cdot 2(3,4\text{-}Me_2C_6H_3NH_2)$	$P\bar{1}$	15.990(5)	8.334(3)	8.809(7)	103.11(4)	100.26(5)	89.47(4)	1	40
104	$[Cd(dadcn)_2Ni(CN)_4]\cdot 2PhNH_2$	$P\bar{1}$	14.045(5)	8.844(3)	9.304(4)	102.96(4)	101.79(4)	88.38(4)	1	40
105	$[Cd(dadcn)_2Ni(CN)_4]\cdot 2(o\text{-}MeC_6H_4NH_2)$	$P\bar{1}$	14.669(6)	8.980(3)	9.122(4)	109.06(4)	102.91(4)	78.04(4)	1	40
106	$[Cd(dadcn)_2Ni(CN)_4]\cdot 2(2,3\text{-}Me_2C_6H_3NH_2)$	$P\bar{1}$	14.76(2)	9.043(7)	9.124(6)	109.08(9)	102.28(9)	79.01(9)	1	40
107	$[Cd(dadcn)_2Ni(CN)_4]\cdot 2(2,6\text{-}Me_2C_6H_3NH_2)$	$P\bar{1}$	15.114(5)	9.032(6)	8.938(6)	108.55(4)	103.84(4)	81.33(4)	1	40
108	$[Cd(dadcn)_2Ni(CN)_4]\cdot 2(2,4\text{-}Me_2C_6H_3NH_2)$	$C2/c$	31.27(2)	9.031(4)	17.15(1)	90	109.39(5)	90	4	40
109	$[Cd(dadcn)_2Ni(CN)_4]\cdot 2(2\text{-}Cl\text{-}4\text{-}MeC_6H_3NH_2)$	$P\bar{1}$	15.135(3)	9.002(3)	9.238(3)	109.04(2)	98.34(2)	98.15(2)	1	40
110	$[Cd(dadcn)_2Ni(CN)_4]\cdot 2(2,5\text{-}Me_2C_6H_3NH_2)$	$P\bar{1}$	14.18(9)	9.03(3)	9.07(3)	108.8(2)	100.0(3)	99.0(3)	1	40
111	$[Cd(dadcn)_2Ni(CN)_4]\cdot 2quin$	$P\bar{1}$	16.069(2)	8.5095(6)	9.1079(9)	109.918(6)	102.327(8)	94.201(1)	1	40
	$[M(en)_2Ni(CN)_4]\cdot 2PhNH_2$, $[M(en)_2Ni(CN)_4]$, $[\{Cd(en)\}_2(en)\{Ni(CN)_4\}_2]\cdot 4PhOH$, and related complexes									
112	$[Ni(en)_2Ni(CN)_4]\cdot 2PhNH_2$	$P2_1/c$	9.452(3)	10.125(3)	13.440(3)	90	107.27(2)	90	2	41
113	$[Cu(en)_2Ni(CN)_4]\cdot 2PhNH_2$	$P2_1/c$	9.547(4)	10.621(5)	12.746(3)	90	107.89(2)	90	2	41
114	$[Zn(en)_2Ni(CN)_4]\cdot 2PhNH_2$	$P2_1/c$	9.550(3)	10.407(2)	13.026(2)	90	107.50(1)	90	2	41
115	$[Cd(en)_2Ni(CN)_4]\cdot 2PhNH_2$	$P2_1/c$	9.924(2)	10.545(3)	12.510(1)	90	107.63(1)	90	2	41
116	$[Ni(en)_2Ni(CN)_4]$	$P2_1/n$	7.104(3)	10.671(3)	9.940(2)	90	114.68(2)	90	2	42a
117	$[Cu(en)_2Ni(CN)_4]$	$P\bar{1}$	6.460(9)	7.230(10)	7.864(15)	106.81(13)	91.51(14)	106.94(12)	1	42b
118	$[Zn(en)_2Ni(CN)_4]$	$P2_1/n$	7.173(3)	10.606(4)	10.091(6)	90	115.91(4)	90	2	42c
119	$[Cd(en)_2Ni(CN)_4]$	$P2_1/n$	11.654(3)	9.270(3)	13.951(4)	90	106.26(1)	90	4	43
		$P2_1/n$	11.628(2)	9.257(1)	13.926(1)	90	106.285(7)	90	4	44
		$Pbca$	20.078(2)	9.140(2)	15.655(2)	90	90	90	8	44
120	$[\{Cd(en)\}_2(en)\{Ni(CN)_4\}_2]\cdot 4PhOH$	$P\bar{1}$	11.868(1)	13.030(1)	7.7113(6)	105.956(7)	94.951(8)	91.584(9)	1	41
121	$[Cd(en)Ni(CN)_4]$	$Pbna$	10.198(3)	11.229(2)	9.038(2)	90	90	90	4	45
122	$[Cd(en)_3][Ni(CN)_4]$	$C2/c$	16.699(2)	8.894(2)	14.320(2)	90	117.351(9)	90	4	44

Table I. Continued

		Space group	*a*/Å	*b*/Å	*c*/Å	*α*/°	*β*/°	*γ*/°	*Z*	Ref.
	Non-Hofmann-type [CdLNi(CN)$_4$]·*x*G clathrates									
123	[Cd(den)Ni(CN)$_4$]·$C_4H_8O_2$	*Pnma*	12.312(2)	12.480(3)	11.456(3)	90	90	90	4	38
124	[Cd(den)Ni(CN)$_4$]·$C_5H_{10}O$	*Pnma*	12.193(4)	11.603(6)	12.334(5)	90	90	90	4	38
125	[Cd(den)Ni(CN)$_4$]·*cyclo*-$C_6H_{11}OH$	*Pnma*	12.382(3)	11.330(3)	12.778(4)	90	90	90	4	38
126	[Cd(den)Ni(CN)$_4$]·*p*-$MeC_6H_4NH_2$	*I*2/*m*	12.141(3)	12.270(4)	11.320(4)	90	90.20(3)	90	4	38
127	[Cd(den)Ni(CN)$_4$]·$^1/_2$(den·PhMe)	*I*2/*m*	12.375(2)	12.939(2)	11.086(3)	90	90.24(2)	90	4	38
128	[Cd(den)$_2$Cd(den){Ni(CN)$_4$}$_2$]	*I*2/*m*	7.532(2)	13.012(3)	14.655(2)	90	93.51(2)	90	4	38
129	[Cd(mtn)Ni(CN)$_4$]·$^1/_2$(*cyclo*-C_6H_{12})	*P*4/*mbm*	14.209(2)	14.209	7.876(1)	90	90	90	4	46
130	[Cd(dmtn)Ni(CN)$_4$]·$^1/_2CHCl_3$	*P*4/*mbm*	14.284(1)	14.284	7.6596(4)	90	90	90	4	47
131	[Cd(tenH)$_2${Ni(CN)$_4$}$_2$]·4$PhNH_2$	$P2_1/n$	10.516(2)	10.594(3)	21.058(4)	90	92.24(2)	90	2	48
	Cd-Ni(CN)$_4$-pXdam series									
132	[Cd(pXdam)$_2$Ni(CN)$_4$]·*m*-$MeC_6H_4NH_2$	$P\bar{1}$	8.149(2)	9.577(1)	9.865(2)	81.03(1)	94.08(2)	106.08(1)	1	37
133	[Cd(pXdam)$_2$Ni(CN)$_4$]·(PhOH·H_2O)	$P2_1/m$	8.615(3)	17.568(2)	9.950(2)	90	105.30(2)	90	2	37
134	[Cd(pXdam)$_2$Ni(CN)$_4$]·quin	$P2_1/m$	8.505(1)	17.737(1)	10.106(1)	90	102.64(1)	90	2	37
135	[Cd$_2$(pXdam)$_3${Ni(CN)$_4$}$_2$]·2C_4H_5N	*C*2/*c*	19.820(2)	7.738(2)	31.213(1)	90	109.138(5)	90	4	37
136	[Cd($PhNH_2$)$_2$(pXdam)Ni(CN)$_4$]	*C*2/*c*	22.240(1)	9.254(1)	16.241(1)	90	130.668(3)	90	4	37
137	(pXdamH_2)[Ni(CN)$_4$]	$P\bar{1}$	7.392(3)	7.921(2)	6.247(1)	90.89(2)	101.49(2)	70.92(2)	1	37
	CdNi(CN)$_4$·2[$NH_2(CH_2)_nNH_2$]·*h*H_2O complexes									
138	[Cd(tn)$_2$Ni(CN)$_4$]	$P2_1/n$	10.474(2)	13.696(4)	15.644(2)	90	92.90(2)	90	4	44
139	[Cd(dabtn)$_2$Ni(CN)$_4$]·2H_2O	$P\bar{1}$	8.253(2)	8.527(1)	7.921(2)	97.84(2)	107.48(2)	104.39(1)	1	44
140	[Cd(daptn)$_2$Ni(CN)$_4$]·H_2O	$C222_1$	9.794(2)	12.961(3)	16.049(3)	90	90	90	4	44
141	[Cd(H_2O)$_2$(dahxn)$_2$][Ni(CN)$_4$]	$P\bar{1}$	8.470(2)	9.750(3)	8.114(3)	111.59(2)	106.68(2)	71.53(2)	1	44
142	[Cd(dahpn)$_2$Ni(CN)$_4$]·H_2O	*Pnma*	9.621(4)	38.925(6)	19.953(4)	90	90	90	12	44
143	[Cd(danon)$_2$Ni(CN)$_4$]	*C*2/*c*	20.839(6)	9.141(4)	15.206(4)	90	105.58(2)	90	4	44
144	[Cd(mea)(daptn)Ni(CN)$_4$]	*C*2/*c*	13.479(5)	10.197(3)	13.954(5)	90	115.06(2)	90	4	49
145	[Cd(mea)(dahxn)Ni(CN)$_4$]·H_2O	*C*2/*c*	9.247(2)	13.434(6)	16.367(3)	90	105.60(2)	90	4	49
	Phenylalkylammonium tetracyanonickelate(II)									
146	[{$Ph(CH_2)_2NH_3$}$_2$Ni(CN)$_4$]	$P\bar{1}$	8.850(4)	8.825(4)	23.000(8)	93.97(4)	98.77(4)	64.75(2)	3	50
147	[{$Ph(CH_2)_2NH_3$}$_2$Ni(CN)$_4$]·$^2/_3H_2O$	$P\bar{1}$	9.159(5)	8.967(4)	22.583(5)	91.42(3)	90.52(3)	53.45(3)	3	50
148	[{$Ph(CH_2)_2NH_3$}$_2$Ni(CN)$_4$]·C_6H_6	*C*2/*c*	15.747(2)	9.152(3)	19.337(2)	90	103.53(1)	90	4	50

Table I. Continued

		Space group	*a*/Å	*b*/Å	*c*/Å	*α*/°	*β*/°	*γ*/°	*Z*	Ref.
149	$[\{Ph(CH_2)_2NH_3\}_2Ni(CN)_4]\cdot PhNMe_2$	*Pccn*	16.329(1)	8.785(1)	20.378(3)	90	90	90	4	50
150	$[\{Ph(CH_2)_2NH_3\}_2Ni(CN)_4]\cdot CHCl_3$	$P\bar{1}$	8.753(1)	8.677(1)	18.912(2)	103.11(1)	102.21(1)	67.18(1)	2	50
151	$[\{Ph(CH_2)_2NH_3\}_2Ni(CN)_4]\cdot p\text{-}MeC_6H_4NH_2$	$P\bar{1}$	9.310(4)	9.263(3)	19.122(4)	98.99(2)	98.35(3)	61.09(2)	2	50
152	$[\{Ph(CH_2)_3NH_3\}_2Ni(CN)_4]\cdot C_6H_6$	$P\bar{1}$	8.992(2)	8.726(2)	10.307(4)	93.32(3)	96.96(3)	62.12(1)	1	50
153	$[\{Ph(CH_2)_4NH_3\}_2Ni(CN)_4]\cdot {}^2/_3H_2O$	$P\bar{1}$	9.346(2)	8.950(2)	27.117(10)	95.28(3)	90.41(2)	61.38(1)	3	50
	Miscellaneous									
154	$(dadcnH)_2[Ni(CN)_4]$	$P\bar{1}$	9.437(3)	10.094(3)	9.205(3)	110.16(2)	112.72(3)	69.16(2)	1	51
155	[meaH·(18-Crown-6)]$_2$[Ni(CN)$_4$]	$P2_1/n$	10.458(2)	8.267(3)	24.045(2)	90	94.09(1)	90	2	51
156	[Cd(2,2'-bpy)Ni(CN)$_4$]	$C2/c$	6.790(1)	17.238(1)	12.464(1)	90	91.14(1)	90	4	52

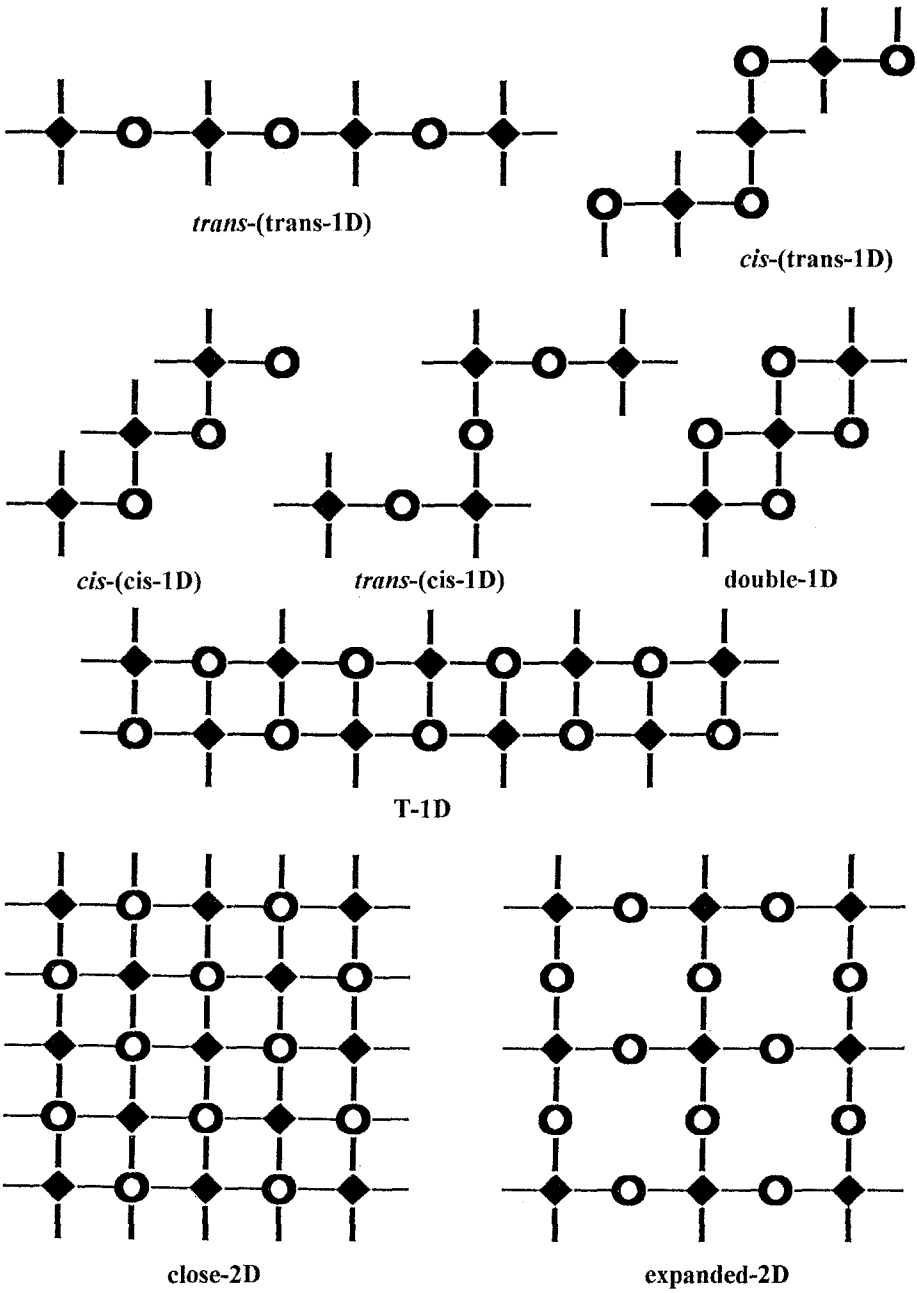

Figure 4. Catenation modes of $Ni(CN)_4$. Solid square with four bars: $Ni(CN)_4$; open circle: second coordination centre. From left top to right bottom: *trans*-(trans-1D), *cis*-(trans-1D), *cis*-(cis-1D), *trans*-(cis-1D), double-1D, T-1D, close-2D, and expanded-2D.

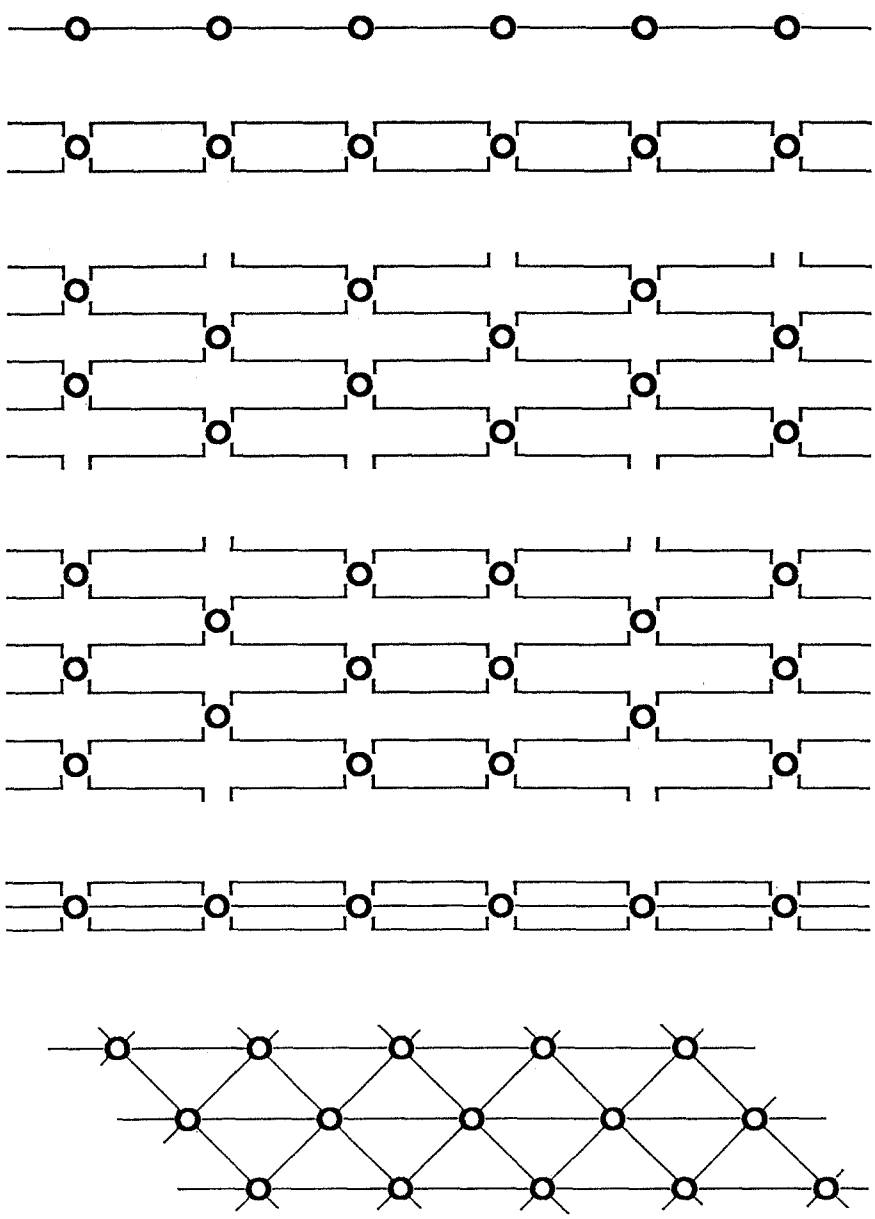

Figure 5. Catenation modes of bidentate ligand **aa** between second coordination centres (open circles). From top to bottom: single-1D in M(**aa**) composition; double-1D in M(**aa**)$_2$; single-2D in M(**aa**)$_2$; single,double-2D in M(**aa**)$_2$; triple-1D in M(**aa**)$_3$; and triangle-2D in M(**aa**)$_3$.

A 2D ice structure is found in the interlayer space of the Hofmann-H_2O-type hydrates $[Fe(H_2O)_2Ni(CN)_4]\cdot 4H_2O$ **14** and $[Cd(H_2O)_2Ni(CN)_4]\cdot 4H_2O$ **15;** for the latter the single crystal structure was reported independently by two groups [21,22], although Ham *et al.* [22] did not describe the 2D network of the water molecules as

2D ice. As shown in Figure 6, the host 2D network has the same topology as that of the Hofmann-type, but the NH_3 is replaced by H_2O. The interlayer space between the much puckered 2D metal complex networks is occupied by the intercalated H_2O molecules which are hydrogen-bonded to the Cd-ligated H_2O to form the 2D network of H_2O molecules with the hexagonal meshes in boat form configurations. Since each O atom is able to provide two H atoms and two lone pairs for hydrogen-bond formation, three of the four crystallographically independent O atoms should be unsaturated in the use of H atoms and lone pairs with regard to the hydrogen bonds; the remaining one is ligated to the Cd atom using one lone pair for the coordination and the other lone pair and two H atoms for network formation. Assuming each edge of the hexagons involve one H atom and lone pair, three H atoms and one lone pair are missing in the network [21].

3.3. HOFMANN-DIAM-TYPE 3D STRUCTURE

The Hofmann-diam-type $[CdLNi(CN)_4]\cdot xG$ clathrates **36–71** where L is a bidentate bridging ligand such as diaminoalkane, xylylenediamine, etc. have the same topology of the hosts as the stacked 2D networks of the Hofmann-type which are spanned successively by a *catena*-μ-(Cd—L—)$_\infty$ linkage to give a 3D latticework. With regard to α,ω-diaminoalkanes $NH_2(CH_2)_nNH_2$ as L, the 3D structures have been obtained for n = 2–9, among which well-defined single crystal structures for odd-n hosts, n = 3, 5, 7 [36m] and 9 [36k], have recently been reported in comparison with those for even-n. The structural features of the Hofmann-α,ω-diaminoalkane-type clathrates for n = 3 have been interpreted in our series of papers [36]. *p*-Xylylenediamine [37] and piperazine (den) [38] give the Hofmann-diam-type host structures for certain guests, e.g., $[Cd(pXda)Ni(CN)_4]\cdot o\text{-}MeC_6H_4NH_2$ **61**, $[Cd(den)Ni(CN)_4]\cdot C_6H_6$ **62**, etc.

The above-mentioned Hofmann-type and Hofmann-diam-type structures all have a close-2D network (cf. Figure 4) with the square mesh spanned by CN groups. $[Ni(CN)_4]^{2-}$ behaves as a cross joint using the four N-ends, each of which is linked to the second coordination centre also behaving as a cross joint in the close-2D network. The bridging ligand in the Hofmann-diam-type behaves as a *catena*-μ linkage builder with the second coordination centre Cd to give an infinite single skeletal chain —[Cd—L—]$_\infty$, viz., in the single-1D catenation mode. However, in the course of the investigations to develop the Hofmann-diam-type by strategy (2), we have obtained a great variety of multi-dimensional supramolecular structures involving $[Ni(CN)_4]^{2-}$ and the L behaving differently from the Hofmann-type and Hofmann-diam-type; both novel host structures of clathrates and polymeric complexes without guests have been obtained. Their structural features are outlined in the following sections.

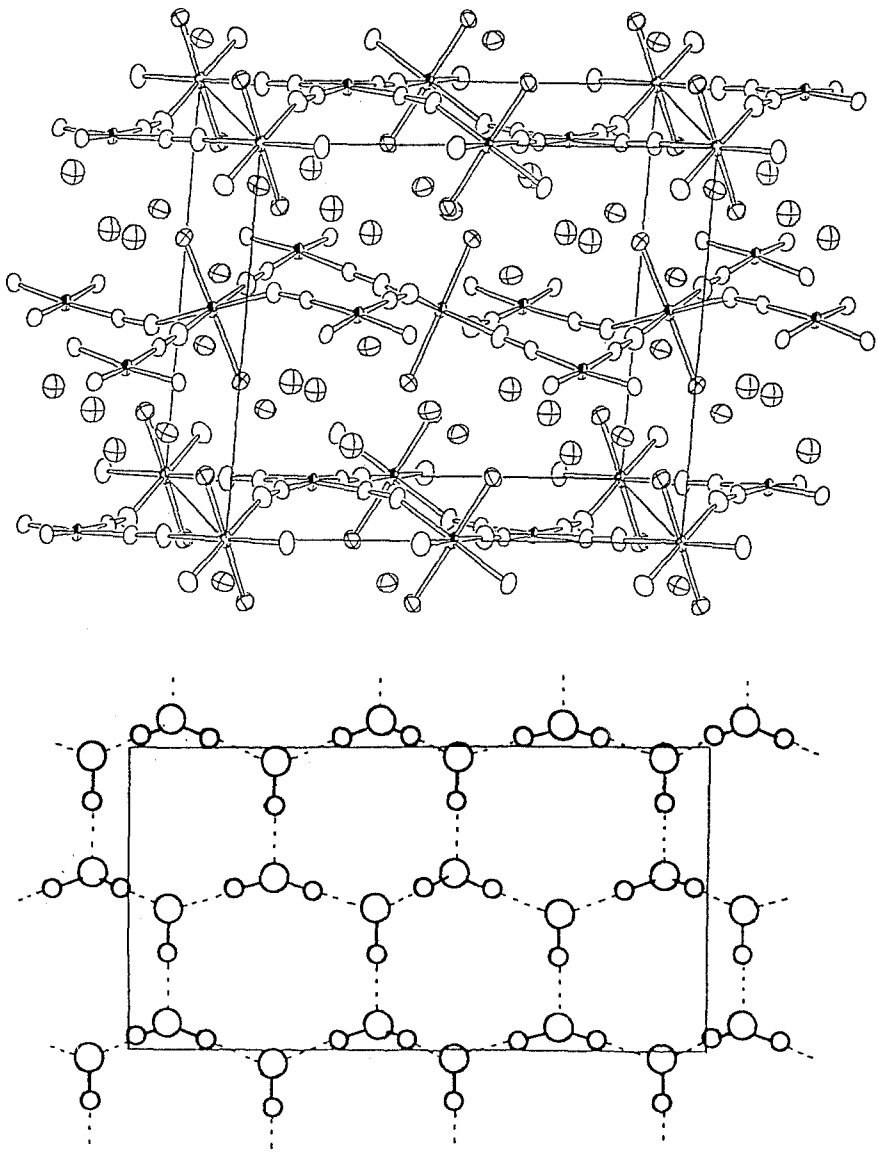

Figure 6. Structure of $[Cd(H_2O)_2Ni(CN)_4]\cdot 4H_2O$ **15**. *Top*: a perspective view of the unit cell with the puckered close-2D network of $[CdNi(CN)_4]$ stacked along the *a* axis intercalating H_2O molecules; O atoms are shown with anisotropic peripheries. *Bottom*: 2D network of hydrogen-bonded H_2O molecules with tentative positions of H atoms.

3.4. ISOMERISM OF HOST STRUCTURES

3.4.1. $[Cd(pn)Ni(CN)_4]$ *hosts*

The host complex $[Cd(pn)Ni(CN)_4]$, whose composition is the same as that of the Hofmann-pn-type $[Cd(pn)Ni(CN)_4]\cdot{}^3/_2C_4H_5N$ **39**, **40**, provides channel cavities

Table II. [Cd(pn)Ni(CN)4]·xG clathrates **72–86**.

Channel type	Space group	xG		
U (snake-like)	*A2/a*	$0.32C_7H_{16}$ (**72**)	$0.36C_6H_{14}$ (**73**)	$0.5C_5H_{12}$ (**74**)
(urea-host-like)		$0.5Et_2O$ (**75**)	$0.5HO(CH_2)_2OH$ (**76**)	$0.5Me(CH_2)_3Br$ (**77**)
		$0.36Me(CH_2)_4Br$ (**78**)		
T (nodal)	*Pnma*	$0.5Cl_2CHCHCl_2$ (**79**)	0.5MeCHClEt (**80**)	$0.5MeCHClCH_2Cl$ (**81**)
(thiourea-host-like)		0.5MeCHOHMe (**82**)	$0.5Cl(CH_2)_2Cl$ (**83**)	$0.5Br(CH_2)_2Br$ (**84**)
		$0.5Cl(CH_2)_3Cl$ (**85**)		
	$Pn2_1a$	$0.5(Me_2CO{\cdot}H_2O)$ (**86**)		

for aliphatic guests by adopting different structures in the catenation modes of the $Ni(CN)_4$ entities and in the ligating behaviour of the pn: **72–86** [39]. In comparison with the Hofmann-pn-type, the close-2D network is twisted into the combination of a double-1D extension and folded expanded-2D network at every Cd to which the pn is chelated. As shown in Figure 7, the channel cavity is surrounded by the double-1D extension of $>[Ni<(CN—Cd—NC)_2>]_\infty$ at the top and the bottom and by the $Ni[—CN—\{Cd(pn)\}—_{1/4}]_4$ moiety of the folded expanded-2D network at the sides. The pn chelate ring is arranged point-symmetrically to give a snake-like bending of the channel in the hosts of **72–78** with straight-chain aliphatic guests, whereas the arrangement is mirror-symmetric to give a nodal structure in the hosts of **69–86** with branched-chain and dihalogeno-substituted aliphatic guests. These channel structures are comparable with those of the spiral channel in the urea–host inclusion compounds and the nodal channel in the thiourea–host compounds (Table II). Thus, the [Cd(pn)Ni(CN)4] complex exhibits the three different host structures depending on the geometry of the guest molecules.

3.4.2. [Cd(danon)$_2$Ni(CN)$_4$] *and* [Cd(dadcn)$_2$Ni(CN)$_4$] *hosts*

The Hofmann-diam-type clathrates have been obtained for the α,ω-diaminoalkanes, $NH_2(CH_2)_nNH_2$, up to n = 9 [Cd(danon)Ni(CN)4]·$^1/_2$(o-$C_6H_4Me_2$) **60** [36k], so far examined in our laboratory. Under similar preparation conditions, danon (n = 9) and dadcn (n = 10) afford clathrates with the composition [Cd(danon or dadcn)$_2$Ni(CN)$_4$]·2G **87–111** for a number of aromatic guests, mainly of aniline derivatives [40], in which composition the number of diaminoalkane ligands is doubled in comparison with the Hofmann-diam-type. As illustrated for [Cd(dadcn)$_2$Ni(CN)$_4$]·2(2,3-$Me_2C_6H_3NH_2$) **106** in Figure 8, the host complex has a layer structure of Cd atoms spanned by bridging diam ligands, the layer being additionally spanned by ambidentate $Ni(CN)_4$ moieties to afford wide and flat channels for the guest molecules. As listed in Table III, catenation modes for the diam ligand and $Ni(CN)_4$ depend upon the guest molecule. With regard to the diam ligand, double-1D, single-2D and single,double-2D catenations are observed

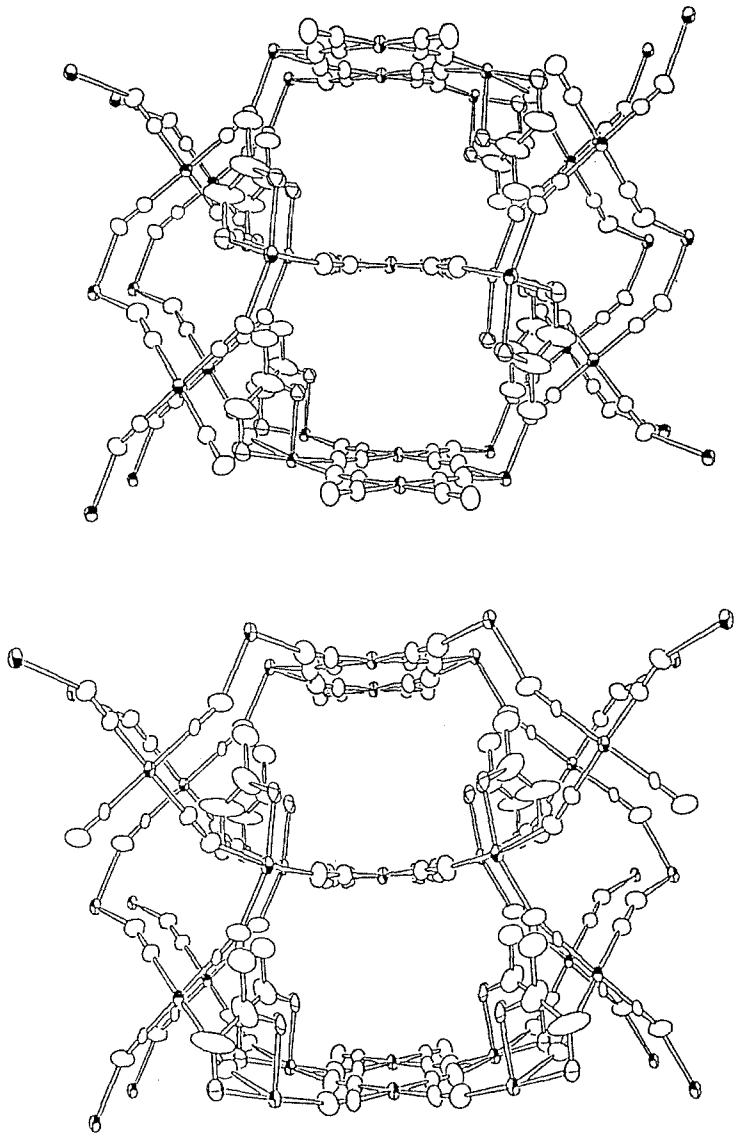

Figure 7. Urea-like and thiourea-like hosts of $[Cd(pn)Ni(CN)_4]$. *Top*: cross section of the channels with a snake-like bending in which channel the pn chelate rings are arranged point-symmetrically. *Bottom*: cross section of the channels with nodes of the pn chelate rings arranged mirror-symmetrically.

for danon, double-1D and single-2D for dadcn; $Ni(CN)_4$ behaves as trans-1D and cis-1D linkage builders. However, the host structures are substantially similar to one another with the layers of double-1D belts or single-2D or single,double-2D network spanned by the $Ni(CN)_4$ moieties. The reason why the linkage mode varies with the guest molecule is uncertain.

Table III. Catenation modes of diam and $Ni(CN)_4$ in $[Cd(danon\ or\ daden)_2Ni(CN)_4]\cdot 2G$ **87–111**.

	$[Cd(danon)_2Ni(CN)_4]\cdot 2G$		$[Cd(dadcn)_2Ni(CN)_4]\cdot 2G$	
G	danon	$Ni(CN)_4$	dadcn	$Ni(CN)_4$
$PhNH_2$			double-1D	trans-1D (**104**)
o-$MeC_6H_4NH_2$	single-2D	cis-1D (**94**)	double-1D	trans-1D (**105**)
m-$MeC_6H_4NH_2$			double-1D	trans-1D (**101**)
p-$MeC_6H_4NH_2$			double-1D	trans-1D (**102**)
m-$Me_2C_6H_4$	single-2D	cis-1D (**95**)		
p-$Me_2C_6H_4$	single-2D	cis-1D (**96**)		
m-$ClC_6H_4NH_2$	double-1D	cis-1D (**89**)		
4-$CNC_6H_4NH_2$	single-2D	trans-1D (**99**)		
2,3-$Me_2C_6H_3NH_2$	double-1D	cis-1D (**88**)	double-1D	trans-1D (**106**)
2,4-$Me_2C_6H_3NH_2$	single-2D	cis-1D (**93**)	single-2D	cis-1D (**108**)
2,5-$Me_2C_6H_3NH_2$	single-2D	cis-1D (**97**)	single-2D	trans-1D (**110**)
2,6-$Me_2C_6H_3NH_2$	double-1D	cis-1D (**87**)	double-1D	trans-1D (**107**)
3,4-$Me_2C_6H_3NH_2$			double-1D	trans-1D (**103**)
3,5-$Me_2C_6H_3NH_2$	double-1D	trans-1D (**92**)		
4-Me-2-$NO_2C_6H_3NH_2$	single-2D	cis-1D (**98**)		
2-Cl-6-$NO_2C_6H_3Me$	double-1D	cis-1D (**90**)		
2-Cl-4-$MeC_6H_3NH_2$			single-2D	trans-1D (**109**)
quin (C_9H_7N)	double-1D	cis-1D (**91**)	single-2D	trans-1D (**111**)
2,4,6-$Me_3C_6H_2NH_2$	single,double-2D	cis-1D (**100**)		

3.5. VARIEGATED HOST STRUCTURES INVOLVING THE $Ni(CN)_4$ ENTITY

3.5.1. $[Cd(en)_2Ni(CN)_4]\cdot 2PhNH_2$ *and related clathrates*

The Hofmann-en-type host $[Cd(en)Ni(CN)_4]$ appears to be unable to accommodate aniline molecule as a guest because the span length of the en between the close-2D networks, ca. 8 Å, is not long enough for the molecular dimension along the apparent twofold axis, ca. 7 Å in the scale of van der Waals contact. The aniline clathrates $[M(en)_2Ni(CN)_4]\cdot 2PhNH_2$ (M = Ni, Cu, Zn or Cd) **112–115**, the composition being similar to those of the danon- and dadcn-bridged hosts described in Section 3.4.2., have a 1D chain structure of the host complex constructed of the bis-en-chelated M and $Ni(CN)_4$ behaving as a trans-1D linkage builder [41]. The interchain space among the $[—M(en)_2—$*trans*$-NC—Ni(CN)_2—CN—]_\infty$ 1D chains is separated by the protrusion of the en chelate-rings to generate the cavity for the guest aniline molecule. Similar 1D chain metal complex structures are obtained without guests $[M(en)_2Ni(CN)_4]_\infty$ for M = Ni **116**, Cu **117** and Zn **118** with the catenation mode of $Ni(CN)_4$ in trans-1D [42] as well as in $[Ni(en)_2Pd(CN)_4]$ [53], whereas for Cd **119** the mode is cis-1D [43,44].

Although no well-defined single crystal structures are yet available for aniline- and phenol-guest Hofmann-type clathrates, powder X-ray diffraction data suggest they are isostructural. However, when the guest is phenol in the Cd-en-$Ni(CN)_4$ system, the obtained clathrate, $[\{Cd(en)\}_2(en)\{Ni(CN)_4\}_2]\cdot 4PhOH$ **120**, exhibits a

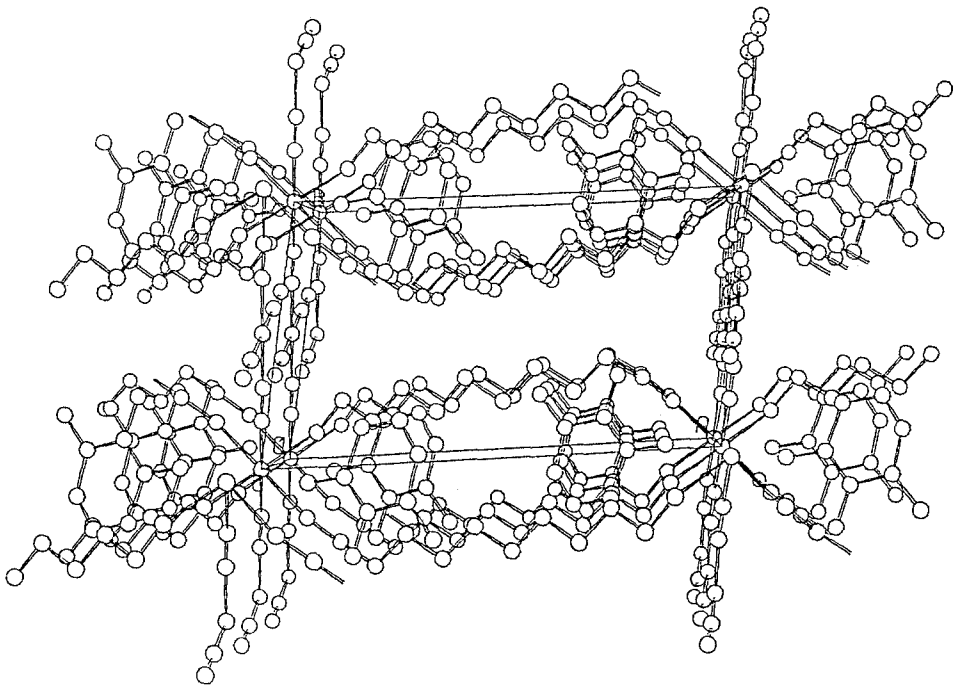

Figure 8. Structure of $[Cd(dadcn)_2Ni(CN)_4]\cdot 2(2,3\text{-}Me_2C_6H_3NH_2)$ **106** as a view along the *c* axis. Cd on the origin and its equivalents are linked along the *a* axis by double-1D catenation of dadcn; the double-1D belts are interconnected through $Ni(CN)_4$ in trans-1D catenation along the *bc* plane; the guests are intercalated between the double-1D belts stacked along the *c* axis.

complicated 3D host structure [41], as shown in Figure 9. There are two kinds of en and $Ni(CN)_4$, different in catenation modes. The Cd atom is chelated by one en and linked to another Cd by the other en; one $Ni(CN)_4$ participates in the double-1D catenation involving the Cd atoms; the double-1D linkages are linked by the other $Ni(CN)_4$ behaving as an ambidentate *trans-*μ ligand.

3.5.2. $[Cd(den)Ni(CN)_4]\cdot x$G *clathrates of non-Hofmann-diam-type and related structures*

3D host structures different in topology from the Hofmann-den-type are obtained with some alicyclic and aromatic guests such as 1,4-dioxane, tetrahydropyran, cyclohexanol, *p*-toluidine, etc. **123–128** [38].

As shown in Figure 10 for the clathrate $[Cd(den)Ni(CN)_4]\cdot{}^1/_2(den\cdot PhMe)$ **127** and the non-guest complex $[Cd(den)_2Cd(den)\{Ni(CN)_4\}_2]$ **128**, the 3D metal complex structures involve two sets of the expanded-2D networks interconnected at the Cd atoms. In the clathrate host the Cd atoms in the expanded-2D networks are additionally spanned by den ligands which behave as a single-1D linkage builder.

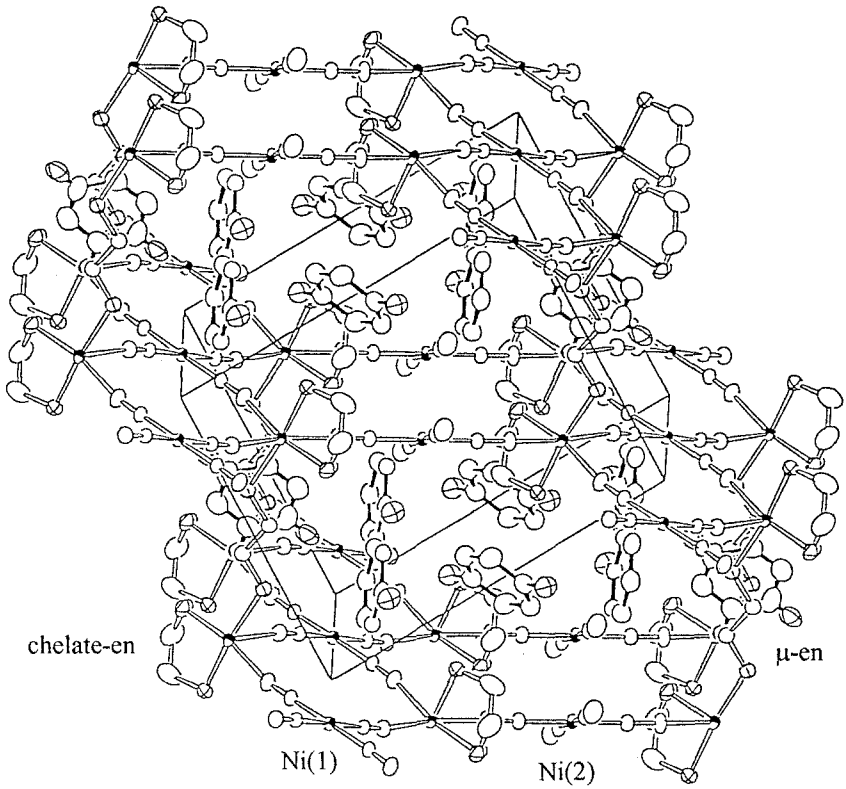

Figure 9. Structure of $[\{Cd(en)\}_2(en)\{Ni(CN)_4\}_2]\cdot 4PhOH$ **120**. Cd and Ni are shown with anisotropic sections; skeleton of the guest with solid bonds; O of PhOH with anisotropic peripheries including those disordered from the symmetry requirements; Ni(1) in the double-1D catenation and Ni(2) in the *trans*-μ bridging.

The exemplified clathrate accommodates both aromatic toluene and alicyclic den as guests in a 1:1 ratio, being a comparatively rare case of a mixed-guest clathrate. The structure of the exemplified complex is derived from an apparent liberation of the toluene guest from the toluene-den clathrate; the bridging den and the guest den in the former turn to a unidentate den and bridging den in the latter, respectively.

3.5.3. $[Cd(mtn)Ni(CN)_4]\cdot{}^1/_2G$ *clathrates*

A typical combination of expanded-2D and double-1D catenation of $Ni(CN)_4$ is seen in the 3D hosts of $[Cd(mtn)Ni(CN)_4]\cdot{}^1/_2(cyclo\text{-}C_6H_{12})$ **129** [46] and $[Cd(dmtn)Ni(CN)_4]\cdot{}^1/_2CHCl_3$ **130** [47] clathrates. The flat expanded-2D network in which mtn- or dmtn-chelated Cd intervenes between the $Ni(CN)_4$ entities extends on the [001] plane of the tetragonal unit cell; the Cd atoms are involved in the double-1D extension with the other $Ni(CN)_4$ entities running along the {220} plane. A square box-like cavity accommodating the guest is formed between the expanded-2D networks walled by the double-1D extensions (Figure 11).

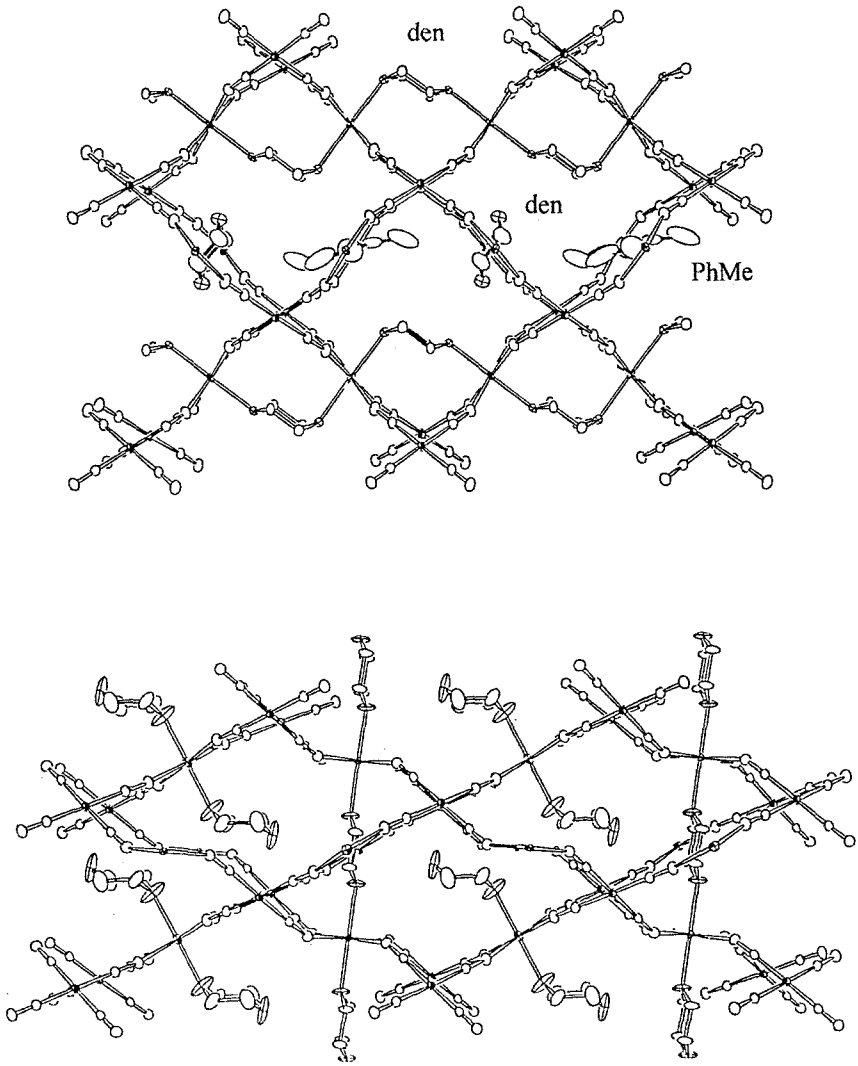

Figure 10. Structures of $[Cd(den)Ni(CN)_4]\cdot{}^1/_2(den\cdot PhMe)$ clathrate **127** (top) and the non-guest complex $[Cd(den)_2Cd(den)\{Ni(CN)_4\}_2]$ **128** (bottom). The structure of **128** can be derived from that of **127** by the following virtual process: delete the guest PhMe in **127**; cut off the single-1D catenation of den in **127** to give *trans*-bis-coordination of unidentate dens in **128**; span the Cd atoms cut off of the single-1D catenation in **127** by the guest den to give new single-1D catenation in **128**.

3.5.4. $[Cd(tenH)_2\{Ni(CN)_4\}_2]\cdot 2PhNH_2$

In contrast with the ambidentate bridging behaviour of en $NH_2CH_2CH_2NH_2$ and den $NH(CH_2CH_2)_2NH$, ten $N(CH_2CH_2)_3N$ behaves unidentately as the monoprotonated ligand $tenH^+$ in $[Cd(tenH)_2\{Ni(CN)_4\}_2]\cdot 4PhNH_2$ **131** (Figure 12) [48]. The $Ni(CN)_4$ behaves as a trans-1D linkage builder but the chains are intercon-

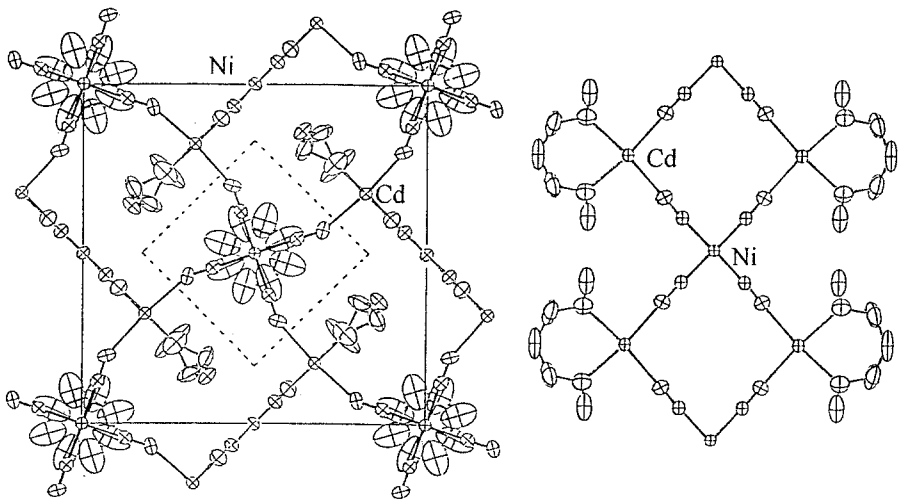

Figure 11. Structure of $[Cd(mtn)Ni(CN)_4]\cdot{}^1/_2(cyclo\text{-}C_6H_{12})$ **129** .The expanded 2D network extends on the *ab* plane (left) involving mtn-chelated Cd atoms which join the double-1D extension at the side of the cavity (right). The guest *cyclo*-C_6H_{12} molecule and the methyl group of mtn are disordered.

nected at every Cd atom to extend a pseudo-expanded-2D network from which bulky tenH ligands protrude into the interlayer space between the 2D networks to give a host structure resembling that of the Hofmann-type. The interlayer cavity is walled not only by the bulky tenH but also the unbridged CN groups protruding from the expanded-2D network. The expanded mesh size is thus counterbalanced to imprison the guest aniline molecule in the interlayer cavity.

3.5.5. Cd-$Ni(CN)_4$-pXdam-G *system*

Besides the Hofmann-pXdam-type clathrate $[Cd(pXdam)Ni(CN)_4]\cdot$ *o*-$MeC_6H_4NH_2$ **61**, clathrates and complexes **132–137** with a variety of compositions and structures crystallise under similar experimental conditions; a few structures are exemplified in Figure 13 [37].

Double-1D $>[Cd<(pXdam)_2>]_\infty$ catenation is seen in $[Cd(pXdam)_2Ni(CN)_4]\cdot$*m*-$MeC_6H_4NH_2$ **132**, $[Cd(pXdam)_2Ni(CN)_4]\cdot(PhOH\cdot H_2O)$ **133** and $[Cd(pXdam)_2Ni(CN)_4]\cdot$quin **134**; the pXdam is doubled in their compositions in contrast to the Hofmann-pXdam-type. The close-2D network in the Hofmann-pXdam-type host is broken into trans-1D in **132** but into cis-1D in **133** and **134**. In the host structure of $[Cd_2(pXdam)_3\{Ni(CN)_4\}_2]\cdot 2C_4H_5N$ **135** three single spans of pXdam extend from one Cd to three Cd atoms, the respective Cd atoms being interconnected further by two $Ni(CN)_4$ moieties, one as a cis-1D and another as a double-1D linkage builder, to afford a cage cavity for the guest pyrrole molecule. Aniline is not accommodated as a guest but ligates to the Cd at *trans* positions in complex

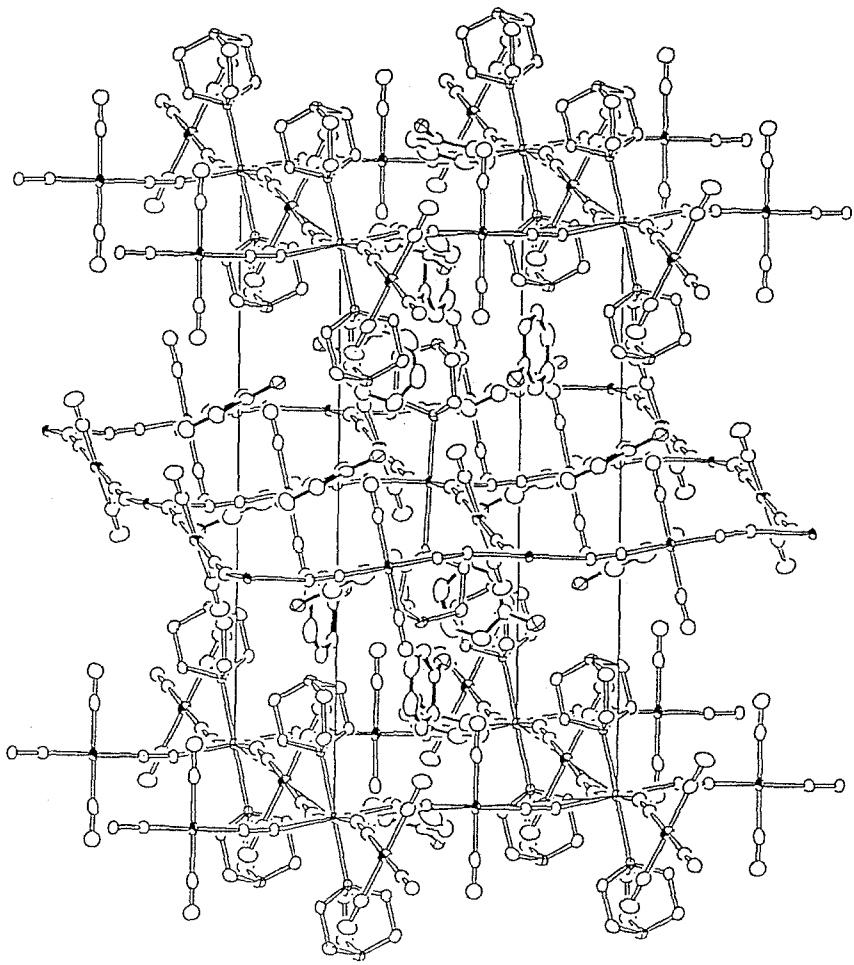

Figure 12. $[Cd(tenH)_2\{Ni(CN)_4\}_2]\cdot 4PhNH_2$ **131**. The 2D network is spanned by the *trans*-1D catenation of $Ni(CN)_4$ among the octahedral Cd atoms, each of which is coordinated by a pair of tenH ligands at trans positions. Skeleton of the guest $PhNH_2$ is shown with solid bonds.

$[Cd(PhNH_2)_2(pXdam)Ni(CN)_4]$ **136** whose 3D structure is constructed of single-2D catenation for pXdam and cis-1D for $Ni(CN)_4$. A *p*-xylylenediammonium salt $(pXdamH_2)[Ni(CN)_4]$ **137** crystallises from the mother solution without guest similar to the case of $(dadcnH)_2[Ni(CN)_4]$ **154**, although the latter is the salt of the monoprotonated diamine [51].

3.6. Cd-$Ni(CN)_4$-DIAM SYSTEMS

In contrast to the 3D hosts of the Hofmann-diam-type clathrates $[CdNH_2(CH_2)_nNH_2Ni(CN)_4]\cdot xG$ from n = 2 to 9 with the same topology, the complexes of the general formula $CdNi(CN)_4\cdot 2[NH_2(CH_2)_nNH_2]\cdot hH_2O$ (h = 0,

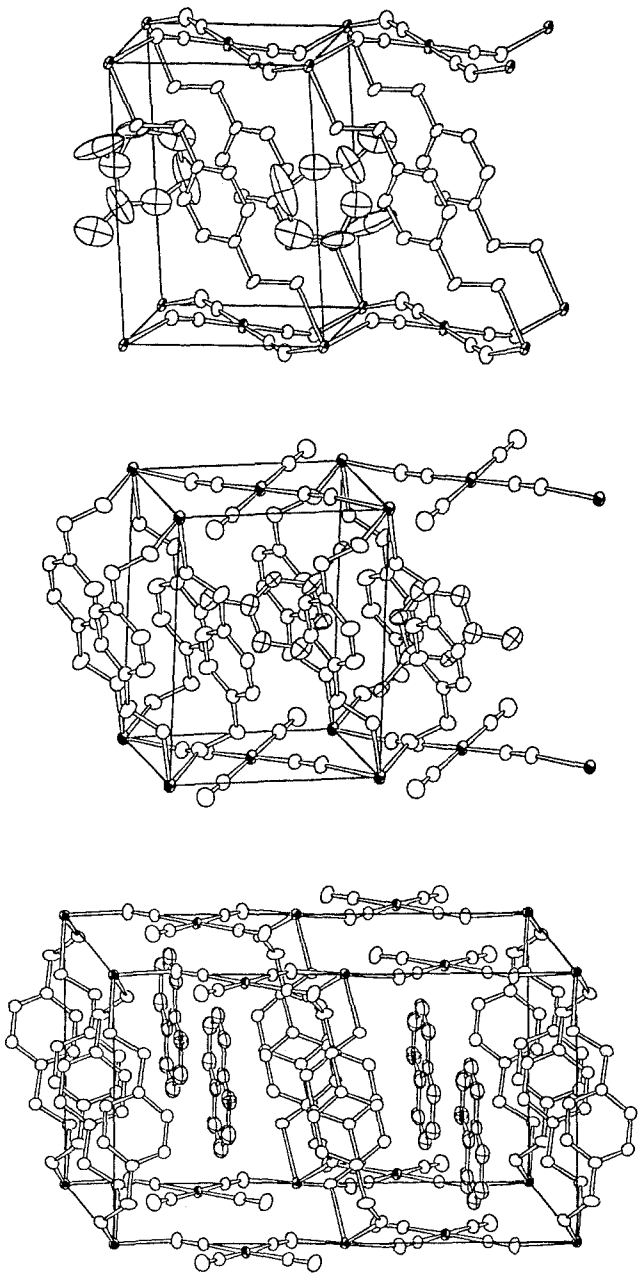

Figure 13. Structures of $[Cd(pXdam)Ni(CN)_4]\cdot o\text{-}MeC_6H_4NH_2$ **61** with the Hofmann-pXdam-type host (top), $[Cd(pXdam)_2Ni(CN)_4]\cdot m\text{-}MeC_6H_4NH_2$ **132** with the host of double-1D pXdam and trans-1D $Ni(CN)_4$ spans (middle), and $[Cd(pXdam)_2Ni(CN)_4]\cdot$quinoline **134** with the host of double-1D pXdam and *trans*-(cis-1D) $Ni(CN)_4$ spans.

1 or 2) without accommodation of bulky guests, have variegated structures different in the catenation behaviour of the diamine and the $Ni(CN)_4$ [44]. The α,ω-diaminoalkanes from $n = 2$ to 7, and 9, though missing for 8, give a great variety of multi-dimensional structures; the diamine behaves as chelating, or bridging in double-1D, single-2D or single-3D mode, and the tetracyanonickelate(II) anion in cis-1D or trans-1D, or as a discrete anion in the crystal structure.

As illustrated in Figure 14, en is chelated in the bis-en complex **119;** two polymorphs, monoclinic and orthorhombic, have been obtained. The $Ni(CN)_4$ moieties involved in the cis-1D catenation are arranged in *cis* positions with respect to the Cd atom in the 1D chain structure; the mode is *cis*-(cis-1D). The polymorphism is due to the difference in the relative array of the 1D chains in the crystal structure. The tris-en complex **122** has the structure of an ionic crystal, namely the packing of $[Cd(en)_3]^{2+}$ and $[Ni(CN)_4]^{2-}$. The mono-en complex $[Cd(en)Ni(CN)_4]$ **121** is left after thermal liberation of the guest molecules from the Hofmann-en-type clathrate as a crystalline powder; the isomorphous crystal is also obtained from an aqueous solution at lower pH (by increasing the pH, the bis- and thereafter the tris-en complexes crystallise out). The en turns from a bridging ligand in the clathrate host to a chelating one in the complex upon the liberation of the guest; the close-2D network is transformed to a 3D lattice in which one $Ni(CN)_4$ is connected to four en-chelated Cd atoms [45].

The tn-bridged complex **138** has a 2D network structure with single-2D catenation of the tn ligands, but the Cd—tn—Cd bridge along one direction is additionally spanned by *cis*-(cis-1D) catenation of the $Ni(CN)_4$ moiety. A bis-tn-chelate structure of $Cd(tn)_2$, like $Cd(en)_2$, appears to be too bulky to keep the crystal packing dense like that in **119** and **120**. The skeletal length of dabtn in **139** is too long not only for chelating ligation but also for formation of a single-2D network adjustable with cis-1D catenation of $Ni(CN)_4$; the double-1D catenation gives a $Cd<(dabtn)_2>Cd$ span length appropriate for the additional span by a trans-1D $Ni(CN)_4$ moiety. That of the double-1D daptn span in **140** becomes shorter than the dabtn span because of the flexibility of the daptn skeleton so that the double-1D span is reinforced by a *trans*-(cis-1D) linkage of $Ni(CN)_4$ to give a triple 1D chain structure. The increase of the methylene unit by 1 from daptn breaks $Ni(CN)_4$ catenation in the dahxn complex **141**; a discrete $Ni(CN)_4$ moiety is intercalated between the double-1D $>[Cd<(dahxn)_2>]_\infty$ extensions; the octahedral coordination of the Cd is accomplished by the two aqua ligands at *trans* positions. The water molecules in both dabtn and daptn complexes fill up the spaces formed in the crystal packing.

The dahpn complex **142** has a fourfold interpenetrating 3D sub-lattice spanned by a single bridge of dahpn; multiple interpenetration, in other words a self-clathrate structure, is often observed for the lattice with relatively long spans, as mentioned later in Sections 4 and 5. The pseudo-tetrahedral dahpn extensions from one Cd to four other Cd atoms give a distorted diamondoid 3D sub-lattice; there are a pair of two crystallographically independent sub-lattices in the unit cell; the sub-lattices, four in total, interpenetrating one another are successively interconnected at Cd

atoms in the nearest distance through ambidentate $Ni(CN)_4$ moieties in *trans*-(cis-1D) catenation mode. The water molecule is accommodated in the space formed in the 3D structure. The structure of the danon complex **143** corresponds to the guest-free host of $[Cd(danon)_2Ni(CN)_4]\cdot 2G$ in single-2D danon and cis-1D $Ni(CN)_4$ described in Section 3.4.2. The danon skeleton appears to be flexible enough to fill up the space by itself without any interpenetration. The absence of the daotn complex suggests the skeletal length and flexibility are critical at $n = 8$ to give either a multiply interpenetrating or a single framework complex structure.

Two complexes, $[Cd(mea)(daptn)Ni(CN)_4]$ **144** and $[Cd(mea)(dahxn)Ni(CN)_4]\cdot H_2O$ **145**, involving an additional mea ligand, show further variations of the catenation behaviour of the respective ligands and resulting multi-dimensional structures [49]. In the former, the *catena*-μ linkages of —[Cd-daptn-]$_\infty$, —[Cd-mea-]$_\infty$ and —[*trans*-NC—Ni(CN)$_2$—CN—] sharing every Cd atom form a 3D latticework, two of which are interpenetrated to each other to give a double framework structure. The mea in the latter is chelated to the Cd atom so that the number of the spans from a Cd decreases to 4: the 3D latticework is pseudo-diamondoid, like that observed in the dahpn complex **142**. The void space in the pseudo-diamondoid lattice is filled up by two other latticeworks to give a triply interpenetrating framework structure.

Table IV summarises the catenation modes of the secondary ligands and $Ni(CN)_4$ entities observed for the structures described in Sections 3.3, 3.4 and 3.5.

3.7. PHENYLALKYLAMMONIUM TETRACYANONICKELATES

Complexes **146**, **147**, **153**, and clathrates **148–152** were obtained by applying strategy (4) to replace the octahedral *trans*-$[M(NH_3)_2]^{2+}$ entity of the Hofmann-type structure by two phenylalkylammonium cations $Ph(CH_2)_nNH_3^+$ (n = 2, 3 and 4) [50]. As exemplified in Figure 15, the complexes of the hosts and those without guests have a layer structure derived from the Hofmann-type close-2D network. The network is broken at every octahedral site by the phenylalkylammonium cation which connects a couple of N-ends from two $Ni(CN)_4$ moieties at the ammonio group through hydrogen bonds to form a double-1D extension of $>[Ni<(CN\cdots H—NH\{(CH_2)_nPh\}—H(\cdots NC)_2>]_\infty$ arrayed in parallel in place of the close-2D network. The phenylalkyl groups protrude from both sides of the double-1D belt into the interlayer space.

In the anhydrate complex $[\{Ph(CH_2)_2NH_3\}_2Ni(CN)_4]$ **146** and two hydrate complexes $[\{Ph(CH_2)_2NH_3\}_2\ Ni(CN)_4]\cdot{}^2/_3H_2O$ **147** and $[\{Ph(CH_2)_4NH_3\}_2\cdot Ni(CN)_4]\cdot{}^2/_3H_2O$ **153**, there are two kinds of sheets formed by the array of the double-1D belts; one is a double-decked and the other a single sheet. In the double-decked sheet the phenylalkyl groups protrude always in the same direction at both sides of each 1D belt, viz. in a double-Z mode. From the single sheet the protrusion is possible either in the same (single-

Table IV. Catenation modes of L and $Ni(CN)_4$ in various structures.

Compound	Ligand	$Ni(CN)_4$	H_2O	Crystal structure
$[Cd(en)Ni(CN)_4]$ **121**	chelate	(close-2D)-3D		3D latticework
$[Ni(en)_2Ni(CN)_4]\cdot 2PhNH_2$ **112**	chelate	trans-1D		1D chain
$[Cu(en)_2Ni(CN)_4]\cdot 2PhNH_2$ **113**	chelate	trans-1D		1D chain
$[Zn(en)_2Ni(CN)_4]\cdot 2PhNH_2$ **114**	chelate	trans-1D		1D chain
$[Cd(en)_2Ni(CN)_4]\cdot 2PhNH_2$ **115**	chelate	trans-1D		1D chain
$[\{Cd(en)\}_2(en)\{Ni(CN)_4\}_2]\cdot .4PhOH$ **120**	chelate	double-1D		3D latticework
	single-μ	trans-μ		
$[Cd(den)Ni(CN)_4]\cdot G$ **62 - 71**	single-1D	close-2D		3D latticework
$[Cd(den)Ni(CN)_4]\cdot G$ **123 - 127**	single-1D	expanded-2D		3D latticework
$[Cd(den)_2Cd(den)\{Ni(CN)_4\}_2]$ **128**	unidentate	expanded-2D		3D latticework with
	single-1D			interpenetration of den
$[Cd(mtn)Ni(CN)_4]\cdot {}^1/_2(cyclo\text{-}C_6H_{12})$ **129**	chelate	expanded-2D		3D latticework
		double-1D		
$[Cd(dmtn)Ni(CN)_4]\cdot {}^1/_2CHCl_3$ **130**	chelate	expanded-2D		3D latticework
		double-1D		
$[Cd(tenH)_2\{Ni(CN)_4\}_2]\cdot 4PhNH_2$ **131**	unidentate	(trans-1D)-2D		3D latticework
$[Cd(pXdam)Ni(CN)_4]\cdot o\text{-}MeC_6H_4NH_2$ **61**	single-1D	close-2D		3D latticework
$[Cd(pXdam)_2Ni(CN)_4]\cdot m\text{-}MeC_6H_4NH_2$ **132**	double-1D	trans-1D		2D network
$[Cd(pXdam)_2Ni(CN)_4]\cdot G$ **133, 134**	double-1D	cis-1D		2D network
$[Cd_2(pXdam)_3\{Ni(CN)_4\}_2]\cdot 2C_4H_5N$ **135**	single-2D*[1]	cis-1D		3D latticework
		double-1D		
$[Cd(PhNH_2)(pXdam)Ni(CN)_4]$ **136** pXdam	single-2D	cis-1D		2D network
$PhNH_2$	unidentate			
$(pXdamH_2)[Ni(CN)_4]$ **137**	discrete	discrete		ionic
$[Ni(en)_2Ni(CN)_4]$ **116**	chelate	trans-1D		1D chain
$[Cu(en)_2Ni(CN)_4]$ **117**	chelate	trans-1D		1D chain
$[Zn(en)_2Ni(CN)_4]$ **118**	chelate	trans-1D		1D chain
$[Cd(en)_2Ni(CN)_4]$ **119**	chelate	cis-1D		1D chain
$[Cd(tn)_2Ni(CN)_4]$ **138**	single-2D*[2]	cis-1D*[2]		2D network
$[Cd(dabtn)_2Ni(CN)_4]\cdot 2H_2O$ **139**	double-1D	trans-1D	guest	2D network
$[Cd(daptn)_2Ni(CN)_4]\cdot H_2O$ **140**	double-1D	cis-1D	guest	triple-1D chain
$[Cd(H_2O)_2(dahxn)_2][Ni(CN)_4]$ **141**	double-1D	discrete	unidentate	1D chain
$[Cd(dahpn)_2Ni(CN)_4]\cdot H_2O$ **142**	single-3D	cis-1D	guest	4-fold 3D latticework
$[Cd(danon)_2Ni(CN)_4]$ **143**	single-2D	cis-1D		3D latticework
$[Cd(mea)(daptn)Ni(CN)_4]$ **144** mea	single-1D	trans-1D		2-fold 3D latticework
daptn	single-1D			
$[Cd(mea)(dahxn)Ni(CN)_4]\cdot H_2O$ **145** mea	chelate	trans-1D		3-fold 3D latticework
dahxn	single-2D			
$[Cd(en)_3][Ni(CN)_4]$ **122**	chelate	discrete		ionic
$(dadcnH)_2[Ni(CN)_4]$ **154**	discrete	discrete		H-bonded 1D chain
$[meaH\cdot(18\text{-crown-}6)]_2[Ni(CN)_4]$ **155**	discrete	discrete		ionic
$[Cd(2,2'\text{-bpy})Ni(CN)_4]$ **156**	chelate	close-2D*[6]		3D latticework

*1. A graphite-like 2D network is given by trifurcate extension of the single-2D catenation.

*2. One single-1D array in the single-2D extension is additionally spanned by the cis-1D.

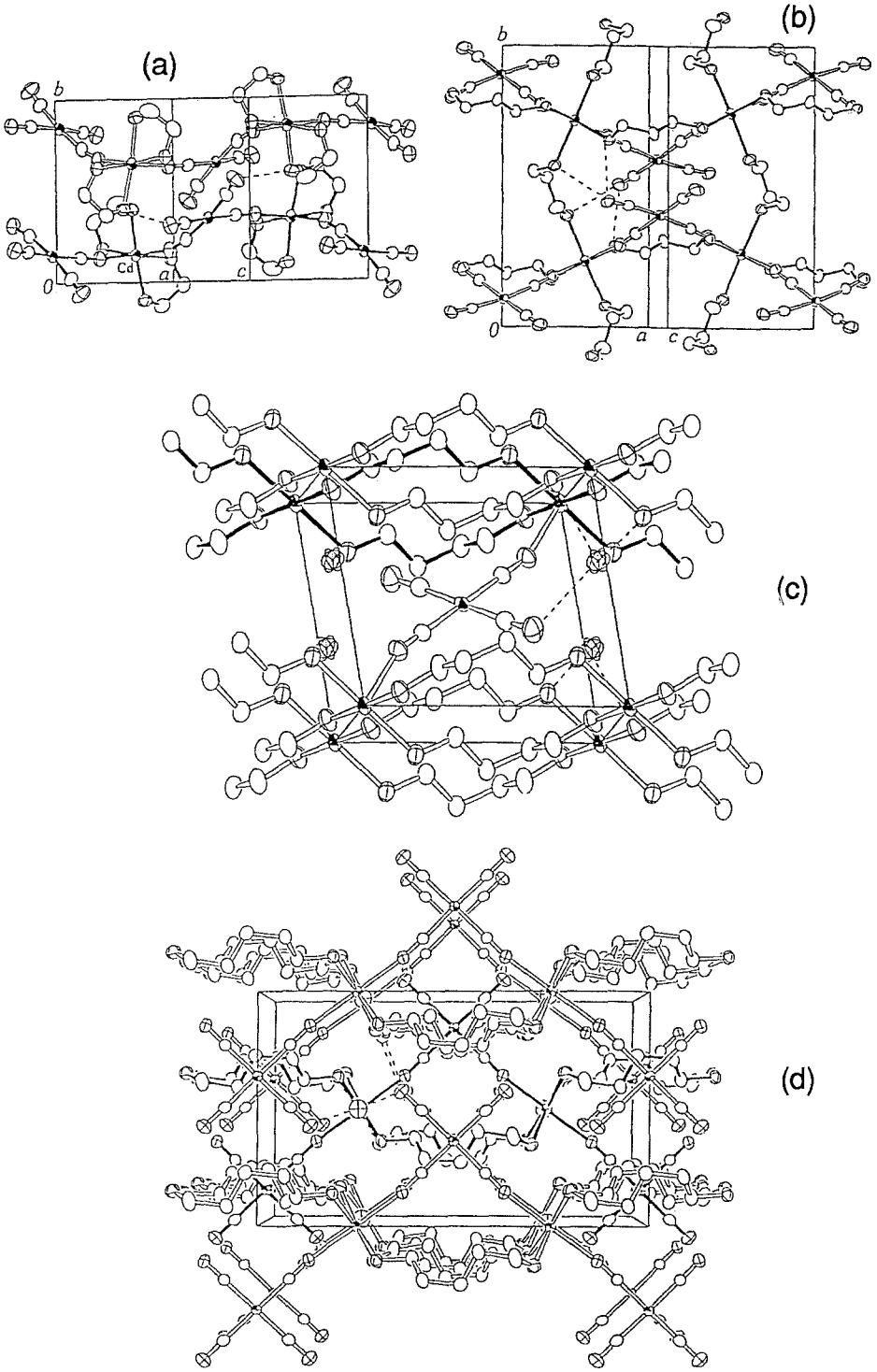

Figure 14a–d.

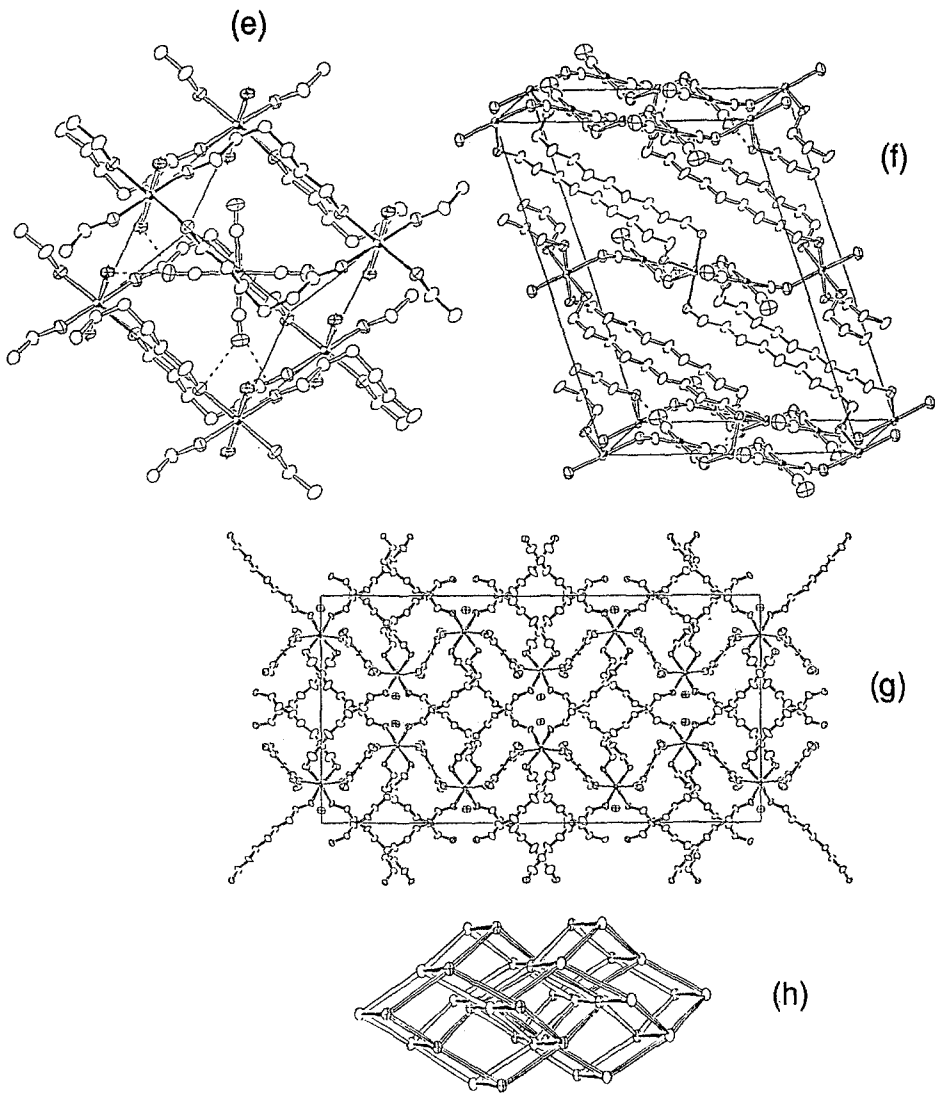

Figure 14e–g. Structures of $CdNi(CN)_4 \cdot 2diam \cdot hH_2O$ series. (a) $[Cd(en)_2Ni(CN)_4]$ **119** (monoclinic form) with chelating en and *cis*-(cis-1D) $Ni(CN)_4$ catenation. (b) $[Cd(tn)_2Ni(CN)_4]$ **138** with single-2D tn spans; a couple of the edges of the mesh are additionally spanned by *cis*-(cis-1D) catenation of $Ni(CN)_4$. (c) $[Cd(dabtn)_2Ni(CN)_4] \cdot 2H_2O$ **139**; double-1D dabtn belts are bridged by *trans*-(trans-1D) $Ni(CN)_4$. (d) $[Cd(daptn)_2Ni(CN)_4] \cdot H_2O$ **140**; double-1D daptn belt is reinforced by *trans*-(cis-1D) catenation of $Ni(CN)_4$. (e) $[Cd(H_2O)_2(dahxn)_2][Ni(CN)_4]$ **141**; discrete $Ni(CN)_4$ is intercalated between double-1D belts of dahxn. (f) $[Cd(danon)_2Ni(CN)_4]$ **143** with single-2D catenation of danon and *trans*-(cis-1D) catenation of $Ni(CN)_4$. (g) $[Cd(dahpn)_2Ni(CN)_4] \cdot H_2O$ **142** with *trans*-(cis-1D) catenation of $Ni(CN)_4$ and single-3D span of dahpn. (h) fourfold interpenetration of diamondoid sub-lattice spanned by dahpn ligands in **142** (solid bar is the linking by $Ni(CN)_4$ in *trans*-(cis-1D) catenation).

Z) or in the opposite direction (single-E); the anhydrate and the hydrates take double-Z and single-E modes. As for the clathrate structures, so far determined, $[\{Ph(CH_2)_2NH_3\}_2Ni(CN)_4]\cdot C_6H_6$ **148**, $[\{Ph(CH_2)_3NH_3\}_2Ni(CN)_4]\cdot C_6H_6$ **152**, and $[\{Ph(CH_2)_2NH_3\}_2Ni(CN)_4]\cdot PhNMe_2$ **149** have the single-sheet stacking with a single-E mode for both benzene clathrates but a single-Z mode for the *N*, *N*-dimethylaniline clathrate; $[\{Ph(CH_2)_2NH_3\}_2Ni(CN)_4]\cdot CHCl_3$ **150** and $[\{Ph(CH_2)_2NH_3\}_2Ni(CN)_4]\cdot p\text{-}MeC_6H_4NH_2$ **151** have the double-decked sheets with a double-Z mode. The respective clathrate structures without the double-decked or single sheet are derived by a formal replacement of the phenylalkyl group protruding from the absent double-decked or single sheet by the guest molecules.

4. Supramolecular Structures Involving Tetrahedral $Cd(CN)_4$

4.1. General

Strategy (3) gives Hofmann-Td-type $[Cd(NH_3)_2M'(CN)_4]\cdot 2G$ and en-Td-type $[Cd(en)M'(CN)_4]\cdot 2G$ (M′ = Cd, Hg) clathrates from the Hofmann-type and Hofmann-en-type upon replacing the square planar $Ni(CN)_4$ by tetrahedral $M'(CN)_4$. The close-2D network in the Hofmann-type and Hofmann-en-type hosts changes to the CN-bridged 3D latticework owing to the tetrahedral linkage of the tetrahedral tetracyanometallate to the octahedral Cd. When M′ is Cd, i.e., in almost all cases of our structures, octahedral Cd(o) and tetrahedral Cd(t) coexist with a 1:1 ratio in the Hofmann-Td-type and related structures.

In the course of our investigations to develop novel host structures with or without use of secondary ligands, we have obtained multi-dimensional structures built of the CN linkages among Cd(o) and Cd(t), and five-coordinated Cd(p) in some structures, in various ratios. In comparison with the varieties of the structures, their compositions are rather simple and can be denoted as adducts of cadmium cyanide $uCd(CN)_2 \cdot vL(\text{or } G)\cdot wH_2O$ for many of the compounds. Their crystallographic data are listed in Table V, in which some related data of cyanocuprates(I) are also included.

4.2. Hofmann-Td-type and related structures

4.2.1. *Structures with the ratio Cd(o):Cd(t) = 1:1*

In the structures of the Hofmann-Td-type **201**–**203** and -Td-en-type **207** and **208**, the close-2D network in the Hofmann-type host is twisted at every tetrahedral M′ by ca. 90° changing the host to a 3D structure linked by the CN bridges between the octahedral Cd and tetrahedral M′. Two kinds of cavities, α and β, are formed in the 3D lattice. Cavity α is isostructural to that in the Hofmann-type with the shape of a rectangular box; cavity β has the shape of a twisted biprism that is derived by

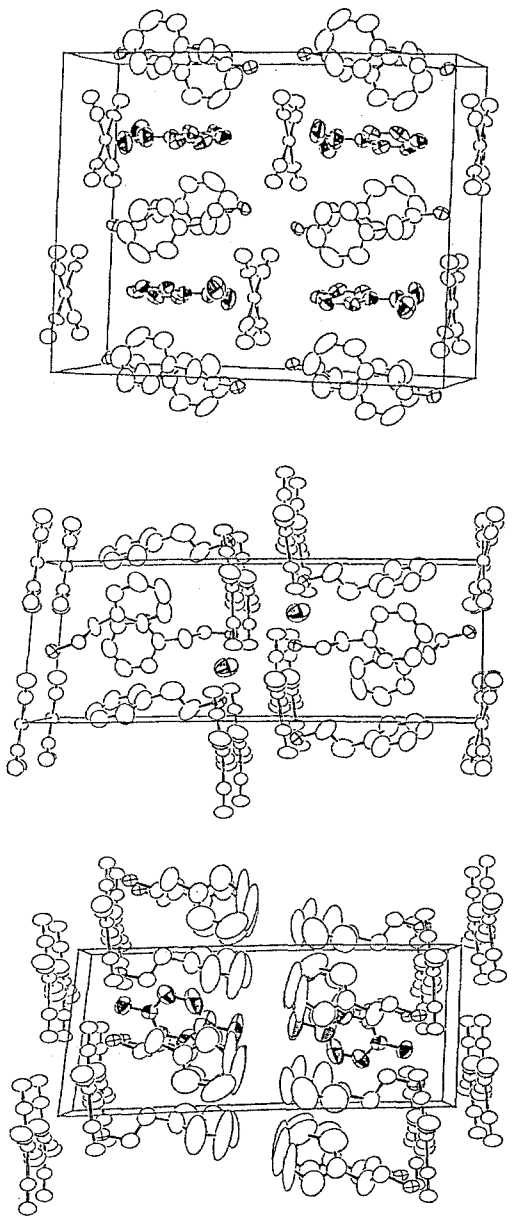

Figure 15. Structures of $[\{Ph(CH_2)_2NH_3\}_2Ni(CN)_4]\cdot PhNMe_2$ **149** (top), $[\{Ph(CH_2)_2NH_3\}_2Ni(CN)_4]\cdot{}^2/_3H_2O$ **147** (middle), and $[\{Ph(CH_2)_2NH_3\}_2Ni(CN)_4]\cdot$ *p*-$MeC_6H_4NH_2$ **151** (bottom). Anisotropic sections are shown for guest atoms; anisotropic peripheries for the ammonio-N. Each of the double-1D belts involving $Ni(CN)_4$and onium groups runs perpendicular to the page. **149** has the sheet structure of single-E; **147** double-Z and single-Z; **151** double-Z.

Table V. Crystallographic data for the structures involving $Cd(CN)_4$ and related structures.

		Space group	*a*/Å	*b*/Å	*c*/Å	*α*/°	*β*/°	*γ*/°	*Z*	Ref.
	Hofmann-Td-type and related clathrates and complexes									
201	$[Cd(NH_3)_2Cd(CN)_4]\cdot 2C_6H_6$	$C2/c$	12.063(2)	12.174(2)	14.621(1)	90	90.976(9)	90	4	54
202	$[Cd(NH_3)_2Hg(CN)_4]\cdot 2C_6H_6$	$P\bar{1}$	8.534(5)	8.537(5)	14.619(8)	90.5(1)	89.2(1)	89.3(1)	2	55
203	$[Cd(NH_3)_2Cd(CN)_4]\cdot 2PhNH_2$	$C2/c$	12.1951(9)	12.078(1)	14.6921(7)	90	93.436(5)	90	4	54
204	$[Cd(H_2O)_2Cd(CN)_4]\cdot 2C_4H_8O_2$	$C2/c$	12.054(5)	11.334(6)	15.249(2)	90	91.62(2)	90	4	20
205	$[Cd(py)_2Cd(CN)_4]$	$Cccm$	9.386(2)	14.358(2)	14.439(2)	90	90	90	4	56
206	$[Cd(PhNH_2)_2Cd(CN)_4]\cdot {}^1/_2PhNH_2$	$P2_1/n$	15.169(2)	16.019(2)	8.866(1)	90	95.73(1)	90	4	54
207	$[Cd(en)Cd(CN)_4]\cdot 2C_6H_6$	$P4_222$	8.265(1)	8.265	15.512(3)	90	90	90	2	57
208	$[Cd(en)Cd(CN)_4]\cdot 2PhNH_2$	Cc	11.027(1)	12.0767(9)	15.837(1)	90	92.059(9)	90	4	54
209	$[Cd(en)Cd(CN)_4]$	$I4_1/acd$	14.366(1)	14.366	23.771(4)	90	90	90	16	57b
210	$[Cd(tn)Cd(CN)_4]$	$I4_1/a$	14.486(2)	14.486(2)	24.009(3)	90	90	90	16	58
211	$[Cd(pn)Cd(CN)_4]\cdot CH_2ClCH_2Cl$	$P2_1/n$	8.278(2)	14.904(2)	14.477(1)	90	91.24(1)	90	4	59
212	$[\{Cd(CN)(py)_2\}_3\{Cd_2(CN)_7\}]$	$R\bar{3}c$	13.987(2)	13.987	43.769(8)	90	90	120	6	56
213	$[\{Cd(CN)(den)\}_3\{Cd_2(CN)_7\}]\cdot 3PhNH_2$	$P\bar{6}2c$	14.165(3)	14.165	15.036(3)	90	90	120	2	60
214	$[\{Cd(CN)(den)\}_3\{Cd_2(CN)_7\}]\cdot 3o\text{-}MeC_6H_4NH_2$	$P\bar{6}2c$	14.202(2)	14.202	15.217(2)	90	90	120	2	60
215	$[\{Cd(den)\}_2(CN)\{Cd_2(CN)_7\}]\cdot 3C_4H_8O_2$	$Pnam$	20.033(2)	13.517(2)	14.991(2)	90	90	90	4	60
216	$[\{Cd(den)\}_2(CN)\{Cd_2(CN)_7\}]\cdot 2.5C_6H_6$	$A2_1am$	19.203(3)	27.732(3)	15.028(3)	90	90	90	8	60
217	$[\{Cd(den)\}_3\{Cd_2(CN)_7\}_2]\cdot 4PhNMe_2$	$Pnam$	16.838(5)	28.560(6)	15.293(5)	90	90	90	4	60
218	$[\{Cd(den)\}_2\{Cd_4(CN)_{12}\}]\cdot 4PhOMe$	$P4_2/mnm$	14.235(4)	14.235	15.077(5)	90	90	90	2	60
219	$[\{Cd(iquin)_2\}\{Cd(CN)_3(iquin)_2\}_2]$	$P2_1/c$	8.178(2)	20.557(2)	16.244(3)	90	97.20(2)	90	2	56
220	$[Cd(den)\{Cd(CN)_3(den)\}_2]$	$C2/c$	11.229(2)	20.323(3)	12.022(2)	90	97.88(1)	90	4	60
221	$[Cd(den)_2\{Cd(CN)_3\}_2]$	$C2/m$	17.4920(9)	9.244(1)	7.013(1)	90	95.908(8)	90	2	60
222	$[Cd_2(tn)_2\{Cd(CN)_4\}_2]\cdot 4PhOH$	$P2_1$	12.036(3)	12.762(4)	15.186(1)	90	90.93(1)	90	2	58
223	$[Cd(CN)_2pyrz]$	$Ccc2$	7.428(1)	13.278(2)	8.005(3)	90	90	90	4	61
224	$[Cd(CN)_2qxln]$	$P2_1/n$	9.673(3)	11.209(3)	9.679(3)	90	107.44(3)	90	4	61
225	$[Cd(CN)_2bpb]$	$C2/c$	24.555(8)	7.239(2)	8.348(3)	90	106.16(4)	90	4	61
	Silica-mimetic clathrates and related structures									
226	$Cd(CN)_2$	$Pn\bar{3}m$	6.300(1)	6.300	6.300	90	90	90	2	62

Table V. Continued

		Space group	a/Å	b/Å	c/Å	α/°	β/°	γ/°	Z	Ref.
		$P\bar{4}3m$	6.301(1)	6.301	6.301	90	90	90	2	63
		$P\bar{4}3m$	6.32*[1]	6.32	6.32	90	90	90	2	64
227	$Zn(CN)_2$	$Pn\bar{3}m$	5.9086(7)	5.9086	5.9086	90	90	90	2	62
		$P\bar{4}3m$	5.9002(9)	5.9002	5.9002	90	90	90	2	63
		$P\bar{4}3m$	5.89*[1]	5.89	5.89	90	90	90	2	65
228	$[Cd(CN)_2]\cdot CHCl_3$	$Fd\bar{3}m$	12.647(6)	12.647	12.647	90	90	90	8	62
		$Fd\bar{3}m$	12.638(3)	12.638	12.638	90	90	90	8	66
229	$[Cd(CN)_2]\cdot Pr^iCl$	$Fd\bar{3}m$	12.638(6)	12.638	12.638	90	90	90	8	67
		$Fd\bar{3}m$	12.668(3)	12.668	12.668	90	90	90	8	62
230	$[Cd(CN)_2]\cdot CHMeClCH_2Cl$	$Fd\bar{3}m$	12.691(2)	12.691	12.691	90	90	90	8	62
231	$[Cd(CN)_2]\cdot Bu^iCl$	$Fd\bar{3}m$	12.692(2)	12.692	12.692	90	90	90	8	62
232	$[Cd(CN)_2]\cdot CCl_4$	$Fd\bar{3}m$	12.714(1)	12.714	12.714	90	90	90	8	62
233	$[Cd(CN)_2]\cdot CMeCl_3$	$Fd\bar{3}m$	12.717(1)	12.717	12.717	90	90	90	8	62
234	$[Cd(CN)_2]\cdot cyclo\text{-}C_6H_{11}Me$	$Fd\bar{3}m$	12.729(2)	12.729	12.729	90	90	90	8	62
235	$[Cd(CN)_2]\cdot CMe_2Cl_2$	$Fd\bar{3}m$	12.731(1)	12.731	12.731	90	90	90	8	62
236	$[Cd(CN)_2]\cdot CHMeCl_2$	$Fd\bar{3}m$	12.732(2)	12.732	12.732	90	90	90	8	62
237	$[Cd(CN)_2]\cdot cyclo\text{-}C_6H_{12}$	$Fd\bar{3}m$	12.735(1)	12.735	12.735	90	90	90	8	62
238	$[Cd(CN)_2]\cdot CFCl_2CF_2Cl$	$Fd\bar{3}m$	12.742(1)	12.742	12.742	90	90	90	8	62
239	$[Cd(CN)_2]\cdot CHCl_2CHCl_2$	$Fd\bar{3}m$	12.743(1)	12.743	12.743	90	90	90	8	62
240	$[Cd(CN)_2]\cdot Bu^tCl$	$Fd\bar{3}m$	12.743(1)	12.743	12.743	90	90	90	8	62
241	$[Cd(CN)_2]\cdot CMe_3Et$	$Fd\bar{3}m$	12.744(1)	12.744	12.744	90	90	90	8	62
242	$[Cd(CN)_2]\cdot CMe_4$	$Fd\bar{3}m$	12.757(2)	12.757	12.757	90	90	90	8	62
243	$[Cd(CN)_2]\cdot CCl_3CF_3$	$Fd\bar{3}m$	12.767(2)	12.767	12.767	90	90	90	8	62
244	$[Cd(CN)_2]\cdot 0.5Bu^i{}_2O$	$Fd\bar{3}m$	12.645(8)	12.645	12.645	90	90	90	8	67
245	$[Cd(CN)_2]\cdot 0.5Pe^i{}_2O$	$Fd\bar{3}m$	12.69(1)	12.69	12.69	90	90	90	8	67
246	$[CdHg(CN)_4]\cdot 2CCl_4$	$Fd\bar{3}m$	12.7138(5)	12.7138	12.7138	90	90	90	4	62
247	$[CdHg(CN)_4]\cdot 2cyclo\text{-}C_6H_{12}$	$Fd\bar{3}m$	12.734(1)	12.734	12.734	90	90	90	4	62
248	$[CdZn(CN)_4]\cdot 2CCl_4$	$Fd\bar{3}m$	12.243(2)	12.243	12.243	90	90	90	4	62
249	$[CdCu(CN)_4]\cdot[NMe_4\cdot CCl_4]$	$F\bar{4}3m$	12.189(2)	12.189	12.189	90	90	90	4	62

*[1] Based on powder X-ray diffraction data.

Table V. Continued

		Space group	*a*/Å	*b*/Å	*c*/Å	*α*/°	*β*/°	*γ*/°	*Z*	Ref.
250	$[CuZn(CN)_4]\cdot[NMe_4\cdot CCl_4]$	$F\bar{4}3m$	11.771(2)	11.771	11.771	90	90	90	4	62
251	$[CuZn(CN)_4]\cdot[NMe_4]$	$F\bar{4}3m$	11.671(2)	11.671	11.671	90	90	90	4	62
		$F\bar{4}3m$	11.609(3)	11.609	11.609	90	90	90	4	63
252	$[Cd(CN)_2]\cdot CHCl_2CH_2Cl$	$P4_12_12$	8.978(6)	8.978	11.934(3)	90	90	90	4	67
253	$[Cd(CN)_2]\cdot Pr^iBr$	$P4_12_12$	9.124(1)	9.124	11.335(3)	90	90	90	4	67
254	$[Cd(CN)_2]\cdot Pr^iCN$	$P4_12_12$	12.483(3)	12.483	12.719(3)	90	90	90	8	67
255	$[Cd(CN)_2]\cdot 0.5(Bu^n{}_2O\cdot H_2O)$	$P6_3/mmc$	8.888(3)	8.888	14.945(6)	90	90	120	4	67
	Clay-like layer structures									
256	$[Cd_3(CN)_7(dmtnH)]\cdot C_6H_6$	$C2/m$	20.662(7)	9.219(4)	14.819(5)	90	115.43(3)	90	4	68
257	$[Cd_3(CN)_7(dmtnH)]\cdot C_6H_5F$	$C2/m$	20.589(5)	9.172(2)	14.891(6)	90	115.60(3)	90	4	69,70
258	$[Cd_3(CN)_7(dmtnH)]\cdot CCl_4$	$C2/m$	20.405(5)	9.067(3)	15.181(6)	90	111.48(3)	90	4	68
259	$[Cd_3(CN)_7(dmtnH)]\cdot Bu^iOH$	$C2/m$	20.481(3)	9.091(2)	15.030(3)	90	111.29(1)	90	4	68
260	$[Cd_3(CN)_8]\cdot[2NMe_4\cdot CCl_2{=}CCl_2]$	$R\bar{3}m$	8.7675(7)	8.7675	14.695(2)	90	90	120	1	68
261	$[Cd_3(CN)_{6.3}I_{1.7}]\cdot[2NMe_4\cdot CCl_2{=}CCl_2]$	$C2/m$	15.467(3)	8.541(7)	12.84(2)	90	92.01(7)	90	2	70
262	$[Cd_3(CN)_8]\cdot[2NHMe_3\cdot C_6H_6]$	$C2/m$	17.979(5)	9.027(3)	11.187(4)	90	99.70(3)	90	2	68
263	$[Cd_3(CN)_7(H_2O)]\cdot SMe_3$	$Pnam$	20.761(3)	11.331(1)	8.277(2)	90	90	90	4	68
264	$[Cd_3(CN)_{6.5}I_{0.5}(H_2O)]\cdot SMe_3$	$Pnam$	20.745(5)	11.362(2)	8.299(2)	90	90	90	4	70
265	$[Cd_3(CN)_8(mtnH)_2]\cdot[2C_6H_6\cdot C_6H_6]$	$Cmca$	15.162(4)	23.772(3)	11.551(1)	90	90	90	4	68
	Zeolite-mimetic 3D structures									
266	$[Cd_3(CN)_7]\cdot[NMe_4\cdot SnMe_4]$	$R\bar{3}m$	8.849(1)	8.849	31.086(3)	90	90	120	3	71
267	$[Cd_3(CN)_7]\cdot[NEt_4\cdot CH_2Cl_2]$	$R\bar{3}m$	8.778(4)	8.778	30.64(3)	90	90	120	3	71
268	$[Cd_3(CN)_7]\cdot[detnH\cdot CHCl_3]$	$R\bar{3}m$	8.850(3)	8.850	30.538(4)	90	90	120	3	71
269	$[Cd_3(CN)_7]\cdot[NMe_4\cdot trans\text{-}CHCl{=}CHCl]$	$Pn2_1m$	11.115(3)	13.287(3)	8.664(3)	90	90	90	2	71
270	$[Cd_3(CN)_7]\cdot[dmtnH\cdot CH_2ClCH_2Cl]$	$Pn2_1m$	11.026(5)	13.54(1)	8.721(2)	90	90	90	2	69,71
271	$[Cd_3(CN)_7]\cdot[detnH\cdot C_6H_6]$	$Pn2_1m$	11.026(5)	13.54(1)	8.721(2)	90	90	90	2	71
272	$[Cd_3(CN)_7]\cdot[SMe_3\cdot 2C_6H_6]$	$Pnam$	21.934(7)	13.483(2)	8.875(3)	90	90	90	4	71
273	$[Cd_3(CN)_7]\cdot[SMe_3\cdot PhMe]$	$Pnam$	21.862(5)	13.389(5)	8.996(3)	90	90	90	4	72
274	$[Cd_3(CN)_7]\cdot[SMe_3\cdot PhEt]$	$Pnam$	21.855(3)	13.511(4)	8.975(3)	90	90	90	4	72
275	$[Cd_3(CN)_7]\cdot[NMe_4\cdot{}^3/_2C_6H_6]$	$Pnam$	21.628(3)	13.998(3)	8.945(1)	90	90	90	4	71
276	$[Cd_3(CN)_7]\cdot[NMe_4\cdot PhMe]$	$Pnam$	22.33(2)	13.297(6)	8.846(4)	90	90	90	4	71

Table V. Continued

		Space group	*a*/Å	*b*/Å	*c*/Å	*α*/°	*β*/°	*γ*/°	*Z*	Ref.
277	$[Cd_3(CN)_7]\cdot[NMe_4\cdot{}^2/_3(o\text{-}C_6H_4Me_2)]$	*Pnam*	22.230(2)	13.570(6)	8.873(2)	90	90	90	4	72
278	$[Cd_3(CN)_7]\cdot[NMe_4\cdot{}^2/_3(m\text{-}C_6H_4Me_2)]$	*Pnam*	22.267(3)	13.498(5)	8.832(2)	90	90	90	4	72
279	$[Cd_3(CN)_7]\cdot[NMe_4\cdot PhEt]$	*Pnam*	22.461(2)	13.498(2)	8.859(1)	90	90	90	4	72
280	$[Cd_3(CN)_7]\cdot[NMe_4\cdot{}^2/_3(1,3,5\text{-}C_6H_3Me_3)]$	*Pnam*	22.256(4)	13.489(4)	8.868(3)	90	90	90	4	71
281	$[\{Cd_3(CN)_7\}_2NMe_3\}]\cdot 2[NHMe_3\cdot CH_2ClCH_2Cl]$	*Pnam*	43.39(1)	13.602(5)	8.773(3)	90	90	90	4	71
282	$[Cd_3(CN)_7]\cdot[NMe_4\cdot 2CH_2ClCH_2Cl]$	$P6_3/mmc$	8.787(2)	8.787	20.97(3)	90	90	120	2	71
283	$[Cd_3(CN)_7]\cdot[NMe_4\cdot 2CH_2{=}CCl_2]$	$P6_3/mmc$	8.775(3)	8.775	20.546(8)	90	90	120	2	71
284	$[Cd_3(CN)_7]\cdot[NMe_4\cdot 2EtCN]$	$P6_3/mmc$	8.714(5)	8.714	20.437(8)	90	90	120	2	71
285	$[Cd_3(CN)_7]\cdot[NMe_4\cdot 2CHCl_2CHCl_2]$	$P6_3/mmc$	8.814(4)	8.814	20.567(3)	90	90	120	2	71
286	$[Cd_3(CN)_7]\cdot[NMe_4\cdot 2CH_2Cl_2]$	$P6_3/mmc$	8.775(2)	8.775	20.546(8)	90	90	120	2	71
287	$[Cd_3(CN)_7]\cdot[NMe_4\cdot p\text{-}C_6H_4Me_2]$	$P6_3/mmc$	8.857(2)	8.857	20.716(3)	90	90	120	2	72
288	$[Cd_3(CN)_7]\cdot[SMe_3\cdot p\text{-}C_6H_4Me_2]$	*Pa*	15.026(5)	9.025(2)	19.832(4)	90	94.82(2)	90	4	72
289	$[Cd_3(CN)_7]\cdot[temtnH\cdot CH_2ClCH_2Cl]$	$Pb2_1m$	10.817(5)	27.553(1)	9.048(2)	90	90	90	4	71
290	$[Cd_4(CN)_9]\cdot[K\cdot 4EtCN]$	*Pnam**2	22.773(5)	18.850(9)	8.549(1)	90	90	90	4	73
	Other mineralomimetic structures									
291	$K_2[Cd(CN)_4]$	$Fd\bar{3}m$	12.8601(9)	12.8601	12.8601	90	90	90	4	74
292	$[PPh_4]_3[Cd_2(CN)_7]$	$R\bar{3}c$	18.990(4)	18.990	34.301(4)	90	90	120	6	75
293	$[SbPh_4]_2[Cd(CN)_3]_2$	$P2_1/c$	19.807(5)	8.46(1)	31.079(7)	90	90.40(3)	90	4	76
294	$[\{Cd(Me_2SO)_2(CN)\}_2\{Cd(CN)_4\}]$	*Fddd*	8.504(2)	14.441(1)	45.883(6)	90	90	90	8	77
295	$[Cd(H_2O)_2Cd(CN)_4]\cdot 2dmf$	$P2_1/c$	9.003(7)	12.046(3)	18.870(15)	90	96.23(4)	90	4	77
296	$[Cd(H_2O)_2\{Cd(CN)_3\}_2]\cdot 2Pr^iOH$	*C*2/*c*	14.251(3)	17.797(2)	13.043(2)	90	111.247(8)	90	8	78
297	$[Cd(H_2O)_2\{Cd(CN)_3\}_2]\cdot 2Pr^n{}_2O$	*C*2/*c*	14.044(6)	18.034(6)	12.931(4)	90	111.47(2)	90	4	79
298	$[Cd(H_2O)_2\{Cd(CN)_3\}_2]\cdot 3Bu^tOH$	*Amm*2*3	8.695(1)	8.548(1)	21.092(4)	90	90	90	2	80,81
299	$[Cd(H_2O)_2\{Cd(CN)_2Cd(CN)_3\}_2]\cdot 6Pr^nOH$	*C*2/*m*	15.176(5)	25.732(3)	8.464(2)	90	132.722(9)	90	8	78
300	$[\{Cd(H_2O)_2\}_3(Cd\{(CN)Cd(CN)_3\}_4)]\cdot 6Et_2O$	$P\bar{4}3n$	15.661(5)	15.661	15.661	90	90	90	4	79
301	$[\{Cd(H_2O)_2\}_3(Cd\{(CN)Cd(CN)_3\}_4)]\cdot 6Pr^i{}_2O$	$P\bar{4}3n$	15.762(9)	15.762	15.762	90	90	90	4	79
302	$[\{Cd(H_2O)(CN)_2\}_4Cd(CN)_2].4cyclo\text{-}C_6H_{11}OH$	$I4_1/a$	20.070(2)	20.070	12.733(3)	90	90	90	4	82
303	$[Cd(hmta)\{Cd(CN)_3\}_2]$	*Cmcm*	21.274(4)	7.782(1)	13.272(1)	90	90	90	4	81

*2. The axes setting has been changed from that in the original lit.

*3. The space group *Ammm* has been recommended from NMR data [92c].

Table V. Continued

		Space group	*a*/Å	*b*/Å	*c*/Å	*α*/°	*β*/°	*γ*/°	*Z*	Ref.
304	$[Cd(hmta)\{Cd_2(CN)_5(OH)\}]$	$P2_1/a$	11.358(2)	12.619(2)	12.366(2)	90	104.05(1)	90	4	81
305	$[\{Cd(NC)(hmta)\}_2\{Cd(CN)_4\}]$	$P2_1/c$	8.8967(6)	13.2822(9)	11.1564(8)	90	105.36(5)	90	2	83
	Imidazole-ligated structures									
306	$3Cd(CN)_2{\cdot}2imH{\cdot}C_6H_6$	$P2_1/n$	12.369(2)	14.117(2)	14.423(2)	90	106.58(1)	90	4	84
307	$3Cd(CN)_2{\cdot}2imH{\cdot}PhMe$	$P2_1/n$	12.455(1)	14.332(1)	14.396(1)	90	105.88(1)	90	4	85
308	$3Cd(CN)_2{\cdot}2imH{\cdot}cyclo\text{-}C_6H_{10}O$	$P2_1/n$	13.405(5)	14.379(3)	13.979(3)	90	104.21(3)	90	4	85
309	$3Cd(CN)_2{\cdot}2imH{\cdot}m\text{-}C_6H_4Me_2$	$P6/m$	17.716(5)	17.716	8.923(4)	90	90	120	3	85
310	$3Cd(CN)_2{\cdot}2imH{\cdot}p\text{-}C_6H_4Me_2$	$P2_1/n$	8.942(2)	12.835(5)	12.222(3)	90	92.33(2)	90	2	85
311	$\mathbf{9Cd(CN)_2{\cdot}4imH{\cdot}2H_2O{\cdot}2PhEt}$	$P2_1/c$	17.221(2)	8.499(3)	23.537(2)	90	105.90(1)	90	2	85
	Diethylenetriamine-ligated structures									
312	$5Cd(CN)_2{\cdot}2dien{\cdot}{}^1/_2C_6H_6$	$C2/m$	29.886(7)	8.831(4)	14.456(7)	90	108.90(3)	90	4	86
313	$5Cd(CN)_2{\cdot}2dien{\cdot}{}^1/_2Cl_2C{=}CCl_2$	$C2/m$	29.945(4)	8.826(3)	14.464(3)	90	108.72(2)	90	4	86
314	$5Cd(CN)_2{\cdot}2dien{\cdot}{}^1/_2Pe^tOH$	$C2/m$	30.018(6)	8.798(5)	14.499(4)	90	108.84(2)	90	4	86
315	$11Cd(CN)_2{\cdot}4dien{\cdot}3H_2O$	$C2$	20.150(3)	10.299(4)	17.849(4)	90	99.88(2)	90	2	86
316	$2Cd(CN)_2{\cdot}CuCN{\cdot}2dien{\cdot}H_2O$	$P2_1/c$	8.823(7)	14.918(6)	19.102(3)	90	95.63(3)	90	4	86
	Structures involving Cu(I)-CN linkage									
317	$H_3[CdCu_2(CN)_7]{\cdot}14H_2O$	$Pa\bar{3}$	12.9401(9)	12.9401	12.9401	90	90	90	4	87
318	$[Cd(H_2O)_3Cu(CN)_3]{\cdot}MeCN$	$C2/m$	13.601(3)	8.629(2)	9.958(3)	90	107.90(2)	90	4	88
319	$[H\{Hameden\}_2]{\cdot}[Cu_4(CN)_7]$	P2/n	12.3829(9)	8.5970(9)	12.6633(7)	90	109.984(5)	90	2	89

rotating a half of the rectangular box along the bisecting diagonal plane by ca. 90° (see Figure 16).

The benzene and aniline clathrates are obtained for both Hofmann-Td- and en-Td-type hosts [54–56]. Although it is difficult to accommodate aniline as the guest in the Hofmann-en-type host owing to the short en span between the close-2D networks, the en-Td-type host can accommodate aniline [54]. The 3D lattice involving the tetrahedral $Cd(CN)_4$ is more flexible than the Hofmann-en-type so that the latticework is deformed to accommodate the hydrogen-bonded pair of aniline molecules in the α and β cavities, as shown in Figure 16.

The replacement of the NH_3 ligand in the Hofmann-Td-type by H_2O affords a 1,4-dioxane clathrate $[Cd(H_2O)_2Cd(CN)_4]\cdot 2C_4H_8O_2$ **204** [20] analogous to the case of the Hofmann-H_2O-type $[Cd(H_2O)_2Ni(CN)_4]\cdot 2C_4H_8O_2$ **13** [20]. A similar analogue to the Hofmann-py-type complex $[Cd(py)_2Ni(CN)_4]$ **32** [29] is obtained as $[Cd(py)_2Cd(CN)_4]$ **205** [56] with the topology of the 3D structure the same as the host of the Hofmann-Td-type clathrate. Cavity α in the flexible 3D lattice is occupied by the py ligand but cavity β collapses with no room for any guest.

The residual complex left after thermal liberation of the guest molecules from en-Td-type $[Cd(en)Cd(CN)_4]\cdot 2C_6H_6$ **207** gives a powder X-ray diffraction pattern identical with that of complex **209** $[Cd(en)Cd(CN)_4]$ [57b], whose 3D structure is a doubly interpenetrating latticework of the CN linkages among Cd(t) and en-chelated Cd(o). The 3D latticework in $[Cd(tn)Cd(CN)_4]$ **210** also has the same topology as **209** [58].

Aniline, being a complementary ligand that is more voluminous than py, gives a 3D host structure different in topology from the Hofmann-Td-type: two aniline ligands coordinate to the octahedral Cd at *cis* positions in $[Cd(PhNH_2)_2Cd(CN)_4]\cdot {}^1/_2PhNH_2$ **206** whose cage cavity accommodates the aniline molecule as the guest [54].

Although its composition suggested a pn-Td-type host structure, the 3D host of the $[Cd(pn)Cd(CN)_4]\cdot ClCH_2CH_2Cl$ clathrate **211** involves the pn-chelated octahedral Cd linked by the tetrahedral $Cd(CN)_4$ entities with a topology different from the Hofmann-en-type; two guest molecules are accommodated in the cage cavity [59].

4.2.2. *Structural variations upon change of complementary ligand*

A slight increase of the pyridine concentration in the mother solution of $[Cd(py)_2Cd(CN)_4]$ (= $Cd(CN)_2\cdot py$ in composition) **205** affords complex $[\{Cd(CN)(py)_2\}_3\{Cd_2(CN)_7\}]$ **212** (= $5Cd(CN)_2\cdot 6py$) with a ratio of Cd(o):Cd(t) = 3:2 [56]. The Cd(o) atoms coordinated with the py ligands at trans positions are linked by CN groups to form a triangle on the equatorial plane, while the dimeric $Cd_2(CN)_7$ [= $(NC)_3Cd(t)(CN)Cd(t)(CN)_3$] entity takes a staggered configuration like the pyrosilicate anion $Si_2O_7^{6-}$ with the central Cd-(CN)-Cd array perpendicular to the equatorial plane of the Cd(o) trimeric unit. As shown in Figure 17, a

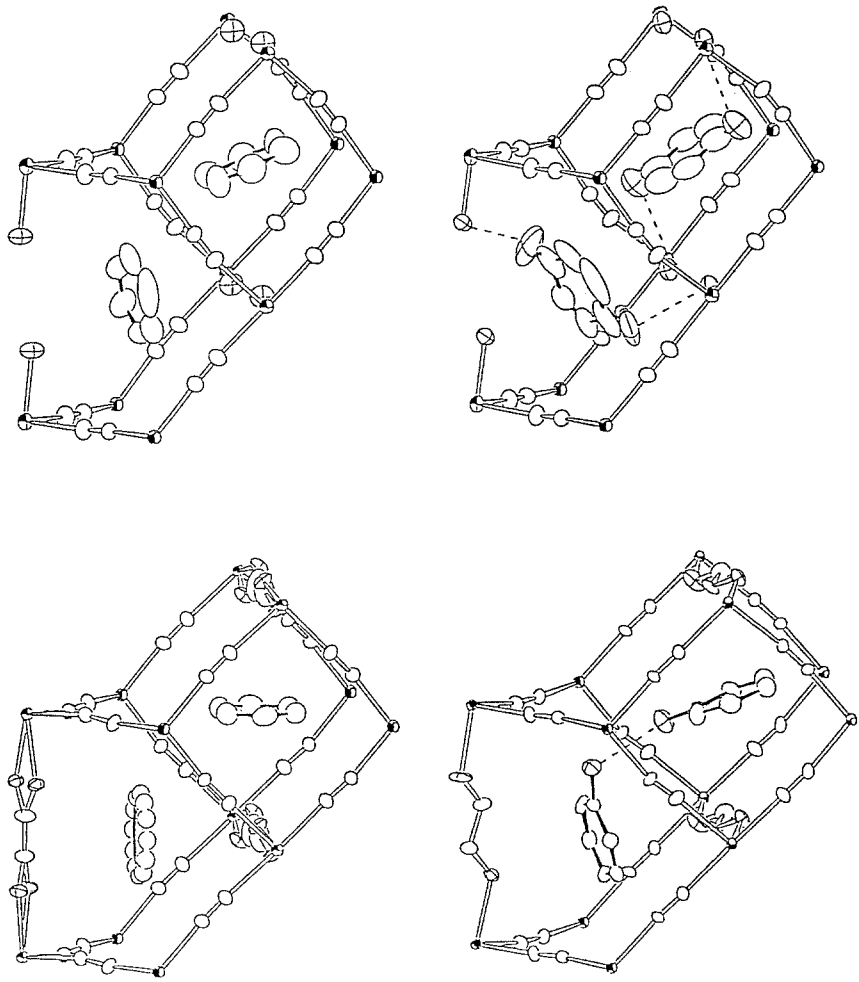

Figure 16. Guests in α and β cavities of Hofmann-Td-type and en-Td-type hosts. *Top left*: C_6H_6 in $[Cd(NH_3)_2Cd(CN)_4]\cdot 2C_6H_6$ **201**; *top right*: $PhNH_2$ in $[Cd(NH_3)_2Cd(CN)_4]\cdot 2PhNH_2$ **203** (both $PhNH_2$ molecules are disordered and hydrogen bonded to the NH_3 of the host); *bottom left*: C_6H_6 in $[Cd(en)Cd(CN)_4]\cdot 2C_6H_6$ **207** (C_6H_6 in β cavity is disordered); *bottom right*: $PhNH_2$ in $[Cd(en)Cd(CN)_4]\cdot 2PhNH_2$ **208** (the $PhNH_2$ molecules in α and β cavities are hydrogen bonded to each other).

CN-bridged 2D network is formed among the trimers and the dimers arranged alternately up and down from the network. The adjacent networks spanned by the dimers in the staggered configuration are stacked with a rotation by 60° so as to fill up the interlayer space by the py ligands at the Cd(o) atoms. In the clathrate structures of $[\{Cd(CN)(den)\}_3\{Cd_2(CN)_7\}]\cdot 3G$ (G = *o*-$MeC_6H_4NH_2$ **214**, $C_4H_8O_2$ **215**) where the Cd(o) in one network is linked directly to the Cd(o) atoms in adjacent networks through the den ligands, the dimer takes an eclipsed configuration to generate cage cavities for the guest molecules. The Cd(o) unit becomes dimeric in **214** and **215**,

and monomeric in **216** [59]. Isoquinoline, being considerably bulkier than py and den as a secondary ligand, gives complex $[\{Cd(iquin)_2\}\{Cd(CN)_3(iquin)_2\}_2]$ **217** in which the *trans*-Cd(o)(iquin)$_2$ and *trans*-Cd(p)(iquin)$_2$ are alternately linked by the CN bridges to extend a 1D belt like the double-1D extension observed for Cd-Ni(CN)$_4$ systems [56]. The five-coordinated Cd(p) is further ligated by an unbridged unidentate CN group. The replacement of iquin by den in the belt structure turns to a 2D structure, where the den ligand bridges between Cd(o) in one belt and Cd(p) in the adjacent belt and *vice versa*.

Another kind of five coordination when a Cd(o) liberates an N-end of a CN-bridge from an adjacent Cd(t) is observed for $[Cd_2(tn)_2\{Cd(CN)_4\}_2]\cdot 4PhOH$ **222** [58]. In its 3D lattice work apparently similar in topology to that of the en-Td-type host, the N end of a CN bridge is not coordinated to Cd(o) but hydrogen-bonded to the NH_2 group of the tn bridging between Cd(o) atoms.

Robson's group reported the 3D latticeworks built of Cd(o) atoms only, which are linked by CN groups and bridging ligands pyrz **223**, qxln **224**, and bpb **225**, respectively [61].

4.3. MINERALOMIMETIC STRUCTURES OF $Cd(CN)_2$ AND $Cd_x(CN)_y$

4.3.1. *Mineralomimetic chemistry*

Clathrate hydrates are well known inclusion structures that occur in nature. Melanophlogite, isomorphous to clathrate hydrate II, is a rare example of a silica (SiO_2) mineral accommodating organic guest molecules. Clathrasils and zeosils are artificial inclusion systems mimicking clathrate hydrates and zeolites [90]. The structural analogy between H_2O (ice) and SiO_2 is also applicable to $Cd(CN)_2$ (see Table VI). They all have the AB_2 composition; A takes a tetrahedral configuration; B bridges between A's to give a 3D structure. Owing to the longer span of Cd—CN—Cd (*ca.* 5.5 Å) compared with those of Si—O—Si (ca. 3.2 Å) and O—H···O (ca. 2.8 Å), the 3D structure of Cd—CN—Cd spans with the same topology as those of Si—O—Si or O—H···O spans may generate a more spacious cavity than those of the latter spans. In addition, since cadmium polycyanocadmates or isopolycyanopolycadmates of composition $Cd_x(CN)_y$ may involve both tetrahedral and octahedral Cd centres in the crystal structures, structures of silicate and oxide minerals involving both tetrahedral and octahedral centres can be mimicked by $Cd_x(CN)_y$. Hence the term mineralomimetic chemistry may be defined as the chemistry of building mineral-like structures using materials that never give stable minerals in nature, where the products have structures, properties, functions, etc. in some respects similar to, but in other respects different from, those of natural minerals. A remarkable difference of mineralomimetic structures from natural minerals is brought about by the longer span of Cd—CN—Cd which is favourable for accommodation of molecular species of larger dimensions than the monatomic cations or water molecules usually included in natural minerals. A number of examples have been demonstrat-

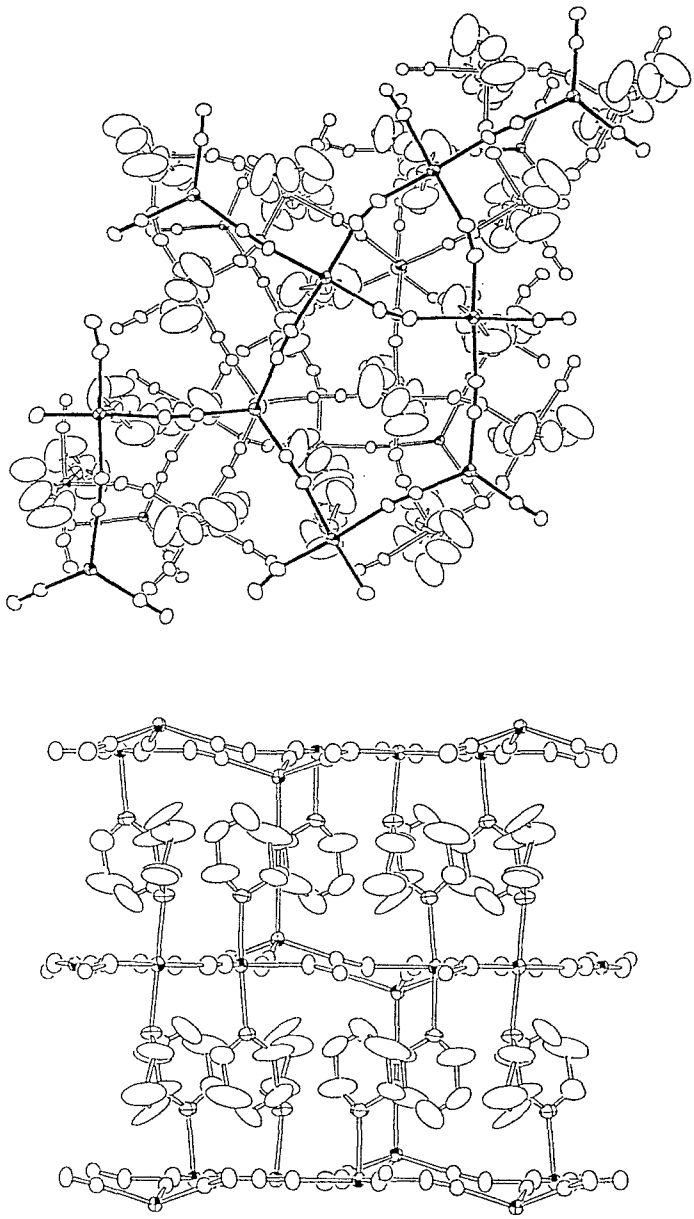

Figure 17. Structure of $[\{Cd(CN)(py)_2\}_3\{Cd_2(CN)_7\}]$ **212**. *Top*: projection along the *c* axis; the trimeric unit of $[Cd(o)(CN)]_3$ and base of the dimeric unit $[(NC)_3Cd(t)(CN)Cd(t)(CN)_3]$ in a staggered conformation form the puckered 2D network with approximately triangle and pentagonal meshes shown with solid bonds. *Bottom*: a side view of the stacked networks from which py ligands protrude to occupy the interlayer space.

Table VI. Structural similarities among SiO_2, H_2O (ice) and $Cd(CN)_2$.

Space group	SiO_2	H_2O	$Cd(CN)_2$
$Fd\bar{3}m$	H-cristobalite	ice I_c	Hc-host
$P4_12_12$	L-cristobalite		Lc-host
	keatite	ice III, ice IX	
$P6_3/mmc$	H-tridymite	ice I_h	Ht-host
$C222_1$ *etc.*	L-tridymite		
$P6_2(6_4)22$	H-quartz		
$P3_1(3_2)21$	L-quartz		
$Pm\bar{3}m$	melanophlogite	clathrate hydrate I	
	$46SiO_2{\cdot}8G$	$46H_2O{\cdot}[6X{\cdot}2Y]$	
$Fd\bar{3}m$		clathrate hydrate II	
		$136H_2O{\cdot}[8X{\cdot}16Y]$	
$Pn\bar{3}m$*	Cu_2O: cuprite	ice VII, ice VIII	neat $Cd(CN)_2$

* All the structures in this line have a double-interpreting latticework of self-clathrate.

ed for silica-mimetic $Cd(CN)_2$, clay-mimetic and zeolite-mimetic $Cd_x(CN)_y$, etc. [7d, 91].

4.3.2. *Silica-mimetic structures*

As shown in Figure 18a, neat $Cd(CN)_2$ **226** as well as neat $Zn(CN)_2$ **227** have an anticuprite type (cuprite: Cu_2O) doubly interpenetrating latticework structure, the single latticework of which is isostructural to the high-temperature phase of cristobalite (H-cristobalite), one of the polymorphs of SiO_2 [62–65]. A number of clathrates with silica-mimetic host structures are derived through the replacement of one latticework by guests [62,66,67]. The clathrates obtained, $Cd(CN)_2{\cdot}G$ or $Cd(CN)_2{\cdot}0.5G$ may be the simplest in composition among the known clathrates.

The host structures of $Cd(CN)_2{\cdot}G$ **228–243** and $Cd(CN)_2{\cdot}0.5G$ **244, 245** are isomorphous to H-cristobalite whose cavity has a T_d symmetry (see Figure 18b). The guests accommodated in the H-cristobalite-mimetic host (Hc host) are tetrahedral or pseudotetrahedral for the series of $CMe_{4-n}Cl_n$ (n = 0–4); those of molecular symmetries considerably lower than T_d are also accommodated in the Hc host. In the cases of **244** and **245**, the di-isoalkyl ether guests randomly share the respective isoalkyl groups in two neighbouring cavities.

The shape of the guest may influence the deformation of the host latticework so much that the cubic Hc host (the space group $Fd\bar{3}m$) is deformed to tetragonal Lc host (L-cristobalite-mimetic: $P4_12_12$) in **252–254** like the thermal transition of SiO_2 from H-cristobalite to L-cristobalite. The H-tridymite structure is mimicked when the guest is a long straight-chain aliphatic molecule Bu^n_2O in $[Cd(CN)_2]{\cdot}0.5(Bu^n_2O{\cdot}H_2O)$ **255**. The Ht host ($P6_3/mmc$) gives a channel cavity for Bu^n_2O which appears to be hydrogen-bonded to H_2O in another cage cavity

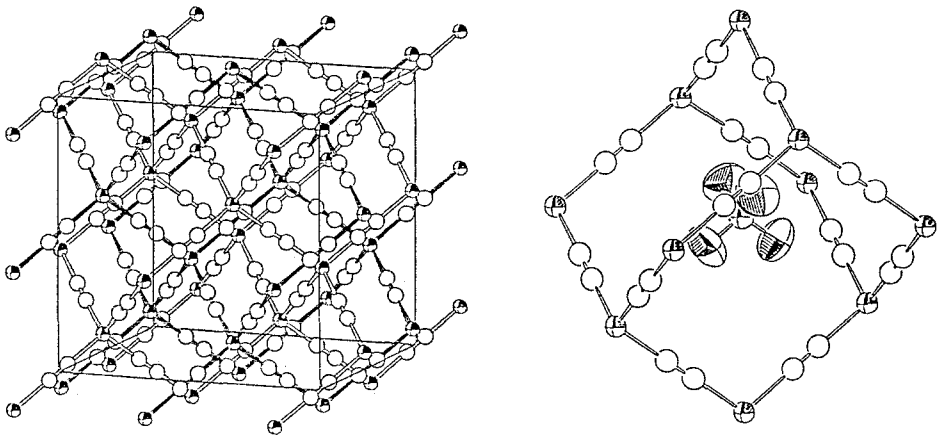

(a) (b)

Figure 18. (a) Self-clathrate structure of neat $Cd(CN)_2$ **226** with doubly interpenetrating 3D latticework. (b) The cavity of a T_d symmetry formed in Hc (high-cristobalite-mimetic) host clathrate $Cd(CN)_2 \cdot CMe_4$ **242** accommodating the CMe_4 guest.

generated in the 3D latticework isomorphous to ice I_h, the ice frozen at 273.15 K and 1 atm. Thus three of the six polymorphs, Hc, Lc, Ht, Lt, Hq (H-quartz) and Lq (L-quartz), have been mimicked by the 3D host structures of $Cd(CN)_2$ [67] (see Figure 19).

As for the X-ray crystallography of the Cd—CN—Cd linkage structures, a problem is the discrimination between C and N in the Cd(t)—CN—Cd(t or p) linkage, although in most cases the Cd(t)—CN—Cd(o) sequence has been ascertained with the Cd—N distance being longer than Cd—C. The Cd(t)—CN—Cd(t) sequence can be determined when the difference between both distances is greater than the sum of three times their e.s.d.'s. Solid-state NMR is a powerful tool for resolving the order–disorder problem as well as to analyse the motional behaviour of guest molecules [82, 92, 93]. In general, the CN group inserted between two Cd(t) atoms is in disorder.

Hc hosts are also possible for the combination of the tetrahedral coordination centres other than Cd such as Hg, Zn, Cu(I), **246–252**. The negatively charged hosts of $[CdCu(CN)_4]^-$ **249** and $[CuZn(CN)_4]^-$ **250** accommodate the neutral guest CCl_4 and NMe_4^+ in the tetrahedral cavities [62]; $[CuZn(CN)_4] \cdot [NMe_4]$ **251** has a neutral, guest-free structure leaving half the number of cavities vacant [62,63]. In these host structures the $Cu(CN)_4$ moiety keeps its integrity as a C-coordinated tetrahedron as determined by both X-ray crystallography and NMR [92c].

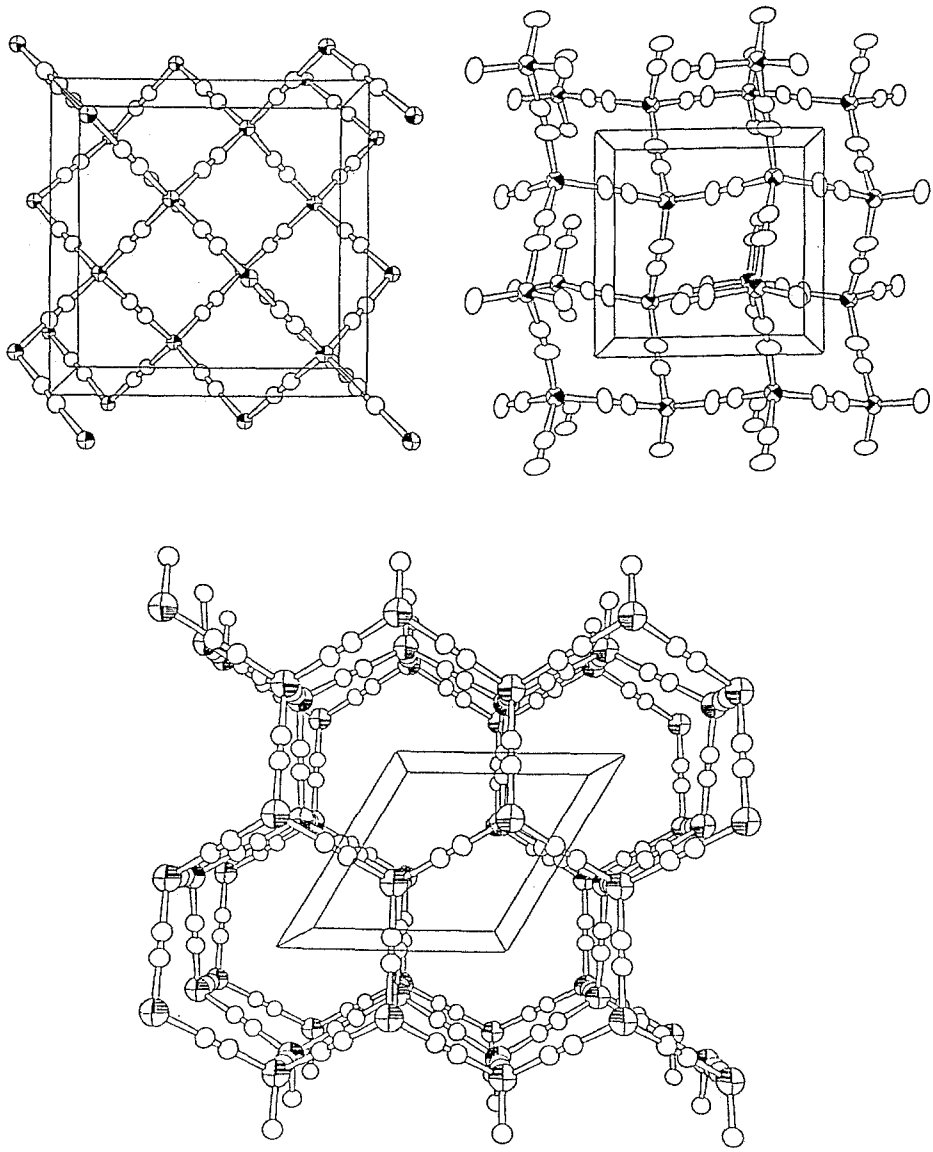

Figure 19. Cubic Hc-host (top left), tetragonal Lc-host (top right) and hexagonal Ht-host (bottom) structures of $Cd(CN)_2$; Cd atoms are shown with anisotropic sections.

4.3.3. *Clay-mimetic 2D layer structures*

The layer of clay minerals is in general composed of an assembly of tetrahedral and octahedral coordination polyhedra sharing oxide anions. In clay chemistry, the notations T—O, T—O—T, etc., have been applied to denote the coordination polyhedra arranged across the layer structure: T for tetrahedral and O for octahedral coordination centres. The layer structures, as in clays, are composed of

Cd(t)—CN—Cd(o)—NC—Cd(t) units, i.e., T—O—T of Cd coordination polyhedra sharing CN groups, as is illustrated in Figure 20. In **256–259**, the negative charge of the $[Cd_3(CN)_7]^-$ host is neutralised by the coordination of the cationic ligand $dmtnH^+$ at Cd(o) so that the neutral guests are intercalated in the interlayer space. The negative charge of the $[Cd_3(CN)_8]^{2-}$ layer in **260** and **262**, and that of partially I^--replaced at the vertex of Cd(t) in **261** is neutralised by the onium cations intercalated in the interlayer space along with the neutral guests. The negatively charged hosts of **263** and **264** have intralayer cavities that accommodate the onium cations. The benzene molecules in **265** are shared between the intralayer cavity and the concave cavity on the surface of the layer.

These clay-mimetic layers demonstrate typical examples of mineralomimetic structures comprised of chemical species that never give stable minerals in nature; they have similarities to and differences from the natural minerals. The similarity is that the layer is composed of T—O—T units; the difference is that the surface of the layer is covered by the vertices of coordination polyhedra in the mineralomimetic structures but by the faces in natural clays. Another point of difference may be in the chemical species: the mimicked structures contain only one Cd species as the coordination centres, both tetrahedral and octahedral. In addition, a few clay-mimetic structures accommodate the guests in the intralayer cavity.

4.3.4. *Zeolite-mimetic 3D lattice structures*

Zeolite-mimetic character may be demonstrated by the 3D structures built of CN linkages among Cd(t) and Cd(o) atoms: a negatively charged 3D latticework host, e.g., $[Cd_3(CN)_7]^-$, $[Cd_4(CN)_9]^-$, accommodates cationic and neutral guests in the polyhedral cavities with polygonal openings edged by Cd—CN—Cd spans. With respect to the 24 structures solved for the $[Cd_3(CN)_7]^-$ hosts **266–289**, which can be classified into six types according to the structural features, a commonly observed feature is that the 1D chain of $—(T—O—T—)_\infty$ runs on the mirror plane of all the unit cells. The one exception is **288** (the space group *Pa* but pseudo-hexagonal). The notation T—O—T has been used to denote a unit of CN-bridged linkage —NC—Cd(t)—CN—Cd(o)—NC—Cd(t)— like that used in clay chemistry, although in zeolite chemistry the usual meaning of T—O—T is the unit of two tetrahedral centres bridged with oxide. The T—O—T unit in the zeolite-mimetic structures is arrayed on a straight line, to a first approximation if slightly bent, but the chain always bends at the T—T joint between the T—O—T units. The three modes of bending, E-TOT, E-TT, E-TOT, Z-TT, and Z-TOT, E-TT have been observed for the 1D chains in the zeolite-like host structures; E-TOT denotes the mode bending towards the opposite directions at both T sides of the T—O—T unit and E-TT towards the opposite sides at the T—T junction; Z indicates the directions are the same. The 3D structure is given by the interconnection of the chains through out-of-the-mirror-plane CN groups. In addition to the bending mode, the difference in array of the bent chains generate four types of 3D structures in E-TOT, E-TT

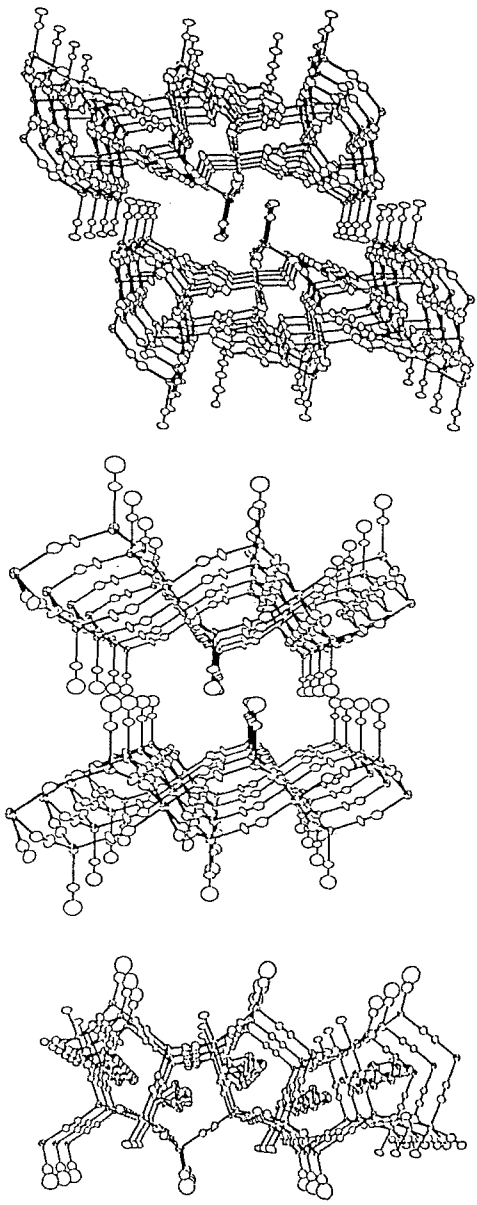

Figure 20. Clay-like layer structures of $[Cd_3(CN)_7(dmtnH)]$ (top), $[Cd_3(CN)_8]^{2-}$ (middle), and $[Cd_3(CN)_7(H_2O)]^-$ (bottom); the last accommodates SMe_3^+ guest in the intralayer cavity.

mode. When an E-TOT, E-TT chain on a mirror plane is assumed in an **o** (ortho) mode of bending, the chain generated by a 2_1 screw rotation never coincides with the **o** chain but in the mode of **a** (anti). Since all the unit cells can be seen to have two net mirror planes on which the 1D chains run, the mode of the chain running on the plane adjacent to the first selected plane may be denoted with a prime **o′** or

Table VII. Classification of the zeolite-mimetic structures.

Type: Compound*[1]	Space group(*Z*)	Bending mode of 1D chain	Cavities
$[Cd_3(CN)_7^-]$ host: Cd(o):Cd(t) = 1:2			
I: **262 - 264**	$R\bar{3}m$(3)	E-TOT,E-TT; **o-o'**	$[4^36^3]$
II: **265 - 267**	$Pn2_1m$(2)	E-TOT,E-TT; **o-a'**	$[4^15^46^1]$, $[4^15^46_1]$
III: **268 - 276**	*Pnam*(4)	E-TOT,E-TT; **o-a'-a--o'**	$[4^35^26^1]$, $[6^28^1]$, $[5^26^1]$
IV **277***[2]	*Pnam*(4)	E-TOT,E-TT; **o**(T)-**a'**(P)-**o**(P)-**a'**(T)-**a**(T)-**o'**(P)-**a**(P)-**o'**(T)	$[4^15^46^1]$, $[4^15^46^1]$, $[4^35^26^1]$, $[6^28^1]$, $[5^26^1]$
V: **278 - 283, 284***[3]	$P6_3/mmc$(2)	E-TOT,Z-TT; **o-o'**	$[6^3]$, $[4^66^3]$
VI: **285**	$Pb2_1m$(4)	Z-TOT,E-TT; **o-a'**	$[4^15^46^1]$, $[4^36^3]$
$[Cd_4(CN)_9]^-$ host: Cd(o):Cd(t) = 1:3			
286	*Pnma*(4)	E-TT,Z-TOT,E-TT; **o-a'-a-o'**	$[4^45^4]$, $[4^15^46^3]$

*1. Shown as the number in Table V.

*2. $[Cd_3(CN)_7Cd_3(CN)_7NMe_3]\cdot 2[NMe_3\cdot CH_2ClCH_2Cl]$; the chain involving Cd(p) is shown with (P) to discriminate from that involving Cd(t) only as Cd(T).

*3. Distorted from the hexagonal symmetry to the monoclinic *Pa*(4).

a′. Thus the classification of the structures listed in Table VII is possible according to their structural features. Some of the representative structures are illustrated in Figure 21.

The interconnection of the 1D chains generates polygons cornered by Cd atoms and edged by —CN— spans; these polygons enclose polyhedral cavities. The cavity is denoted as $[p^nq^m]$, i.e. enclosed by n of p-edged and m of q-edged polygons. In the polyhedral cavities organic onium cations and neutral guests are accommodated. An exceptional case is for type IV **281** in which NMe_3 in a cavity is not protonated but ligates to a Cd from inside of the cavity, the Cd(p) being in a trigonal-bipyramidal five coordination.

Inclusion selectivity for C_6H_6 (B), PhMe (T), three $C_6H_4Me_2$ (X) isomers *o*- (O), *m*- (M) and *p*- (P), and PhEt (E) was examined for fractional enclathration crystallisation processes into types III and V hosts. When the onium guest is NMe_4^+, B-, T-, O-, M-, and E-guest clathrates **275–279** are isomorphous to one another of space group *Pnam* with comparable unit cell dimensions, but P **287** gives a hexagonal ($P6_3/mmc$) structure. When the onium is SMe_3^+, B, T, and E **272–274** are orthorhombic *Pnam* as well as those of NMe_4^+ onium ones, but the host of P-guest clathrate **288** is deformed from hexagonal to monoclinic *Pa*. From B—T—X and X—E mixtures the selectivity of the NMe_4^+-host for the guest is in the order of T>B>P $\gg$ M>O and E>P $\gg$ M>O respectively [94], but that of the SMe_3^+-host P>T>B $\gg$ M>O and P>E $\gg$ M>O [95].

The nonacyanotetracadmate of **290** has a chain of T—O—T—T units; K^+ is accommodated as the cationic guest to neutralise the negative charge of the host along with the neutral guest EtCN [73].

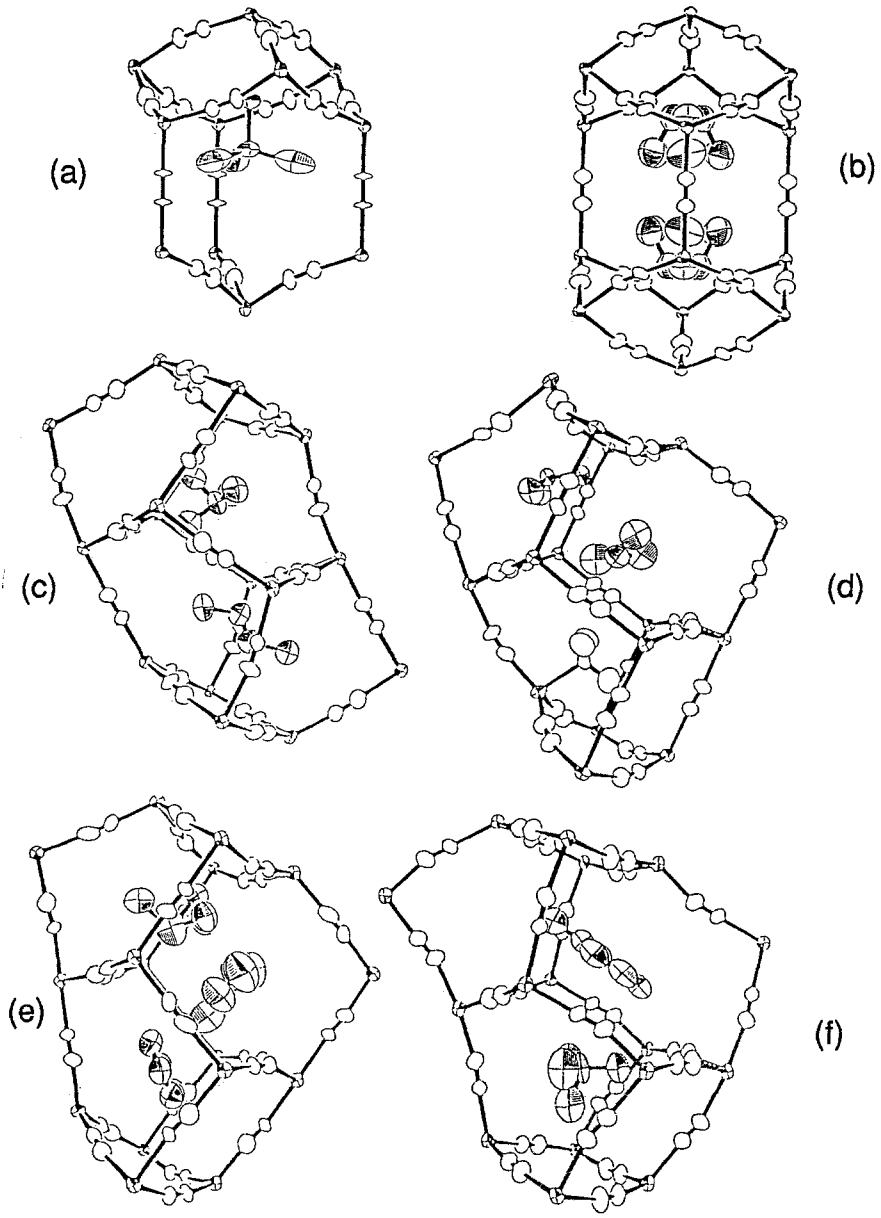

Figure 21a–f. Representative cavity structures in zeolite-mimetic $[Cd_3(CN)_7]^-$ hosts and $[Cd_4(CN)_9]^-$ host structure. (a) $SnMe_4$ or NMe_4^+ in type I **266**; (b) a pair of disordered CH_2ClCH_2Cl in type V **285**; (c) NMe_4^+ and *trans*-CHCl=CHCl in type II **269**; (d) $NHMe_3^+$, CH_2ClCH_2Cl, and unidentate NMe_3 in type IV **281**; (e) NMe_4^+ and two disordered C_6H_6 in type III **275**; (f) temtnH^+ and CH_2ClCH_2Cl in type VI **289**.

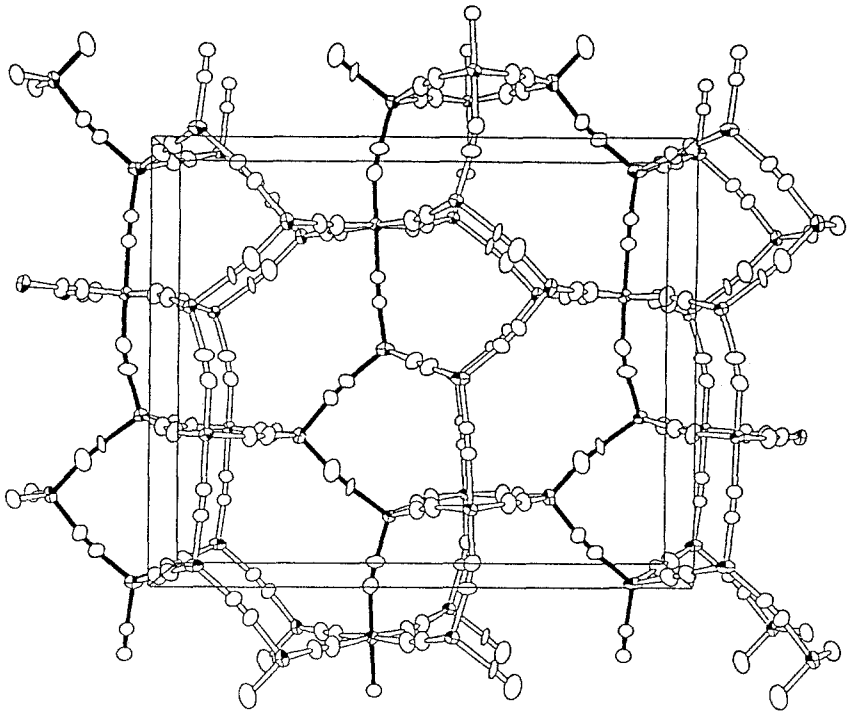

Figure 21g. The host structure of $[Cd_4(CN)_9]^-$ **290** as a projection along the *c* axis; the 1D chains of —[O—T—T—T—]$_n$ running on the same mirror plane at z = 1/2 are shown with solid bonds.

4.3.5. *Other mineralomimetic structures*

$K_2[Cd(CN)_4]$ is one of the starting reagents used to prepare the crystals of cyanocadmate compounds with multi-dimensional structures. The salt has an AB_2X_4 composition like spinel, Al_2MgO_4. The crystal structure of $K_2[Cd(CN)_4]$ **291** was described as a cyano-spinel: Cd takes a tetrahedral position coordinated with four CN groups and K takes an octahedral position surrounded by six N atoms of the CN groups in the space group $Fd\bar{3}m$ [74]. The dimeric pyrosilicate structure $Si_2O_7^{2-}$ was mimicked by a discrete $[Cd_2(CN)_7]^{3-}$ moiety in $[PPh_4]_3[Cd_2(CN)_7]$ **292** [75] and ino-silicate $(SiO_3^{2-})_\infty$ by a linear chain of $[Cd(CN)_3^-]_\infty$ in $[SbPh_4]_2[Cd(CN)_3]_2$ **293**, which formula represents the presence of two crystallographically independent cations and anionic chains in the unit cell [76].

A variety of zeolite-mimetic and related structures have been reported for the compounds with apparently simple compositions : uCd(CN)$_2$ · v(L and/or G)·wH$_2$O. 3Cd(CN)$_2$·2Me$_2$SO reported by Kim *et al.* [77] is formulated as $[\{Cd(Me_2SO)_2(CN)\}_2Cd(CN)_4]$ **294** whose structure is closely related to the Hofmann-Td-type. The 3D lattice involving Cd(o) and Cd(t) in a 2:1 ratio is generated by introducing an extra Cd(o) next to the Cd(o) in the Hofmann-Td-type; two Me_2SO coordinate to each Cd(o) at *trans* positions to fill up the cavi-

ties. $Cd(CN)_2 \cdot dmf \cdot H_2O$, formulated as $[Cd(H_2O)_2Cd(CN)_4] \cdot 2dmf$ **295** [77], may be seen as a polymorph of the Hofmann-H_2O-Td-type. The aqua ligands coordinate to the Cd(o) at *cis* positions and are hydrogen-bonded to the guest dmf molecules. The *cis* coordination of aqua ligands at Cd(o) is also observed for $3Cd(CN)_2 \cdot 2G \cdot 2H_2O$ (G = Pr^iOH **296** [78], $Pr^n{}_2O$ **297** [79]; Cd(o):Cd(t) = 1:2) in which the alcohol and the ether guests are respectively hydrogen-bonded to the aqua ligands. Coordination of aqua ligands at *trans* positions of Cd(o) occurs in $3Cd(CN)_2 \cdot 3Bu^tOH \cdot 2H_2O$ (= $[Cd(H_2O)_2\{Cd(CN)_3\}_2] \cdot 3Bu^tOH$; Cd(o):Cd(t) = 1:2) **298** [80, 81], $5Cd(CN)_2 \cdot 6Pr^nOH \cdot 2H_2O$ (= $[Cd(H_2O)_2\{Cd(CN)_2Cd(CN)_3\}_2] \cdot 6Pr^nOH$; Cd(o):Cd(t) = 1:4) **299** [78], and $8Cd(CN)_2 \cdot 6G \cdot 2H_2O$ $[\{Cd(H_2O)_2\}_3(Cd\{(CN)Cd(CN)_3\}_4)] \cdot 6G$; Cd(o):Cd(t) = 3:5; G = Et_2O **300**, = $Pr^i{}_2O$ **301**) [79]. The structure of **298** can be interpreted in terms of another variation from the Hofmann-Td-type that replacement of two Cd(o) by a Cd(t) for half the number of Cd(o) atoms in the Hofmann-Td-type generates this structure. The expanded cavity accommodates the alcohol guest hydrogen-bonded with the aqua ligand.

In the 3D lattice of **299**, there are two sets of $-(T-O-T-)_\infty$ chains, like those observed for the zeolite-mimetic structures, running approximately on the [001] plane of the $C2/m$ unit cell. The chains do not run in parallel but cross at every Cd(o). The interchain connection occurs at every Cd(t) to generate channel cavities, in which disordered Pr^nOH molecules are assumed to be hydrogen-bonded to the aqua ligands. In the isomorphous **300** and **301**, which have a Cd(o):Cd(t) ratio of 3:5, the five Cd(t) atoms form a neopentane-like assembly of $Cd\{-CN-Cd(CN-)_3\}_4$, the three outer N atoms of each $-Cd(CN-)_3$ moiety being linked to three Cd(o) atoms to generate the 3D host lattice. A pair of ether guests are hydrogen-bonded with the aqua ligands from two Cd(o) atoms to form a square array of O atoms.

The cristobalite-mimetic host of $[\{Cd(H_2O)(CN)_2\}_4Cd(CN)_2] \cdot 4cyclo\text{-}C_6H_{11}OH$ **302** (= $5Cd(CN)_2 \cdot 4cyclo\text{-}C_6H_{11}OH \cdot 4H_2O$) [82] has a Cd(p):Cd(t) ratio of 4:1, i.e., four of the five Cd atoms in the 3D host are coordinated additionally by the aqua ligands respectively, these ligands forming a hydrogen-bonded tetrahedron in one cavity. Each of the cyclohexanol guests accommodated in the four adjacent cavities directs its OH group towards the face of the water tetrahedron. Eventually, those species accommodated in the five cavities are arrayed to form a big tetrahedron $[(H_2O)_4](cyclo\text{-}C_6H_{11}OH)_4$.

Because of the rigid tetrahedral array of ligating N atoms in hmta (hexamethylenetetramine), involvement of hmta with the Cd—CN—Cd linkage structure resulted in three different 3D lattice structures as seen in $[Cd(hmta)\{Cd(CN)_3\}_2]$ **303** (= $3Cd(CN)_2 \cdot hmta$) [81], $[Cd(hmta)\{Cd_2(CN)_5(OH)\}]$ **304** (= $2Cd(CN)_2 \cdot Cd(CN)(OH) \cdot hmta$) [81], and $[\{Cd(NC)(hmta)\}_2Cd(CN)_4]$ **305** (= $3Cd(CN)_2 \cdot 2hmta$) [83].

A series of imH-ligated hosts, involving both imH-ligated Cd(o) and Cd(t), show a variety of structures, depending on the guest, with the same composition

$3Cd(CN)_2 \cdot 2imH \cdot G$ [84, 85]. Benzene, toluene and cyclohexanone gives an isomorphous series of $[\{Cd(o)(imH)\}\{Cd(t1)(CN)_3(imH)\}\{Cd(t2)(CN)_3\}] \cdot G$ (G = C_6H_6 **306**, PhMe **307**, *cyclo*-$C_6H_{10}O$ **308**) like the zeolite-mimetic host. However, the host of the *m*-xylene clathrate $[\{Cd(o)(imH)_2\}\{Cd(t)(CN)_3\}_2] \cdot m\text{-}C_6H_4Me_2$ **309** has a beryl($Al_2Be_3Si_6O_{18}$)-like framework structure. The cyclosilicate structure unit of $(SiO_3)_6$ is mimicked by the hexagonal ring of $\{Cd(t)(CN)_3\}_6$; the BeO_4 tetrahedron sharing the O with the silicate unit is mimicked by $Cd(o)(imH)_2$ which leaves four coordination sites for the CN linkages from the out-of-plane CN groups of the hexagonal ring. The guest m-$C_6H_4Me_2$ molecules are accommodated in the channel formed by stacking of the hexagonal rings and the positions of the Al atoms in beryl. $[Cd(o)\{Cd(t)(CN)_3(imH)\}_2] \cdot p\text{-}C_6H_4Me_2$ **310** has the AB_2 host composition which mimics the structure of rutile (TiO_2). Cd(o) like the octahedral Ti is in a six coordination from six $Cd(t)(CN)_3(imH)$ moieties, each of which extends three CN groups to three Cd(o)'s like O in rutile. The beryl-mimetic and rutile-mimetic structures are illustrated in Figure 22. The ethylbenzene clathrate with the composition different from the others $[\{Cd(o)(imH)_2\}\{Cd(o)(H_2O)\}_2\{Cd(t)(CN)_3(imH)\}_2\{Cd(t)(CN)_3\}_2] \cdot 2PhEt$ **311** has a clay-like layer structure involving intralayer cavities accommodating the guests and ligands. Using dien ($NH_2CH_2CH_2NHCH_2CH_2NH_2$) as complementary ligand, a variety of clathrate structures have been obtained [86].

Tetrahedral $Cu^I(CN)_4$ behaves similarly to the tetrahedral $Cd(CN)_4$ in several multi-dimensional structures. A pyrosilicate-like dimeric structure of $Cu_2(CN)_7$ similar to $Cd_2(CN)_7$ gives a pyrite(FeS_2)-mimetic $[Cd\{Cu_2(CN)_7\}]^{3-}$ 3D framework structure in $(H_{31}O_{14}) \cdot [Cd\{Cu_2(CN)_7\}]$ (= $H_3[Cd\{Cu_2(CN)_7\}] \cdot 14H_2O$) **317**, where 12 H_2O molecules are hydrogen-bonded to make a rotaxane-like ring about the pyrosilicate-like unit (Figure 23). The ring is further hydrogen-bonded to six H_2O molecules, each of which intervenes among three 12 H_2O rings; the array of the rings and intervening H_2O is of the same topology as that of rutile [87]. The layer host of the $[Cd(H_2O)_3Cu(CN)_3] \cdot MeCN$ clathrate **318** has a 2D network of hydrogen-bonded H_2O molecules coordinated at facial positions of the Cd(o) atoms which are arrayed on the surface of the metal complex layer. In the onium guest clathrate $[H(Hameden)_2] \cdot [Cu_4(CN)_7]$ **319** [89], the anionic 3D host framework has a polyacene-like 1D array of condensed hexagonal rings edged by a Cu—CN—Cu linkage, these 1D arrays being interconnected by the CN groups bifurcated at the C end.

5. Supramolecular Structures Involving Linear $Ag(CN)_2$

5.1. GENERAL

Our strategy (5) is to use dicyanoargentate(I) $[Ag(CN)_2]^-$ itself as a bridging ligand. The anion $[Ag(CN)_2]^-$, and its dimeric condensate $[Ag_2(CN)_3]^-$, both behave as a rod ligand to build up multi-dimensional structures by bridging between two secondary coordination centres usually of Cd(o) atoms. Unidentate ligation of

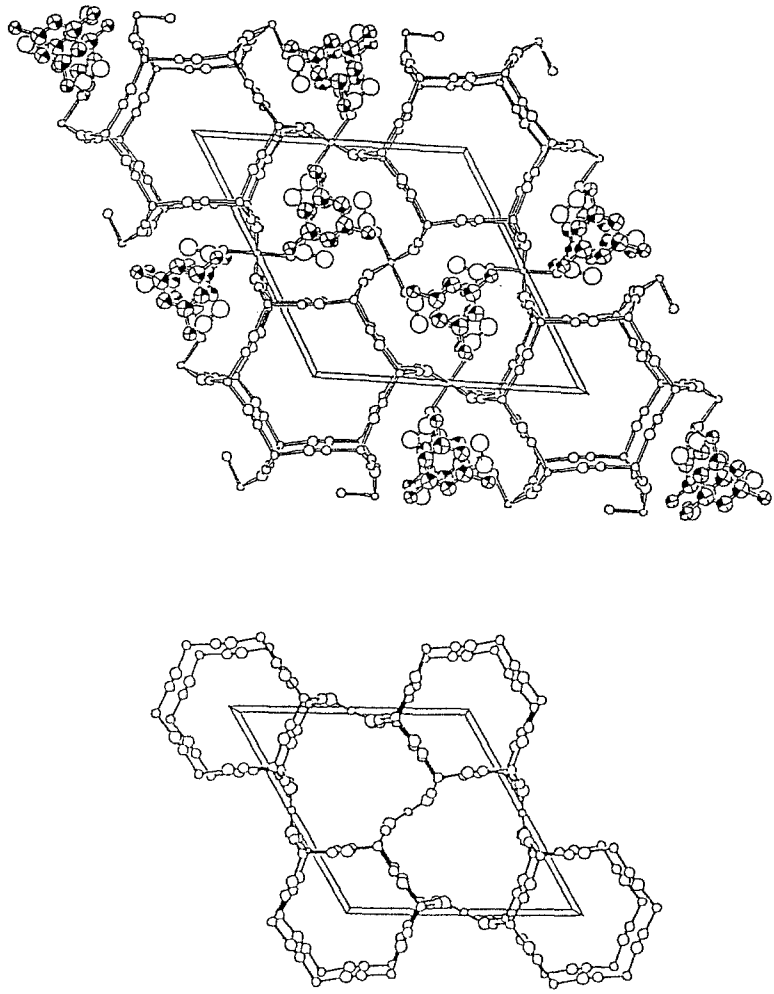

Figure 22a. Beryl-mimetic structure of $[Cd(imH)_2\{Cd(CN)_3\}_2]\cdot m\text{-}C_6H_4Me_2$ **309**. *Top*: projection along the *c* axis; the guests in the channel passing the origin are so disordered that they have not been shown. *Bottom*: Beryl-like $[Cd(CN)_2]_n$ skeleton of the host.

Cd—NCAgCN is observed in the skeletal part of the multi-dimensional structure for several compounds; a discrete anion sometimes plays a role of a space filler. The span length of Cd—NCAgCN—Cd, ca. 11 Å, is doubled in comparison with that of the M—CN—Cd span, ca. 5.5 Å, so that a 2D network and a 3D latticework spanned by Cd—NCAgCN—Cd generate respectively a wider mesh and a more voluminous cavity in comparison with those edged by M—CN—Cd. Eventually, the multi-dimensional structures involving $Ag(CN)_2$ entities show a great variety of topologies, e.g., 2D network embracing two 1D chains, interwoven 2D network by doubly interpenetrating 2D networks, interwoven 3D textile by two sets of interpenetrating 2D networks, doubly interpenetrating 3D latticework, triply

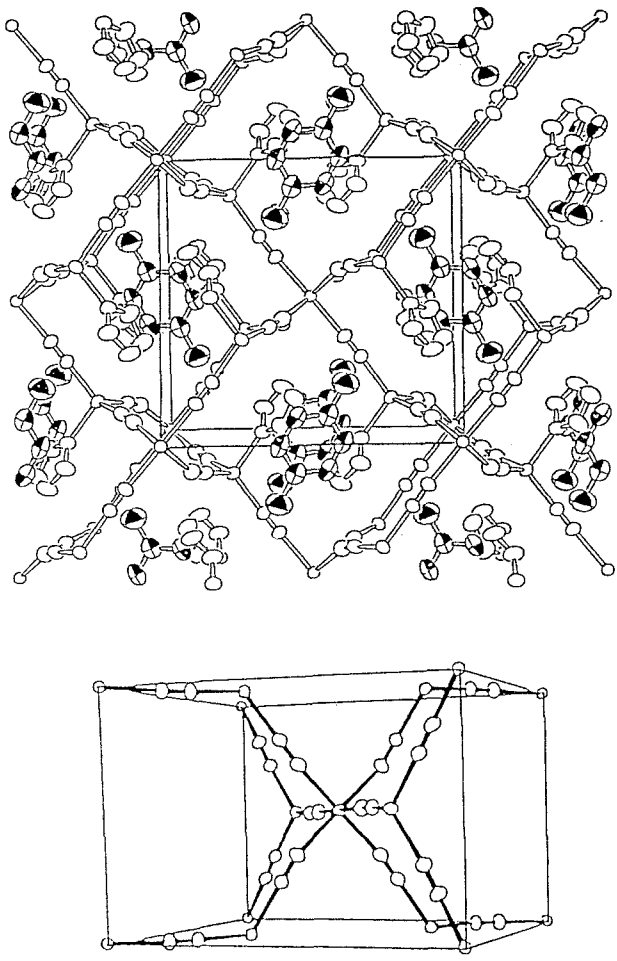

Figure 22b. Rutile-mimetic structure of $[Cd\{Cd(CN)_3(imH)_2\}_2]\cdot p\text{-}C_6H_4Me_2$ **310**. *Top*: projection along the *c* axis. *Bottom*: rutile-like $[Cd(CN)_2]_n$ skeleton of the host.

interpenetrating 3D latticework, etc. In spite of the varieties in structure, the composition of the self-assembled crystals is rather simple: $a\text{Ag(CN)}\cdot b\text{Cd(CN)}_2 \cdot c\text{L}\cdot d\text{G}$. Table VIII summarises their structural data; the compounds have been formulated to discriminate the $Ag(CN)_2$ moieties differing in ligating behaviour as clear as possible.

5.2. Structures derived from the Hofmann-type

The formal replacement of $[Ni(CN)_4]^{2-}$ in the Hofmann-type host $[Cd(NH_3)_2Ni(CN)_4]$ by $2[Ag(CN)_2]^-$ gives $[Cd(NH_3)_2\{Ag(CN)_2\}_2]$ **401** [94]; the mesh of the close-2D network of $[Ni(—CN—Cd_{1/4}—)_4]_\infty$ is expanded to $[Cd(—NCAgCN—Cd_{1/4}—)_4]_\infty$ which is abbreviated to $[Cd\{Ag(CN)_2\}_2]$ hereafter.

Table VIII. Crystallographic data for the structure involving $Ag(CN)_2$ and related structures.

		Space group	*a*/Å	*b*/Å	*c*/Å	*α*/°	*β*/°	*γ*/°	*Z*	Ref.
401	$[Cd(NH_3)_2\{Ag(CN)_2\}_2]$	$P4_2/mbc$	8.128(4)	8.128	17.611(4)	90	90	90	4	94
402	$[Cd(py)_2\{Ag(CN)_2\}_2]\cdot C_6H_6$	$I4_1/22$	12.7816(8)	12.7816	13.062(1)	90	90	90	4	95
403	$[Cd(py)_2\{Ag(CN)_2\}_2]\cdot C_4H_5N$	$I2_12_12_1$	12.861(2)	12.438(3)	13.105(2)	90	90	90	4	95
404	$[Cd(py)_2\{Ag(CN)_2\}_2]$	$C2/m$	8.665(2)	14.139(1)	7.549(1)	90	93.15(2)	90	2	95
405	$[Cd(4\text{-Mepy})_2\{Ag(CN)_2\}_2]\cdot 4\text{-Mepy}$	$Ibca$	25.990(9)	26.954(10)	14.001(6)	90	90	90	16	96
406	$[Cd(4\text{-Mepy})_4\{Ag_2(CN)_3\}][Ag(CN)_2]$	$C2/m$	11.974(7)	19.078(11)	7.634(7)	90	108.55(5)	90	2	96
407	$[Cd(3\text{-Mepy})_2\{Ag(CN)_2\}_2]$	$P2_1/c$	9.172(7)	15.610(2)	15.406(2)	90	104.02(2)	90	4	97
408	$[Cd(4\text{-ampy})_2\{Ag(CN)_2\}_2]-2[Cd\{Ag(CN)_2\}(mea)(4\text{-ampy})\{Ag(CN)_2\}]$	$P\bar{1}$	10.882(3)	12.295(3)	10.824(2)	104.89(2)	104.95(2)	68.68(2)	1	98
409	$[Cd(3\text{-ampy})_2\{Ag(CN)_2\}_2]$	$Pbca$	14.126(2)	19.557(1)	6.534(2)	90	90	90	4	97
410	$[Cd(3\text{-ampy})_3\{Ag(CN)_2\}\{Ag(CN)_2\}]$	$P2_1/c$	13.652(5)	10.907(1)	16.801(2)	90	94.78(2)	90	4	97
411	$[Cd(3\text{-ampy})_4\{Ag(CN)_2\}_2]$	$Pccn$	12.810(6)	11.275(5)	20.914(4)	90	90	90	4	97
412	$[Cd(3,4\text{-dmpy})_4\{Ag_2(CN)_3\}][Ag(CN)_2]$	$P\bar{1}$	10.972(2)	11.776(1)	7.7261(7)	107.599(7)	103.36(1)	72.56(1)	1	97
413	$[Cd(3,5\text{-dmpy})_2\{Ag(CN)_2(3,5\text{-dmpy})\}_2]$	$P2_1/c$	8.941(2)	15.280(2)	13.411(1)	90	101.82(1)	90	2	97
414	$[Cd(imH)_4\{Ag(CN)_2\}_2]$	$Pbmn$	22.206(1)	10.306(1)	10.318(1)	90	90	90	4	99
415	$[Cd(imH)_5\{Ag(CN)_2\}][Ag(CN)_2]$	$P2_1/n$	9.028(4)	13.988(6)	22.079(4)	90	101.02(2)	90	4	99
416	$[Cd(N\text{-Meim})_4\{Ag(CN)_2\}][Ag(CN)_2]$	$C2/m$	11.1292(8)	11.435(3)	11.266(1)	90	94.252(8)	90	2	99
417	$[Cd(2\text{-MeimH})_4\{Ag(CN)_2\}][Ag(CN)_2]\cdot H_2O$	$Pnnm$	11.212(2)	11.156(5)	23.646(5)	90	90	90	4	99
418	$[Cd(4,4'\text{-bpy})\{Ag(CN)_2\}_2]$	$P2_1/c$	8.891(4)	11.464(3)	17.656(4)	90	133.73(2)	90	2	100
419	$[Cd(1,3\text{-bppn})\{Ag(CN)_2\}_2]$	$C2/c$	18.656(5)	12.553(4)	16.657(3)	90	130.134(8)	90	4	97
420	$[Cd(pyz)\{Ag_2(CN)_3\}\{Ag(CN)_2\}]$	$P2/c$	9.235(2)	7.560(3)	11.274(1)	90	101.71(2)	90	2	100
421	$[Cd(mXdam)_2\{Ag(CN)_2\}_2]\cdot o\text{-}Me_2C_6H_4$	$P\bar{1}$	10.303(1)	10.764(1)	7.627(1)	99.38(1)	109.71(1)	93.42(1)	1	97
422	$[Cd(mXdam)\{Ag(CN)_2\}_2]\cdot 0.75PhCl$	$Pbam$	9.562(3)	21.280(2)	9.940(2)	90	90	90	4	97
423	$K[Co\{Au(CN)_2\}_3]$	$P312$	6.82802(5)	6.82802	7.80807(9)	90	90	120	1	101
424	$Rb[Cd\{Ag(CN)_2\}_3]$	$P312$	7.151(2)	7.151	8.1758(8)	90	90	120	1	102
425	$K[Cd\{Ag(CN)_2\}_3]$	$P312$	6.951(1)	6.951	8.2365(9)	90	90	120	1	97
426	$[Co\{Au(CN)_2\}_2]$	$P6_422$	8.434(4)	8.434	20.695(6)	90	90	120	6	103
427	$[Zn\{Ag(CN)_2\}_2]$	$P6_422$	8.4520(10)	8.452	20.622(11)	90	90	120	6	104

Table VIII. Continued

		Space group	*a*/Å	*b*/Å	*c*/Å	*α*/°	*β*/°	*γ*/°	*Z*	Ref.
428	$[K(15\text{-Crown-}5)_2][Cd\{Ag(CN)_2\}_3]\cdot 2C_6H_6$	*Pnma*	16.267(4)	21.849(5)	14.223(5)	90	90	90	4	105
429	$[K(15\text{-Crown-}5)_2][Cd\{Ag(CN)_2\}_3]\cdot 2C_4H_5N$	$R\bar{3}m$	12.850(2)	12.850	23.976(2)	90	90	120	3	97
430	$[K(15\text{-Crown-}5)_2][Cd\{Ag(CN)_2\}_3]\cdot 2PhNO_2$	*Pnma*	16.071(1)	21.996(1)	14.530(2)	90	90	90	4	97
431	$[Rb(15\text{-Crown-}5)_2][Cd\{Ag(CN)_2\}_3]\cdot 2PhMe$	*Pnma*	16.509(10)	21.966(5)	14.177(4)	90	90	90	4	105
432	$[Rb(15\text{-Crown-}5)_2][Cd\{Ag(CN)_2\}_3]\cdot 2PhNO_2$	*Pnma*	16.173(4)	22.025(5)	14.498(7)	90	90	90	4	97
433	$[Cd_2(18\text{-Crown-}6)[Cd(H_2O)_2\{Ag(CN_2\}_3]$	*C*2/*m*	13.481(2)	8.697(1)	17.1236(9)	90	103.449(4)	90	2	97

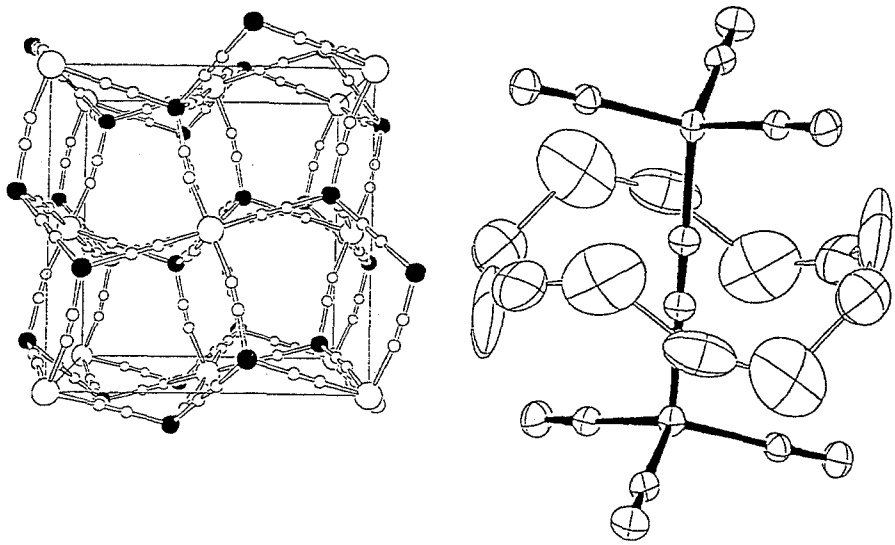

Figure 23. Structure of $H_3[Cd\{Cu_2(CN)_7\}]\cdot 14H_2O$ **317**. *Left*: pyrite-mimetic 3D latticework: Cd is shown with large circle and Cu with solid circle. *Right*: rotaxane structure of hydrogen-bonded 12 H_2O molecules about the central Cu—(CN)—Cu bond of the $[Cu_2(CN)_7]^{5-}$ moiety in a staggered conformation.

The expanded space is filled up by the interpenetration of the networks puckered and distorted to a considerable extent. The replacement of the ammine ligand by bulkier py makes the 2D network of $[Cd\{Ag(CN)_2\}_2]$ almost flat, and the interlayer space between the networks is occupied by the py ligands. The expanded mesh of the interpenetrating network accommodates the guest C_6H_6 in **402** and C_4H_5N in **403** [95]. Complex $[Cd(py)_2\{Ag(CN)_2\}_2]$ **404** has a 2D layer structure of the network with the insertion of the py rings into the meshes of adjacent upper and lower networks [95].

The 4-Mepy clathrate $[Cd(4\text{-Mepy})_2\{Ag(CN)_2\}_2]\cdot$4-Mepy **405** is obtained by introducing a methyl group at the 4-position of the py ligand [96]. As shown in Figure 24a, the layer of the 2D host is interwoven by two puckered 2D $[Cd\{Ag(CN)_2\}_2]$ networks. The cross section of the layer has a shape approximated to a stationary wave of 26.945(10) Å wavelength and ca. 4.95 Å amplitude. The interwoven structure generates an intralayer channel at the antinodal zone of the wave, and the stacking of the layer generates an interlayer channel between the nodes. Both cavities are occupied by the 4-Mepy ligands; the guest 4-Mepy is trapped in the mesh of the network like a boat floating on the wave (Figure 24b) . From the mother solution for **405**, $[Cd(4\text{-Mepy})_4\{Ag_2(CN)_3\}][Ag(CN)_2]$ **406** crystallises out, too. The complex has a 1D chain structure of the successive linkage between the four-blade propeller of $[Cd(4\text{-Mepy})_4]^{2+}$ and the shaft of dimeric condensate —NCAg(CN)AgCN—; the discrete $[Ag(CN)_2]^-$ anion is accommodated in the interchain space (Figure 24c) [96].

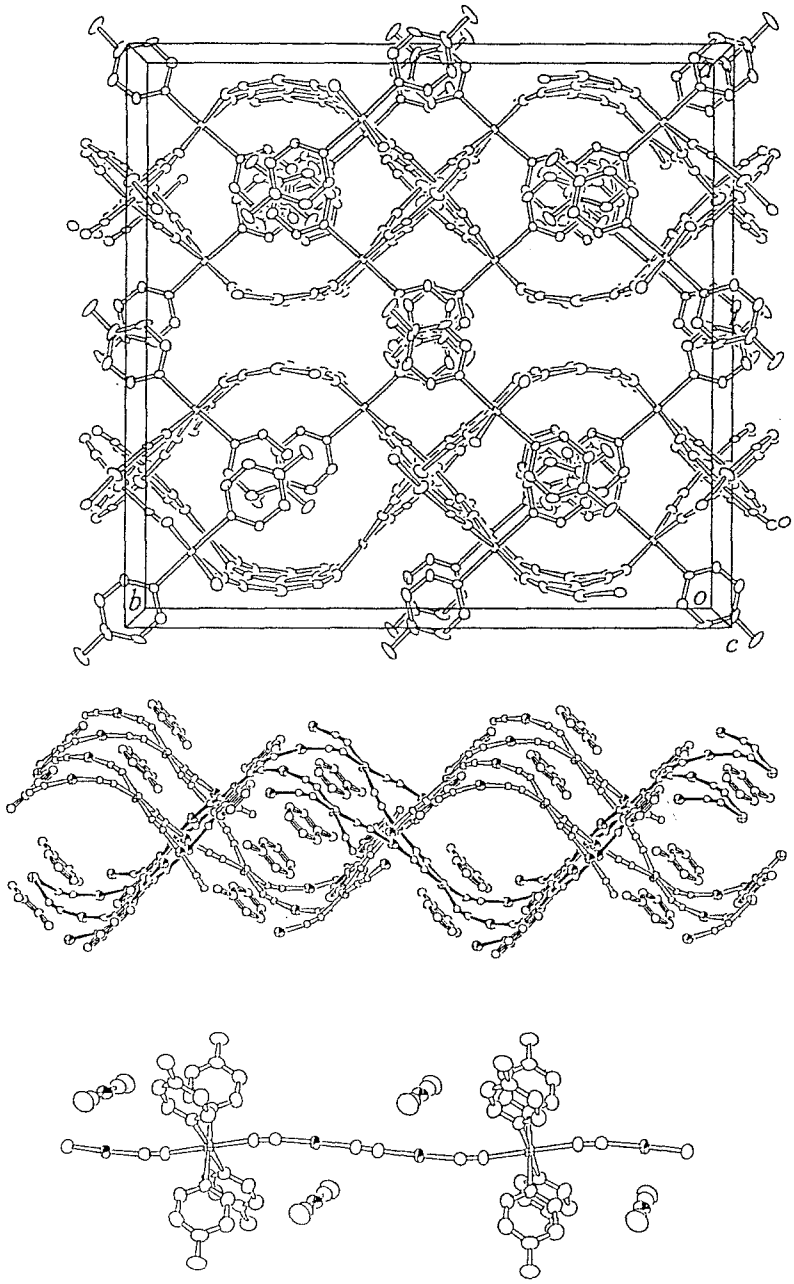

Figure 24. Top: projection along the c axis of $[Cd(4\text{-Mepy})_2\{Ag(CN)_2\}_2]\cdot$4-Mepy **405** showing a 'stationary wave' structure of doubly interpenetrating network; middle: the interpenetrating networks and the guests floating on the wave in **405**; *bottom*: 1D chain structure of $[Cd(4\text{-Mepy})_4\{Ag_2(CN)_3\}][Ag(CN)_2]$ **406** involving linear dimeric unit —NCAg(CN)AgCN— and discrete $[Ag(CN)_2]^-$ accommodated in the interchain space.

The methyl group of 3-Mepy in $[Cd(3\text{-}Mepy)_2\{Ag(CN)_2\}_2]$ **407** plays a role of clasp between two of the 2D networks. The mesh of one network is interpenetrated by the 3-Mepy ligand from another network so that the two networks are adhered to each other to form a double layer. The double layer is stacked to form the layered crystal structure [97]. In $[Cd(4\text{-}ampy)_2\{Ag(CN)_2\}_2]\cdot 2[Cd\{Ag(CN)_2\}\{Ag(CN)_2\}(mea)(4\text{-}ampy)]$ **408**, the 2D network embraces a couple of 1D chains of the —[Cd—NCAgCN—] unit in which the Cd atom is ligated by a chelating mea, and one unidentate 4-ampy and —NCAgCN to accomplish the six coordination [98]. Each mesh of the 2D network is inserted by the unidentate rods of—NCAgCN from the 1D chains running above and beneath the network. The self-clathrate structures of **407** and **408** are illustrated in Figure 25.

A self-clathrate structure such as that in **408** is not observed for the structures involving 3-ampy ligands in the ratios of Cd:3-ampy = 1:2, 1:3 and 1:4, in which structures the 2D network of $[Cd\{Ag(CN)_2\}_2]$ disappears [97]. $[Cd(3\text{-}ampy)_2\{Ag(CN)_2\}_2]$ **409** has a 1D chain structure. 3-Ampy behaves as a bridging ligand to link the octahedral Cd atoms in a double-1D mode, i.e., four of the six coordination sites of the octahedral Cd are ligated by two amino-N and py-N from four 3-ampy ligands; the six coordination of Cd is accomplished by a couple of unidentate —NCAgCN rods. The 3-ampy ligates unidentately to the octahedral Cd in $[Cd(3\text{-}ampy)_3\{Ag(CN)_2\}\{Ag(CN)_2\}]$ **410**; the bridging —NCAgCN— links the Cd atoms successively to form a 1D chain; the six coordination of the Cd is accomplished by the equatorial ligation of the unidentate —NCAgCN. $[Cd(3\text{-}ampy)_4\{Ag(CN)_2\}_2]$ **411** is a four-blade propeller-shaped molecular complex *trans*-$[Cd(3\text{-}ampy)_4\{Ag(CN)_2\}_2]$ in which all the ligands are unidentate.

Two lutidines, 3,4-dmpy and 3,5-dmpy, also behave differently [97]. Complex $[Cd(3,4\text{-}dmpy)_4\{Ag_2(CN)_3\}][Ag(CN)_2]$ **412** is isostructural to **406**, though the space group is different, with respect to the 1D chains of the four-blade propellers linked successively by the dimeric condensates; a discrete $[Ag(CN)_2]^-$ is accommodated in the interchain space. The 2D network structure in $[Cd(3,5\text{-}dmpy)_2\{Ag(CN)_2(3,5\text{-}dmpy)\}]$ **413** involves the Ag in a three coordination with 3,5-dmpy which fills up the mesh of the network and the interlayer space between the stacked networks.

5.3. IMIDAZOLE-LIGATED STRUCTURES

Imidazole (imH) and its derivatives N-Meim blocked at the pyrrole-NH by a methyl group and 2-MeimH not blocked but substituted at the 2-position give the complexes $[Cd(imH)_4\{Ag(CN)_2\}_2]$ **414**, $[Cd(imH)_5\{Ag(CN)_2\}][Ag(CN)_2]$ **415**, $[Cd(N\text{-}Meim)_4\{Ag(CN)_2\}_2][Ag(CN)_2]$ **416**, and $[Cd(2\text{-}MeimH)_4\{Ag(CN)_2\}][Ag(CN)_2]\cdot H_2O$ **417**, respectively [99]. All the CdL_4 moieties form a four-blade propeller structure with the ligands coordinated equatorially to the octahedral Cd. **414** is a molecular complex with the

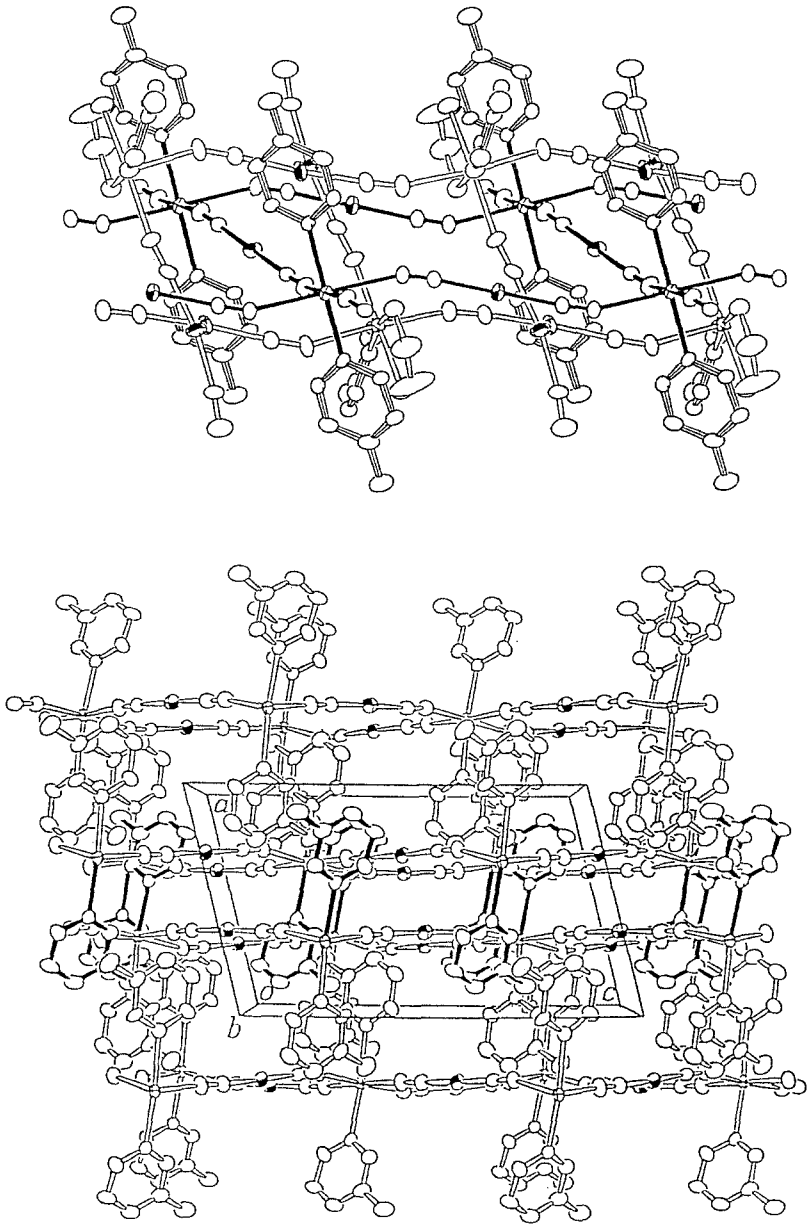

Figure 25. Layer structures of $[Cd(4\text{-ampy})_2\{Ag(CN)_2\}_2]\cdot 2[Cd\{Ag(CN)_2\}\{Ag(CN)_2\}(mea)(4\text{-ampy})]$ **408** (top) and $[Cd(3\text{-ampy})_2\{Ag(CN)_2\}_2]$ **407** (bottom). In the former, the 2D network shown with solid bonds embraces a couple of the 1D chains above and beneath the network. In the latter, the 3-Mepy ligands shown with solid bonds play a role of adhesive between a couple of 2D networks adjacent to each other; the 3-Mepy interpenetrating through the mesh provides the methyl group as a clasp to hold the couple of 2D network.

NCAgCN—Cd—NCAgCN shaft. The propellers in **416** and **417** are linked by bridging —NCAgCN— groups successively to form a 1D chain structure; a discrete $[Ag(CN)_2]^-$ is accommodated in the interchain space. Molecular complex **415** has an umbrella-like shape with the top and ribs of imHs and a shank of —NCAgCN about the octahedral Cd.

5.4. STRUCTURES INVOLVING SECONDARY BRIDGING LIGANDS

Like the Hofmann-diam-type in the Hofmann-type series, secondary ligands having a bridging function may give multi-dimensional structures spanned not only by —NCAgCN— but also by the secondary ligand such as 4,4′-bipyridine (4,4′-bpy), pyrazine (pyrz), etc. Complex $[Cd(4,4'\text{-bpy})\{Ag(CN)_2\}_2]$ **418** has a doubly interpenetrating 3D latticework structure built of the stacking of $[Cd\{Ag(CN)_2\}_2]$ 2D networks pillared by 4,4′-bpy bridges (Figure 26) [100]. The 4,4′-bpy ligands coordinating to Cd at *trans* positions in one network bridge between the Cd and the Ag atoms in the second adjacent networks by interpenetrating the meshes of the adjacent networks above and beneath. Another doubly interpenetrating 3D latticework of the same topology is possible for 1,3-di(4-pyridyl)propane (1,3-bppn) in $[Cd(1,3\text{-bppn})\{Ag(CN)_2\}_2]$ **419** [97]; the lattice structure is considerably distorted from that of **418** owing to intervening of the flexible trimethylene skeleton between the two pyridyl groups. Combination of the three rods —NCAg(CN)AgCN—, —NCAgCN—, and pyrz different in span length gives a triply interpenetrating 3D latticework structure in $[Cd(pyrz)\{Ag(CN)_2\}\{Ag_2(CN)_3\}]$ **420** (Figure 27) [100]. Each of the three *catena*-μ ligands makes a single-1D array sharing the Cd atoms to form a parallelepiped unit; each of the edges penetrates two faces of other parallelepipeds and each face is interpenetrated by two edges of the others to give the triple interpenetration.

In contrast to these interpenetrating self-clathrate structures, the structure of the aromatic guest clathrate $[Cd(mXdam)_2\{Ag(CN)_2\}_2]\cdot o\text{-}Me_2C_6H_4NH_2$ **421** is less complicated [97]. The host structure of the double-1D $>[Cd(mXdam)_2]>]_\infty$ catenation and unidentate ligation of —NCAgCN is similar to that in $[Cd(3\text{-ampy})_2\{Ag(CN)_2\}_2]$ **409**; however the double-1D span length of 10.303(1) Å is long enough to generate the cavity for the guest molecule in the interlayer space (Figure 28). The 2D network of $[Cd\{Ag(CN)_2\}_2]$ is recovered in the host of $[Cd(mXdam)\{Ag(CN)_2\}_2]\cdot 0.75PhCl$ **422**, where the bridging mXdam reinforces one set of the Cd—NCAgCN—Cd edges to form a hetero-double-1D catenation. The guest is accommodated in the interlayer space non-stoichiometrically [97].

5.5. DISTORTED $Ag(CN)_2$-SPANNED CUBES

3D lattices analogous to the CN-spanned cube of the Keggin–Miles Prussian blue structures are constructed of $Ag(CN)_2$ or $Au(CN)_2$ spans between Cd atoms in place

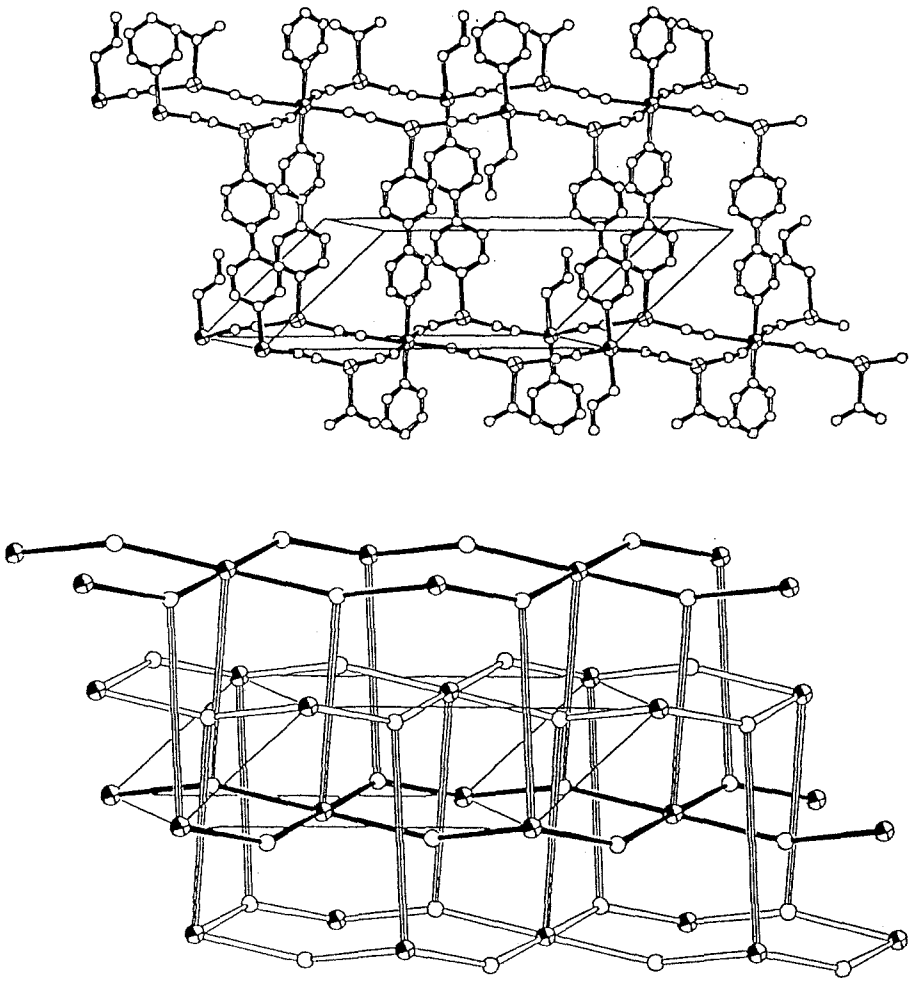

Figure 26. Doubly interpenetrating 3D structure of $[Cd(4,4'\text{-bpy})\{Ag(CN)_2\}_2]$ **418**. *Top*: the single 3D framework ; Cd is shown with anisotropic sections and Ag with peripheries. *Bottom*: illustration of the double interpenetration; Cd is shown with anisotropic sections, Ag with open ball, CN with bar, and 4,4′-bpy with lined bar.

of CN and Fe, although the cubes are distorted to some extent. Both self-clathrates and organic mixed guest clathrates have been obtained.

An earlier example was reported for $K[Co\{Au(CN)_2\}_3]$ **424** [101] whose composition is analogous to one of the complexes assumed by Keggin and Miles [4] $K_2Fe[Fe(CN)_6] = 2K[Fe(CN)_3]$. Although the original paper never referred to its supramolecular structure, it was axiomatic for those who were familiar with crystallography to understand that this dicyanoaurate(I) complex had a triply interpenetrating and trigonally distorted latticework not only forming a self-clathrate structure but also accommodating K^+ cations in the interstitial cavities. Quite the

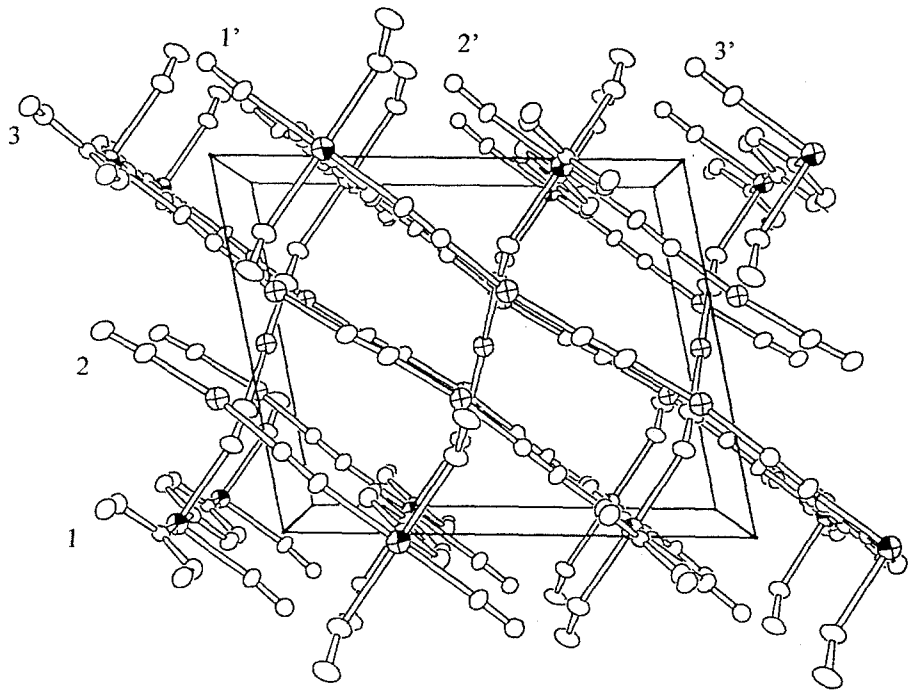

Figure 27. Triply interpenetrating 3D structure of [Cd(pyrz){Ag(CN)$_2$}{Ag$_2$(CN)$_3$}] **420** as a view along the *b* axis. Each of the Cd—NCAgCN—Cd spans between the 2D networks edged by Cd—NCAg(CN)AgCN—Cd and Cd-pyrz-Cd spans runs through the meshes of two networks to the third next: from 1 to 1′, 2 to 2′ and 3 to 3′.

same structure for Rb[Cd{Ag(CN)$_2$}$_3$] **425** [102] was recently revisited, as well as K[Cd{Ag(CN)$_2$}$_3$] **423** [97]. The speculation that a CN-edged cube, though trigonally distorted in the real structures, accommodates a K^+ ion inside thus materialised.

A precedent interesting structure mimicking H-quartz but with a sixfold interpenetration was also reported for a complex of AB_2 composition [Co{Au(CN)$_2$}$_2$] **426** in 1982 [103]; the structure has recently been revisited for [Zn{Au(CN)$_2$}$_2$] **427** [104]. Due to the longer span of M—NCAuCN—M than Si—O—Si, a self-clathrate structure is inevitable to fill up the more voluminous space to stabilise the crystal packing without any other guests.

The single latticework of [Cd{Ag(CN)$_2$}$_3$]$^-$ may be stabilised upon accommodation of voluminous guest(s) (one of) which should be cationic to neutralise the negative charge of the host. As shown in Figure 29, the clathrates [M(15-Crown-5)$_2$][Cd{Ag(CN)$_2$}$_3$]·2G (M = K: G = C_6H_6 **428** , C_4H_5N **429**, $PhNO_2$ **431**; M = Rb: G = PhMe **430**, $PhNO_2$ **432**) demonstrate that the bis(15-Crown-5) complexes of K^+ and Rb^+ are not large enough to fill up the cavity by itself but a couple of the aromatic guests are also required. Upon increasing the ionic radius of the alkali cation, viz., in the case of Cs^+, the crown ether moiety should become

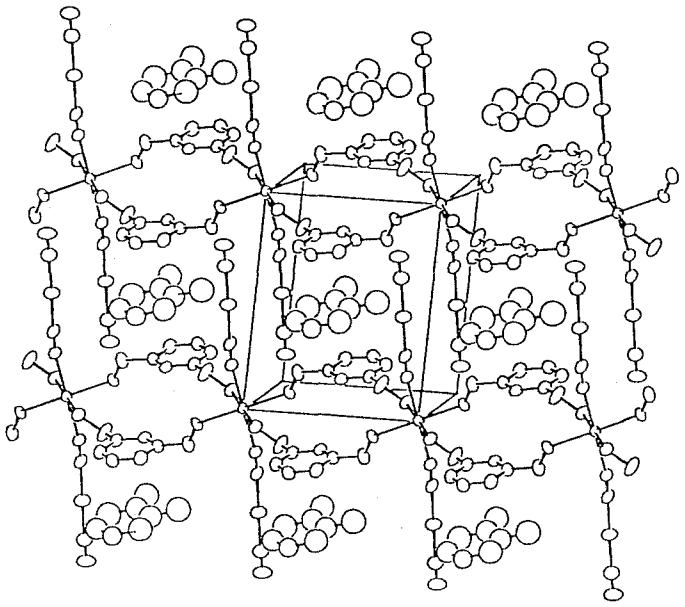

Figure 28. Structure of $[Cd(mXdam)_2\{Ag(CN)_2\}_2]\cdot$ o-$Me_2C_6H_4$ **421**. The double-1D belts of mXdam ligands sandwich the guest in the interlayer cavity separated by the protrusion of unidentate —NCAgCN from the respective Cd atoms.

greater in size to form the bis-Cst complex of the crown. However, $[Cs(18\text{-Crown-}6]^+$ appears unable to give a stable clathrate structure but affords a cation-anion complex $[Cd_2(18\text{-Crown-}6)][Cd(H_2O)_2\{Ag(CN)_2\}_3]$ **433**, in which the $Ag(CN)_2$ moiety behaves as a unidentate rod ligand.

5.6. TOPOLOGICAL VARIETIES IN $Ag(CN)_2$-SPANNED STRUCTURES

Table IX lists the structural features of the respective $Ag(CN)_2$ and $Ag_2(CN)_3$ entities in our multi-dimensional complexes from discrete complexes to triply interpenetrating 3D latticeworks, in which the behaviour of $Ag(CN)_2$ and $Ag_2(CN)_3$ is classified into the three categories: (1) discrete anion, (2) unidentate ligand and (3) bridging ligand. The resulting structures present a great variety of topologies: discrete neutral complexes **411** and **414**; discrete anionic complex **433**; discrete cationic complex **415**; cationic 1D chains **406**, **412**, **416** and **417**; neutral 1D chain **410**; neutral 2D networks almost flat **404** and **422**, and puckered **413**; 3D latticeworks **428**, **429**, **430**, **431** and **432**; double-1D belts involving secondary ligands **409** and **421**; a pair of adhered 2D networks **407**; 2D network embracing a pair of 1D chains **408**; 2D layer interwoven by a pair of 2D networks **405**; interwoven 3D textiles of flat 2D networks **402** and **403** and puckered networks **401**; doubly interpenetrating 3D latticeworks **418** and **419**; and triply interpenetrating 3D latticeworks **420**, **424** and **425**. Linear $Ag(CN)_2$ is the most simple and flexible in

Table IX. Structural features of the respective $Ag(CN)_2$ entities.

Topological feature	Compound
Discrete $[Ag(CN)_2]$	$[Cd(4\text{-}Mepy)_2\{Ag_2(CN)_3\}]$**[Ag(CN)$_2$] 406** $[Cd(3,4\text{-}dmpy)_2\{Ag_2(CN)_3\}]$**[Ag(CN)$_2$] 412** $[Cd(imH)_5\{Ag(CN)_2\}]$**[Ag(CN)$_2$] 415** $[Cd(N\text{-}Meim)_4\{Ag(CN)_2\}_2]$**[Ag(CN)$_2$] 416** $[Cd(2\text{-}MeimH)_4\{Ag(CN)_2\}_2]$**[Ag(CN)$_2$]**$\cdot H_2O$ **417**
Unidentate Cd-NCAgCN protruding from a 1D chain	$[Cd(4\text{-}ampy)_2\{Ag(CN)_2\}_2]$- 2[Cd**{Ag(CN)$_2$}**(mea)(4-ampy){$Ag(CN)_2$}] **408** $[Cd(3\text{-}ampy)_3$**{Ag(CN)$_2$}**$\{Ag(CN)_2\}]$ **410**
trans-NCAgCN-Cd-NCAgCN protruding from a discrete unit	$[Cd(3\text{-}ampy)_4$**{Ag(CN)$_2$}$_2$] 411** $[Cd(imH)_4$**{Ag(CN)$_2$}$_2$] 414** $[Cd(imH)_5$**{Ag(CN)$_2$}**$][Ag(CN)_2]$ **415** $[Cd_2(18\text{-}Crown\text{-}6)][Cd(H_2O)_2\{Ag(CN_2\}_3]$
trans-NCAgCN-Cd-NCAgCN protruding from a double-1D chain	$[Cd(3\text{-}ampy)_2$**{Ag(CN)$_2$}$_2$] 409** $[Cd(mXdam)_2$**{Ag(CN)$_2$}$_2$]**$\cdot o\text{-}Me_2C_6H_4$
1D chain -[Cd-NCAgCN-]$_n$	$[Cd(3\text{-}ampy)_3\{Ag(CN)_2\}$**{Ag(CN)$_2$}**$]$ **410** $[Cd(4\text{-}ampy)_2\{Ag(CN)_2\}_2]$- 2[Cd{$Ag(CN)_2$}(mea)(4-ampy)**{Ag(CN)$_2$}**] **408** $[Cd(N\text{-}Meim)_4$**{Ag(CN)$_2$}$_2$**$][Ag(CN)_2]$ **416** $[Cd(2\text{-}MeimH)_4$**{Ag(CN)$_2$}$_2$**$][Ag(CN)_2]$ **417** $[Cd(pyrz)\{Ag_2(CN)_3\}$**{Ag(CN)$_2$}**] 420**
1D chain -[Cd-NCAg(CN)AgCN-]$_n$	$[Cd(4\text{-}Mepy)_2$**{Ag$_2$(CN)$_3$}**$][Ag(CN)_2]$ **406** $[Cd(3,4\text{-}dmpy)_2$**{Ag$_2$(CN)$_3$}**$][Ag(CN)_2]$ **412** $[Cd(pyrz)$**{Ag$_2$(CN)$_3$}**$\{Ag(CN)_2\}]$ 420**
2D network $[Cd(\text{-}NCAgCN\text{-}Cd_{1/4}\text{-})_4]_n$ single sheet stacked	$[Cd(py)_2$**{Ag(CN)$_2$}$_2$]404** $[Cd(3,5\text{-}dmpy)_2$**{Ag(CN)$_2$}**$(3,5\text{-}dmpy)\}_2]$ **413** $[Cd(mXdam)$**{Ag(CN)$_2$}$_2$**$]\cdot 0.75PhCl$ 422**
coupled sheets adhered	$[Cd(3\text{-}Mepy)_2$**{Ag(CN)$_2$}$_2$] 407**
single sheet embracing 1D chains	$[Cd(4\text{-}ampy)_2$**{Ag(CN)$_2$}$_2$]**- 2[Cd{$Ag(CN)_2$}(mea)(4-ampy){$Ag(CN)_2$}] **408**
single sheet pillared	$[Cd(4,4'\text{-}bpy)$**{Ag(CN)$_2$}$_2$] 418** $[Cd(1,3\text{-}bppn)$**{Ag(CN)$_2$}$_2$] 419**
coupled sheets interwoven	$[Cd(4\text{-}Mepy)_2$**{Ag(CN)$_2$}$_2$**$]\cdot 4\text{-}Mepy$ 405**
interpenetrating 3D textile	$[Cd(NH_3)_2$**{Ag(CN)$_2$}$_2$] 401** $[Cd(py)_2$**{Ag(CN)$_2$}$_2$**$]\cdot C_6H_6$ 402** $[Cd(py)_2$**{Ag(CN)$_2$}$_2$**$]\cdot C_4H_5N$ 403**
2D network $[Cd\{Ag_2(CN)_3\}\{Ag(CN)_2\}]_n$	$[Cd(pyrz)$**{Ag$_2$(CN)$_3$}{Ag(CN)$_2$}**$]$ 420**
3D latticework $[Cd(\text{-}NCAgCN\text{-}Cd_{1/6}\text{-})_6]_n$ single	$[K(15\text{-}Crown\text{-}5)_2][Cd$**{Ag(CN)$_2$}$_3$**$]\cdot 2C_6H_6$ 428** $[K(15\text{-}Crown\text{-}5)_2][Cd$**{Ag(CN)$_2$}$_3$**$]\cdot 2C_4H_5N$ 429** $[K(15\text{-}Crown\text{-}5)_2][Cd$**{Ag(CN)$_2$}$_3$**$]\cdot 2PhNO_2$ 430** $[Rb(15\text{-}Crown\text{-}5)_2][Cd$**{Ag(CN)$_2$}$_3$**$]\cdot 2PhMe$ 431** $[Rb(15\text{-}Crown\text{-}5)_2][Cd$**{Ag(CN)$_2$}$_3$**$]\cdot 2PhNO_2$ 432**
triple interpenetration	Rb[Cd**{Ag(CN)$_2$}$_3$] 424** K[Cd**{Ag(CN)$_2$}$_3$] 425**

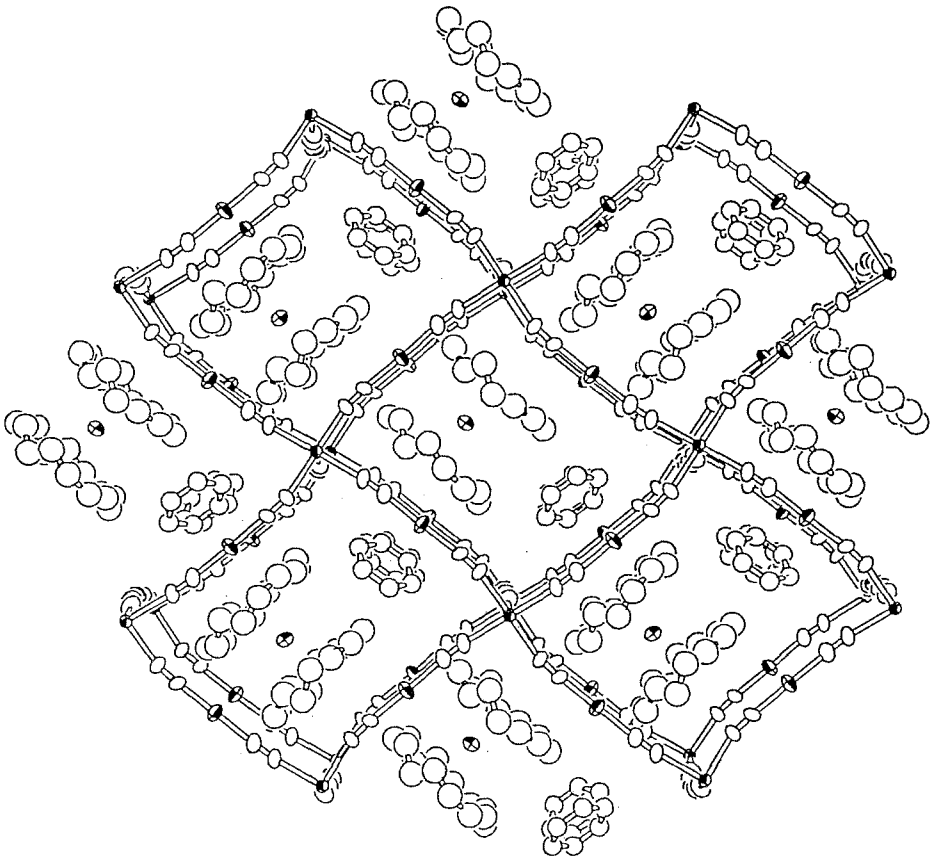

Figure 29. Structure of $[K(15\text{-Crown-}5)_2][Cd\{Ag(CN)_2\}_3]\cdot 2C_6H_6$ **428**; the distorted cubic cavity edged by Cd—NCAgCN—Cd spans accommodates the $[K(15\text{-Crown-}5)_2]^+$ sandwich complex cation and a couple of C_6H_6 molecules; Cd, Ag, and K atoms are shown with anisotropic sections.

structure in comparison with square planar $Ni(CN)_4$ and tetrahedral $Cd(CN)_4$ as the building block to build up CN-linked multi-dimensional structures. By the present stage of our investigations, the secondary coordination centre has been limited only to octahedral Cd. As exemplified for clathrates **428–432**, the longer span of a cage may be advantageous to accommodate the bulkier guest in a relatively simple host structure. As well as selection of the secondary ligand, that of the secondary coordination centre should be a key to develop host structures appropriate to the accommodation of the desired guest.

6. Concluding Remarks

A so-called supramolecular structure may be traced back to the earliest recorded artificial coordination complex in the field of inorganic chemistry–Prussian blue. Zeise's discovery of $K[PtCl_3(C_2H_4)]$ and related complexes in 1827 gave a strong

impetus to chemists in the 19th century to seek molecular complexes formed between metal salts and organic molecules. Thus, one can appreciate that Hofmann's discovery of $Ni(CN)_2 \cdot NH_3 \cdot C_6H_6$ in 1897 was historically not by chance but natural. A long period of inactivity to the middle of this century was due to the lack of tools for structure determination. After the pioneering work by Powell, we owe our progress much to the advancement of X-ray crystallography in both hardware and software.

In comparison with brilliant activities in organic and bio-organic host–guest or supramolecular chemistry, there is much to be explored in inorganic structures. The number of structures cited in this review is only about 300, with rather simple compositions, but the structures display a great variety. In fact the coordination structure of a discrete complex is simple in principle; complexity is generally given by the complexity of ligands. As this review exemplifies, we have known a little of inorganic polymeric structures even for those self-assembled from the systems limited to the square planar, tetrahedral and linear cyanometallates.

Recent theoretical studies [106], and vibrational spectroscopic studies [107, 108] including those after Powell's structure determination, contribute to understanding the host–guest interactions in the Hofmann-type and other clathrates. Solid state NMR is a new tool to analyse static structures and the dynamic behaviour of host-guest systems [93]. A temperature-dependent spin cross-over system of Fe(II) has been found in $[Fe(py)_2Ni(CN)_4]$ [9]. New structures may reveal new aspects of solid materials.

Millions of organic compounds are constructed mainly from linkages among *sp*, sp^2 and sp^3 C atoms. There is no reason why inorganic structures built of the linkages among coordination polyhedra such as linear, trigonal, tetrahedral, square planar, trigonal-bipyramidal, octahedral, etc., should be less complicated than organic structures. It is our fortune that much more remains to be explored not only for multi-dimensional inorganic structures but also for inorganic–organic host–guest structures.

Acknowledgements

I would like to acknowledge much help from my colleagues, Professor Shin-ichi Nishikiori, Doctors Tai Hasegawa, Masato Hashimoto, Takafumi Kitazawa, Ki-Min Park, Hidetaka Yuge, Takayosni Soma and Chong-Hyeak Kim, and Mr. Motoyasu Imamura, M.Sc. and Mr. Atsushi Ebina, M.Sc., whose enthusiastic contributions in my laboratory were essential to the developments I have described in this review. Thanks are also due for the support from a Grant-in-Aid for Scientific Research 07640738 from the Ministry of Education, Science and Culture, Japan.

I am grateful to Dr. J. Eric D. Davies, the Editor-in-Chief, for his appropriate advice and suggestions given to me in the preparation of this article.

References

1. (a) K.A. Hofmann and F.A. Küspert: *Z. Anorg. Allgem. Chem.* **15**, 204 (1897); (b) K.A. Hofmann and F.H. Höchtlen: *Chem. Ber.* **36**, 1149 (1903); (c) K.A. Hofmann and H. Arnoldi: *Chem. Ber.* **39**, 339 (1906).
2. (a) H.M. Powell and J.H. Rayner: *Nature (London)* **163**, 566 (1949); (b) J.H. Rayner and H.M. Powell: *J. Chem. Soc.* 319 (1952).
3. D.E. Palin and H.M. Powell: *J. Chem. Soc.* 208 (1947).
4. J.F. Keggin and Miles: *Nature (London)* **137**, 577 (1936).
5. H.J. Buser and A. Ludi: *J. Chem. Soc., Chem. Commun.* 1299 (1972); H.J. Buser, D. Schwarzenbach, W. Petter and A. Ludi: *Inorg. Chem.* **16**, 2704 (1977); F. Herren, P. Fischer, A. Ludi and W. Hälg: *Inorg. Chem.* **19**, 956 (1977).
6. A. Ludi and H.U. Güdel: *Struct. Bonding (Berlin)*, **14**, 1 (1973); H.J. Buser and A. Ludi: *Chimia* **30**, 100 (1976); A. Ludi, *J. Chem. Educ.* **58**, 1013 (1981); A. Ludi: *Chem. unser Zeit* **22**, 123 (1988).
7. (a) T. Iwamoto: *Isr. J. Chem.* **18**, 240 (1979); (b) T. Iwamoto: *J. Mol. Struct.* **75**, 51 (1981); (c) T. Iwamoto: *The Hofmann-type and Related Inclusion Compounds* (Inclusion Compounds v. 1, J.L. Atwood, J.E.D. Davies and D.D. MacNicol (eds.)), pp. 29–57, Academic Press (1984); (d) T. Iwamoto: *Inclusion Compounds of Multi-Dimensional Cyanometal Complex Hosts* (Inclusion Compounds, v. 5, J.L. Atwood, J.E.D. Davies and D.D. MacNicol (eds.)), pp. 177–212, Oxford University Press (1991).
8. R. Kuroda and Y. Sasaki: *Acta Crystallogr., Sect. B* **30**, 687 (1974).
9. T. Kitazawa, Y. Gomi, M. Takahashi, M. Takeda, M. Enomoto, A. Miyazaki and T. Enoki: *J. Mater. Chem.* in press.
10. T. Iwamoto, T. Miyoshi and Y. Sasaki: *Acta Crystallogr., Sect. B* **30**, 292 (1974).
11. T. Miyoshi, T. Iwamoto and Y. Sasaki: *Inorg. Chim. Acta* **7**, 97 (1973).
12. H.G. Büttner, G.J. Kearley, C.J. Howard and F. Fillaux: *Acta Crystallogr., Sect. B* **50**, 431 (1994).
13. Y. Sasaki: *Bull. Chem. Soc. Jpn.* **42**, 2412 (1969).
14. S. Nishikiori, T. Kitazawa, R. Kuroda and T. Iwamoto: *J. Inclusion Phenom. Mol. Recognit. Chem.* **7**, 369 (1989).
15. S. Nishikiori: in preparation.
16. E. Kendi and D. Ülkü: *Z. Kristallogr.* **144**, 91 (1976).
17. J.H. Rayner and H.M. Powell: *J. Chem. Soc.* 3412 (1958).
18. C. Kappenstein and J. Cernak: *Coll. Czechslovak Chem. Commun.* **52**, 1915 (1987).
19. T. Kitazawa, M. Fukunaga, M. Takahashi and M. Takeda: *Mol. Cryst. Liq. Cryst.* **244**, 331 (1994).
20. H. Yuge, C.-H. Kim, T. Iwamoto and T. Kitazawa: *Inorg. Chim. Acta* (submitted).
21. K.-M. Park, R. Kuroda and T. Iwamoto: *Angew. Chem.*, **105**, 939; *Angew. Chem., Int. Ed. Engl.* **32**, 884 (1993).
22. W.K. Ham, T.J.R. Weakley and C.J. Page: *J. Solid State Chem.* **107**, 101 (1993).
23. S. Nishikiori: Doctoral Thesis, the University of Tokyo, 1986.
24. S. Nishikiori and T. Iwamoto: *Chem. Lett.* 319 (1986).
25. S. Nishikiori: under preparation.
26. S. Nishikiori and T. Iwamoto: *Chem. Lett.* 1129 (1985).
27. S. Nishikiori and T. Iwamoto: *Chem. Lett.* 1775 (1981); *Bull. Chem. Soc. Jpn.* **56**, 3246 (1983).
28. H. Yuge: Doctoral Thesis, the University of Tokyo, 1992.
29. D. Ülkü: *Z. Kristallogr.* **142**, 271 (1975).
30. O. Büyükgüngör and D. Ülkü: *Acta Crystallogr., Sect. C* **43**, 241 (1987).
31. T. Hökelek and D. Ülkü: *Acta Crystallogr., Sect. C* **44**, 832 (1988).
32. R. E. Marsh: *Acta Crystallogr., Sect. C* **45**, 694 (1989)
33. T. Miyoshi, T. Iwamoto and Y. Sasaki: *Inorg. Nucl. Chem. Lett.* **6**, 21 (1970); *Inorg. Chim. Acta* **6**, 59 (1972).
34. T. Iwamoto and M. Kiyoki: *Bull. Chem. Soc. Jpn.* **48**, 2414 (1975).
35. S. Nishikiori, T. Iwamoto and Y. Yoshino: *Bull. Chem. Soc. Jpn.* **53**, 2236 (1980).

36. (a) T. Hasegawa, S. Nishikiori and T. Iwamoto: *J. Inclusion Phenom.* **1**, 365 (1984); (b) S. Nishikiori and T. Iwamoto: *J. Inclusion Phenom.* **2**, 341 (1984); (c) T. Hasegawa, S. Nishikiori and T. Iwamoto: *J. Inclusion Phenom.* **2**, 351 (1984); (d) T. Hasegawa, S. Nishikiori and T. Iwamoto: *Chem. Lett.* 1659 (1985); (e) S. Nishikiori and T. Iwamoto: *Inorg. Chem.* **25**, 788 (1986); (f) T. Hasegawa, S. Nishikiori and T. Iwamoto: *Chem. Lett.* 793 (1986); (g) T. Iwamoto, S. Nishikiori and T. Hasegawa: *J. Inclusion Phenom.* **5**, 222 (1987); (h) T. Hasegawa and T. Iwamoto: *J. Inclusion Phenom.* **6**, 143 (1988); (i) T. Hasegawa and T. Iwamoto: *J. Inclusion Phenom.* **6**, 549 (1988); (j) S. Nishikiori, T. Hasegawa and T. Iwamoto: *J. Inclusion Phenom. Mol. Recognit. Chem.* **11**, 137 (1991); (k) M. Hashimoto, T. Kitazawa, T. Hasegawa and T. Iwamoto: *J. Inclusion Phenom. Mol. Recognit. Chem.* **11**, 153 (1991); (l) T. Hasegawa, S. Franzen, D. Lambright, D.H. Oh, S. Balasubramanian, B. Hedman and K.O. Hodgson: *Inorg. Chem.* **30**, 1441 (1991); (m) H. Yuge, M. Asai, A. Mamada, S. Nishikiori and T. Iwamoto: *J. Inclusion Phenom. Mol. Recognit. Chem.* **22**, 71 (1995).
37. H. Yuge, Y. Noda and T. Iwamoto: *Inorg. Chem.* **35**, 1842 (1996).
38. H. Yuge and T. Iwamoto: in preparation.
39. (a) K.-M. Park , M. Hashimoto, T. Kitazawa and T. Iwamoto: *Chem. Lett.* 1387 (1989); (b) K.-M. Park and T. Iwamoto: *J. Chem. Soc., Chem. Commun.* 72 (1990); *J. Chem. Soc., Dalton Trans.* 1875 (1993); (c) K.-M. Park, U. Lee and T. Iwamoto: *J. Korean Chem. Soc.* **38**, 435 (1994).
40. (a) M. Hashimoto, T. Hasegawa, H. Ichida and T. Iwamoto: *Chem. Lett.* 1387 (1989); (b) M. Hashimoto and T. Iwamoto: *Chem. Lett.* 1531 (1990); (c) M. Hashimoto and T. Iwamoto: in preparation.
41. H. Yuge and T. Iwamoto: *J. Chem. Soc., Dalton Trans.* 1237 (1994).
42. (a) J. Cernak, J. Chomic, D. Baloghova and M. Dunaj-Jurco:*Acta Crystallogr., Sect. C* **44**, 1902 (1988); (b) J. Cernak, I. Potocnak, J. Chomic and M. Dunaj-Jurco: *Acta Crystallogr., Sect. C* **46**, 1098 (1990); (c) J. Lokaj, K. Gyerova, A. Sopkova, J. Sivy, V. Kettmann and V. Vrabel: *Acta Crystallogr., Sect. C* **47**, 2447 (1991).
43. G.B. Jameson, W. Bachmann, H.R. Oswald and E. Dubler: *Acta Crystallogr., Sect. A* **37**, C88 (1981).
44. H. Yuge, A. Mamada, M. Asai, S. Nishikiori and T. Iwamoto: *J. Chem. Soc., Dalton Trans.* 3195 (1995).
45. T. Kitazawa, Y. Mizushima, J. Shiraha, R. Taguchi, A. Katoh, T. Hasegawa, S. Nishikiori and T. Iwamoto: *J. Inclusion Phenom. Mol. Recognit. Chem.* **10**, 29 (1991).
46. S. Nishikiori and T. Iwamoto: *Chem. Lett.* 1127 (1987); S. Nishikiori, Y. Takahashi- Ebisudani, and T. Iwamoto: *J. Inclusion Phenom. Mol. Recognit. Chem.* **8**, 101 (1990).
47. M. Imamura, S. Nishikiori and T. Iwamoto: unpublished.
48. H. Yuge and T. Iwamoto: *Acta Crystallogr., Sect. C* **51**, 374 (1995).
49. H. Yuge and T. Iwamoto: *Acta Crystallogr., Sect. C* **52**, 575 (1996).
50. a) A. Ebina, S. Nishikiori and T. Iwamoto: *J. Chem. Soc., Chem. Commun.* 233 (1994); b) A. Ebina, S. Nishikiori and T. Iwamoto: in preparation.
51. H. Hashimoto and T. Iwamoto: *J. Coord. Chem.* **23**, 269 (1991).
52. M. Hashimoto and T. Iwamoto: *Acta Crystallogr., Sect. C* **50**, 496 (1994).
53. M. Rüegg and A. Ludi: *Theor. Chim. Acta* **20**, 193 (9171).
54. H. Yuge and T. Iwamoto: *J. Inclusion Phenom. Mol. Recognit. Chem.* **14**, 217 (1992).
55. R. Kuroda: *Inorg. Nucl. Chem. Lett.* **9**, 13 (1974).
56. H. Yuge and T. Iwamoto: *J. Chem. Soc., Dalton Trans.* 2841 (1993).
57. a) T. Iwamoto: *Chem. Lett.*, 723 (1973); b) S. Nishikiori and T. Iwamoto: *J. Inclusion Phenom.* **3**, 283 (1985).
58. S. Tsunezawa and T. Iwamoto: 69th Annual Meeting of the Chemical Society of Japan, 3E231, Kyoto, March (1995).
59. K.-M. Park and T. Iwamoto: *J. Inclusion Phenom. Mol. Recognit. Chem.* **11**, 397 (1991).
60. H. Yuge and T. Iwamoto: in preparation.
61. B.F. Abrahams, M.J.Hardie, B.F.Hoskins, R. Robson and E.E. Sutherland: *J. Chem. Soc., Chem. Commun.* 1049 (1994).

62. (a) T. Kitazawa, S. Nishikiori, R. Kuroda and T. Iwamoto: *J. Chem. Soc., Dalton Trans.* 1029 (1994); (b) T. Kitazawa, S. Nishikiori, A. Yamagishi, R. Kuroda and T. Iwamoto: *J. Chem. Soc., Chem. Commun.* 413 (1992); (c) T. Kitazawa, S. Nishikiori, R. Kuroda and T. Iwamoto: *Chem. Lett.* 1729 (1988).
63. B.F. Hoskins and R. Robson: *J. Am. Chem. Soc.* **112**, 1546 (1990).
64. E. Shugam and H. Zhdanov: *Acta Physicochim. U. R. S. S.* **20**, 247 (1945).
65. H.S. Zhdanov: *Compt. Rend. Acad. Sci. U. R. S. S.* **31**, 352 (1941).
66. B.F. Abrahams, M.J. Hardie, B.F. Hoskins, R. Robson and G.A. Williams: *J. Am. Chem. Soc.* **114**, 10641 (1992).
67. T. Kitazawa, T. Kikuyama, M. Takeda and T. Iwamoto: *J. Chem. Soc., Dalton Trans.* 3715 (1995).
68. T. Kitazawa, S. Nishikiori and T. Iwamoto: in preparation.
69. T.Kitazawa, S. Nishikiori, R. Kuroda and T. Iwamoto: *Chem. Lett.* 459 (1988).
70. T. Kitazawa, S. Nishikiori and T. Iwamoto: *Mater. Sci. Forum* **91–93**, 257 (1992).
71. T. Kitazawa, S. Nishikiori and T. Iwamoto: *J. Chem. Soc., Dalton Trans.* 3695 (1994).
72. C.-H. Kim, S. Nishikiori and T. Iwamoto: in preparation.
73. T. Kitazawa, H. Sugisawa, M. Takeda and T. Iwamoto: *J. Chem. Soc., Chem. Commun.* 1855 (1993).
74. B. Ziegler and D. Babel: *Z. Naturforsch.* **46b**, 47 (1991).
75. T. Kitazawa and M. Takeda, *J. Chem. Soc., Chem. Commun.* 309 (1993).
76. T. Kitazawa, M. Akiyama, M. Takahashi and M. Takeda: *J. Chem. Soc., Chem. Commun.* 1112 (1993).
77. J. Kim, D. Whang, Y.-S. Koh and K. Kim: *J. Chem. Soc., Chem. Commun.* 637 (1994).
78. J. Kim, D. Whang, J. I. Lee and K. Kim: *J. Chem. Soc., Chem. Commun.* 1400 (1993).
79. T. Kitazawa, T. Kikuyama, M. Takahashi and T. Takeda: *J. Chem. Soc., Dalton Trans.* 2933 (1994).
80. B.F. Abrahams, B.F. Hoskins and R. Robson:*J. Chem. Soc., Chem. Commun.* 60 (1990).
81. B.F. Abrahams, B.F. Hoskins, J. Liu and R. Robson: *J. Am. Chem. Soc.* **113**, 3045 (1991).
82. S. Nishikiori, C. I. Ratcliffe and J.A. Ripmeester: *J. Am. Chem. Soc.* **114**, 8590 (1992).
83. J. Pickard and G.-T. Gong: *Z. Anorg. Allgem. Chem.* **620**, 183 (1994).
84. C.-H. Kim, T. Soma, S. Nishikiori and T. Iwamoto: *Chem. Lett.* 89 (1996).
85. C.-H. Kim, H. Yuge, S. Nishikiori and T. Iwamoto: in preparation.
86. H. Kurihara, T. Soma and T. Iwamoto: 45th Symposium on Coordination Chemistry, Japan, 3Aα14, Fukuoka, October (1995).
87. H. Nishikiori and T. Iwamoto: *J. Chem. Soc., Chem. Commun.* 1555 (1993).
88. S. Nishikiori and T. Iwamoto: *Chem. Lett.* 1218 (1994).
89. H. Yuge and T. Iwamoto: *J. Inclusion Phenom. Mol. Recognit. Chem.* (in press).
90. H. Gies: *Clathrasils and Zeosils: Inclusion Compounds with Silica Host Framework* (Ch. 1 in *Inclusion Compounds* Vol. 5, J.L. Atwood, J.E.D. Davies and D.D. MacNicol (eds.)), pp. 1–36, Oxford University Press, Oxford (1991).
91. T. Iwamoto: *Clay-like and Zeolite-like Structures Built of Polymeric Cyanocadmates* (in Chemistry of Microporous Crystals, T. Inui, S. Namba and T. Tatsumi (eds.)) pp. 3–10, Kodansha-Elsevier, Tokyo (1991); T. Iwamoto, T. Kitazawa, S. Nishikiori, and R. Kuroda: *Mineralomimetic Inclusion Behavior of Cadmium Cyanide Systems* (in Chemical Physics of Intercalation II, P. Bernier, J.E. Fischer, S. Roth and S.A. Solin (eds.)), pp. 325–332, Plenum, New York (1993); T. Iwamoto, S. Nishikiori and T. Kitazawa: *Supramol. Chem.* **6**, 179 (1995).
92. (a) S. Nishikiori, C. I. Ratcliffe and J.A. Ripmeester: *Can. J. Chem.* 68, 2770 (1990); (b) S. Nishikiori, C.I. Ratcliffe and J.A. Ripmeester: *J. Chem. Soc., Chem. Commun.* 775 (1991); (c) R. Curtis, C.I. Ratcliffe and J.A. Ripmeester: *J. Chem. Soc., Chem. Commun.* 1800 (1992).
93. J.A. Ripmeester and C.I. Ratcliffe: *Solid State NMR Studies of Host-Guest Materials* (Ch. 1 in Spectroscopic and Computational Studies of Supramolecular Systems, J.E.D. Davies (ed.)), pp. 1–27, Kluwer Academic Publishers, Dordrecht (1992).
94. T. Soma and T. Iwamoto: *Chem. Lett.* 271 (1995).
95. T. Soma and T. Iwamoto: *J. Inclusion Phenom. Mol. Recognit. Chem.* (in press).
96. T. Soma and T. Iwamoto: *Chem. Lett.* 821 (1994).

97. T. Soma and T. Iwamoto: in preparation.
98. T. Soma and T. Iwamoto: *Acta Crystallogr., Sect. C* (in press).
99. T. Soma and T. Iwamoto: *Inorg. Chem.* **35**, 1849 (1996).
100. T. Soma, H. Yuge and T. Iwamoto: *Angew. Chem., Int. Ed. Engl.* **33**, 1665 (1994).
101. S.C. Abrahams, J.L. Bernstein, R. Liminga and E.T. Eisenmann: *J. Chem. Phys.* **73**, 4585 (1980).
102. B.F. Hoskins, R. Robson and N.V.Y. Scarlett: *J. Chem. Soc., Chem. Commun.* 2025 (1994).
103. S.C. Abrahams, L.E. Zyontz and J.L. Bernstein: *J. Chem. Phys.* **76**, 5458 (1982).
104. B.F. Hoskins, R. Robson and N.V.Y. Scarlett: *Angew. Chem., Int. Ed. Engl.* **34**, 1203 (1995).
105. T. Soma and T. Iwamoto: *Mol. Cryst. Liq. Cryst.* **276**, 19 (1996).
106. E. Ruiz, S. Alvarez, R. Hoffmann and J. Bernstein: *J. Am. Chem. Soc.* **116**, 8207 (1994); E. Ruiz and S. Alvarez: *Inorg. Chem.* **34**, 3260 (1995); E. Ruiz and S. Alvarez: *J. Phys. Chem.* **99**, 2296 (1995); E. Ruiz and S. Alvarez: *Inorg. Chem.* **34**, 5845 (1995).
107. S. Akyüz, A.B. Dempster and L. Morehouse: *Spectrochim. Acta* **30A**, 1183 (1974); J.E.D. Davies, A.B. Dempster and S. Suzuki: *Spectrochim. Acta* **33A**, 103 (1977); S. Akyüz, A.B. Dempster, J.E.D. Davies and K.T. Holmes: *J. Mol. Struct.* **54**, 1 (1979); N. Ekici, Z. Kantarci and S. Akyüz: *J. Inclusion Phenom. Mol. Recognit. Chem.* **10**, 9 (1991); S. Bayari, Z. Kantarci and S. Akyüz: *J. Inclusion Phenom. Mol. Recognit. Chem.* **17**, 291 (1994).
108. L. Andreeva, B. Minceva-Sukarova and V. Petrusevski: *Croat. Chem. Acta* **65**, 173 (1992).